

The University of Maine

DigitalCommons@UMaine

Electronic Theses and Dissertations

Fogler Library

Summer 8-16-2024

An Enhancement of the Properties of Cellulose Nanofibril Composites for Biomedical Applications

Cameron G. Andrews

The University of Maine, cameron.andrews@maine.edu

Follow this and additional works at: <https://digitalcommons.library.umaine.edu/etd>



Part of the [Biomaterials Commons](#)

Recommended Citation

Andrews, Cameron G., "An Enhancement of the Properties of Cellulose Nanofibril Composites for Biomedical Applications" (2024). *Electronic Theses and Dissertations*. 4036.

<https://digitalcommons.library.umaine.edu/etd/4036>

This Open-Access Thesis is brought to you for free and open access by DigitalCommons@UMaine. It has been accepted for inclusion in Electronic Theses and Dissertations by an authorized administrator of DigitalCommons@UMaine. For more information, please contact um.library.technical.services@maine.edu.

**AN ENHANCEMENT OF THE PROPERTIES OF CELLULOSE NANOFIBRIL
COMPOSITES FOR BIOMEDICAL APPLICATIONS**

By

Cameron Andrews

B.S. University of Maine, 2023

A THESIS

Submitted in Partial Fulfillment of the

Requirements for the Degree of

Master of Science

(in Biomedical Engineering)

The Graduate School

The University of Maine

August 2024

Advisory Committee:

Michael Mason, Professor of Chemical and Biomedical Engineering, Advisor

Mehdi Tajvidi, Associate Professor of Renewable Nanomaterials

Renee Kelly, Associate Vice President for Strategic Partnerships, Innovation, Resources
and Engagement

© 2024 Cameron Andrews

All Rights Reserved

**AN ENHANCEMENT OF THE PROPERTIES OF CELLULOSE NANOFIBRIL
COMPOSITES FOR BIOMEDICAL APPLICATIONS**

By Cameron Andrews

Thesis Advisor: Dr. Michael Mason

An Abstract of the Thesis Presented
In Partial Fulfillment of the Requirements for the
Degree of Master of Science
(in Biomedical Engineering)
August 2024

The use of plastics has increased significantly within the past few years. The versatile properties within this material set have enabled them to be adopted into many different industries. They tend to possess excellent vapor and liquid barrier properties, adjustable mechanical properties, and can be designed for specific heating and electrical applications. One specific industry that has capitalized on plastics is the medical industry. Since the COVID-19 pandemic, a class of subset plastic materials, single-use plastics, have been utilized. These single-use devices are typically used for a short time and quickly discarded. These items can range from masks to gloves and even IV bags. While these materials possess properties that are ideal for their design, they are over-engineered for their purpose. They are generally used within 24 hours but are sometimes designed to last 100s years. Not only that, but they are difficult to dispose of. Incineration can release greenhouse gases into the air, mechanical degradation can produce microplastics, and landfilling is a temporary solution that will create future complications. Therefore, alternative single-use plastic materials must be designed to possess properties similar to current ones but can naturally degrade in a much shorter period.

Cellulose nanofibrils (CNF) emerge as a crucial solution to the single-use plastic problem in the medical industry. Among the many biodegradable materials under research, CNF's sustainability, biocompatibility, and biodegradability make it a compelling candidate for biomedical research. Its unique geometric and surface properties make it chemically and mechanically versatile, including hydrophilicity, high mechanical strength, and moderate porosity in bulk formulations. These properties have led to extensive research into the potential of dense CNF-based solid composites in healthcare-related applications, from disposable surgical tools to resorbable implants. The urgency of finding a solution to the single-use plastic problem in the medical industry cannot be overstated, and CNF offers a promising path forward.

Despite significant progress and even some commercial interest, several key unknowns remain that must be addressed to fully realize the potential of CNF as an alternative to single-use plastics in the medical industry. The rehydration and degradability of CNF when introduced to water are current complications within the material. One potential method is to use a crosslinking agent within the CNF to address this. More potential complications are the low dispersion of minerals throughout the material and low cell viability. To overcome this, an enhanced dispersion method of a biological mineral into CNF will be designed and tested. This will alleviate the current lack of mineral dispersion while also expanding the cell viability of the material. Bioglass will also be added to CNF to explore further and enhance the cell viability of CNF while attempting to retain the desired mechanical properties of the dried material. Finally, adapting a standard metal fabrication process will try to reduce the overall internal strain that CNF naturally possesses. This ongoing research and experimentation demonstrate the commitment to creating a more desired and suitable alternative product to medical-grade plastics.

ACKNOWLEDGEMENTS

First, I would like to thank Dr. Michael Mason for the opportunity to participate in this groundbreaking research. Your guidance and aspirations for this project motivated me to keep moving forward and accomplish as much as possible during this degree. I want to thank Dr. Mehdi Tajvidi and Renee Kelly, who helped me better understand how to purposefully research to successfully set up a product for its potential market applications. Also, everybody in Dr. Tajvidi's lab for helping me perform various mechanical tests. I want to thank Dr. Mitchell Chesley for mentoring and guiding me through the initial stages of my research into this project. Your faith in me gave me the confidence and knowledge to continue pursuing this project following your graduation. I want to thank all of the members of the Mason Lab, especially Abraham Fadahunsi and Blake Turner. Your energy and collaboration helped make the time spent conducting my research enjoyable. I want to thank all of the undergraduate students who have worked with me throughout this project, and your help enabled me to complete my research promptly. I would also like to thank Rajat Rai for his help interpreting my results. I would also like to thank Dr. Emma Perry for her help in obtaining the SEM images used in this thesis. I finally would like to thank Kyle Guerrette and his student design suite workers for their continuous help with this project.

I want to acknowledge all the family and friends who have significantly impacted my undergraduate and graduate journey here at the University of Maine. I would never have made it through this process without the continuous support and belief you all gave me. You pushed me to strive to be successful and impactful during my education, which has gotten me to where I am today.

TABLE OF CONTENTS

ACKNOWLEDGEMENTS.....	iii
LIST OF TABLES.....	vi
LIST OF FIGURES.....	vii
CHAPTER 1 INTRODUCTION.....	1
CHAPTER 2 LITERATURE REVIEW.....	3
2.1. Plastics.....	3
2.2. Plastic Properties.....	6
2.3. Device Requirements.....	9
2.4. Single-Use Devices.....	11
2.5. Alternative Materials.....	14
2.6. Cellulose Nanofibrils.....	18
2.7. Unknowns.....	24
CHAPTER 3 CROSSLINKING OF CELLULOSE NANOFIBRIL COMPOSITES.....	27
3.1. Introduction.....	27
3.2. Polycup.....	29
3.2.1 Bulk CNF Production.....	29
3.2.2 Results.....	34
3.3. Urea.....	45
3.3.1 Thin Film Production.....	45
3.3.2 Results.....	47
3.4. Strontium Chloride.....	51
3.4.1 Results.....	51

3.5. Conclusions.....	55
CHAPTER 4 HOMOGENIZATION METHODS FOR CELLULOSE NANOFIBRIL COMPOSITES.....	56
4.1. Introduction.....	56
4.2. Methods.....	58
4.3. Results.....	60
4.4. Conclusions.....	71
CHAPTER 5 CELLULOSE NANOFIBRIL COMPOSITES WITH BIO-ACTIVE GLASS.....	72
5.1. Introduction.....	72
5.2. Methods.....	73
5.3. Results.....	73
5.4. Conclusions.....	79
CHAPTER 6 STRUCTURAL ANNEALING OF CELLULOSE NANOFIBRIL COMPOSITES.....	80
6.1. Introduction.....	80
6.2. Methods.....	82
6.3. Results.....	83
6.4. Conclusions.....	91
CHAPTER 7 CONCLUSIONS.....	92
7.1 Summary.....	92
7.2 Future Work and Recommendations.....	94
REFERENCES.....	97
BIOGRAPHY OF THE AUTHOR.....	102

LIST OF TABLES

Table 2.1.	Plastic material types, names, characteristics, and applications.	7
Table 2.2	Surface degradation rates and half-lives of specifically-sized common plastics. .	12
Table 2.3	Various cellulose nanomaterials.	17
Table 2.4	Known applications of CNFs.	19
Table 2.5	Unknown properties of CNF.	24

LIST OF FIGURES

Figure 2.1	Global medical plastics market by share and application in 2023.	4
Figure 2.2.	U.S Medical Plastics Market.	5
Figure 2.3.	Dual-Disc CNF Refiner at the University of Maine Process Development Center (PDC).	18
Figure 2.4.	Original cutting directionality of CNF molds.	22
Figure 3.1.	Crosslinking action of polycup and CNF.	29
Figure 3.2.	Bulk CNF production schematic.	30
Figure 3.3.	Cross-section of a macroporous CNF sample.	30
Figure 3.4.	Schematic of Type V tensile testing sample, with dimensions from ASTM standard D638-22.	31
Figure 3.5.	Schematic of flexural testing sample with dimensions from ASTM standard D790-17.	32
Figure 3.6.	Water soaking in Fisher Scientific Oven (left) for absorption and tensile tests using Instron model 5942 (right).	33
Figure 3.7.	Water absorption rate over all time points for each polycup % by wt.	34
Figure 3.8.	Water absorption of CNF samples with varying amounts of polycup over 1 hour.	35
Figure 3.9.	The tensile strength of bulk CNF with polycup over total water absorption time.	37
Figure 3.10.	The tensile strength of bulk CNF with polycup over the first hour of water absorption time.	38
Figure 3.11.	Young’s Modulus of bulk CNF with polycup over total water absorption time. .	39

Figure 3.12.	Young’s modulus of bulk CNF with polycup over the first hour of water absorption.	40
Figure 3.13.	Flexural testing setup with 3-point bending attachment on an Instron model 5942.	42
Figure 3.14.	Flexural strength of CNF scaffolds with polycup across various saturation conditions.	43
Figure 3.15.	Flexural modulus of CNF scaffolds with polycup across various saturation conditions.	44
Figure 3.16.	CNF thin film procedure.	46
Figure 3.17.	Cutting of CNF thin films in the 1D (left) and 2D (right).	47
Figure 3.18.	Tensile strength for urea samples in 2 directions at 60°C and 80°C.	48
Figure 3.19.	Young’s modulus for urea samples in 2 directions at 60°C and 80°C.	49
Figure 3.20:	Tensile strength of urea samples compared against 60°C and 80°C in both the 1D (left) and 2D (right).	50
Figure 3.21:	Tensile strength of urea samples compared against 1D and 2D in both the 60°C (left) and 80°C (right).	51
Figure 3.22.	Tensile strength (left) and modulus (right) of strontium CNF films compared across directions.	52
Figure 3.23.	Tensile strength (left) and modulus (right) of strontium CNF films compared across wt. %.	53
Figure 3.24:	Comparison of tensile strength across all crosslinking agents.	54
Figure 4.1.	CNF thin film with 15% HA untreated.	57
Figure 4.2.	No-treat HA mixing methodology for thin film CNF composites.	59

Figure 4.3.	Sieved HA mixing methodology for thin film CNF composites.	59
Figure 4.4.	Tensile strength of sieved CNF films with HA in the 1D (left) and 2D (right).	60
Figure 4.5.	Young’s Modulus of sieved CNF films with HA in the 1D (left) and 2D (right).	61
Figure 4.6:	Tensile strength of no-treat CNF films with HA in the 1D (left) and 2D (right).	62
Figure 4.7:	Young’s modulus of no-treat CNF films with HA in the 1D (left) and 2D (right).	62
Figure 4.8.	Statistical analysis of saturated mixing types (left) and pre-saturation (right).	63
Figure 4.9:	Statistical analysis of sieve vs no-treat blended mixing types.	64
Figure 4.10.	15% HA/CNF thin film portions with HA treated by blending (left) and left untreated (right).	65
Figure 4.11.	50% HA/CNF blend-mixed film with a 4x SEM image (left), and a 50% HA/CNF untreated film with a 4x SEM image (right).	66
Figure 4.12.	Cutting directions of new CNF molds.	68
Figure 4.13.	Flexural strength (left) and modulus (right) of CNF/HA composites.	69
Figure 4.14.	Compressive strength (left) and modulus (right) of CNF/HA composites.	70
Figure 5.1.	Tensile strength of Bioglass/CNF films.	74
Figure 5.2.	Young’s modulus of Bioglass/CNF films.	75
Figure 5.3.	Flexural strength of 45s Bioglass/CNF composites.	76
Figure 5.4.	Flexural strength of 45s Bioglass/CNF composites.	77
Figure 5.5:	Comparison of Bioglass and HA flexural strength with CNF.	78
Figure 6.1.	Representation of CNF fibers' expected behavior through annealing cycle.	81
Figure 6.2.	Procedure for one annealing cycle.	82

Figure 6.3.	Flexural strength (left) and modulus (right) of 70°C pure CNF across . increasing annealing cycles.	83
Figure 6.4.	6-cycle samples with observed expansion (left, middle) and 2-cycle sample (right).	84
Figure 6.5.	Volume, mass, and density change across increasing annealing cycles.	85
Figure 6.6.	Volume change for differently manufactured CNF across increasing annealing cycles.	86
Figure 6.7.	Mass change for differently manufactured CNF across increasing annealing cycles.	87
Figure 6.8.	Density change for differently manufactured CNF across increasing annealing cycles.	88
Figure 6.9.	Flexural strength of differently manufactured CNF across increasing annealing cycles.	89
Figure 6.10.	Flexural modulus of differently manufactured CNF across increasing annealing cycles.	90

CHAPTER 1: INTRODUCTION

The use of plastics has increased significantly within the past few years. The versatile properties within this material set have enabled them to be adopted into many different industries. They tend to possess excellent vapor and liquid barrier properties, adjustable mechanical properties, and can be designed for specific heating and electrical applications. One specific industry that has capitalized on plastics is the medical industry. Since the COVID-19 pandemic, a class of subset plastic materials, single-use plastics, have been utilized. These devices are typically used for a short time and quickly discarded. These items can range from masks to gloves and even IV bags. While these materials possess properties ideal for their design, their life cycle relative to their useful life would suggest that they are over-engineered. They are generally used within 24 hours but are sometimes designed to last 100s years. Not only that, but they are difficult to dispose of. Incineration can release greenhouse gases into the air, mechanical degradation can produce microplastics, and landfilling is a temporary solution that will create future complications. Therefore, alternative single-use plastic materials must be designed to possess properties similar to current ones but can naturally degrade in a much shorter period.

Cellulose nanofibrils (CNF) are emerging as a promising solution to the medical industry's single-use plastic problem. Their sustainability, biocompatibility, and biodegradability make them an attractive candidate for biomedical research. CNF's unique geometric and surface properties make it chemically and mechanically versatile. It is hydrophilic, has high mechanical strength, and has moderate porosity in bulk formulations. These properties have sparked extensive research into the potential of dense CNF-based solid composites in healthcare-related applications, from disposable surgical tools to resorbable implants.

Despite much progress and even some commercial interest, several key unknowns must first be addressed. This thesis will explore these unknowns. Chapter 2 gives an in-depth background into medical plastic usage and potential replacement materials. Chapter 3 will examine the crosslinking of CNF to attempt to reduce its rehydration and degradability when fully dried. Chapter 4 will explore a method of dispersion of a biological mineral into CNF. This will alleviate the current lack of mineral dispersion while also expanding the cell viability of the material. Chapter 5 will progress further regarding the cell viability of CNF while attempting to retain the desired mechanical properties of the dried material. Finally, Chapter 6 will experiment with a modification to a standard metal fabrication process to try to reduce the overall internal strain of the material. This will aid the material manufacturing process and create a more uniform product. These unknowns will be explored to create a more desired and suitable alternative product to medical-grade plastics.

CHAPTER 2: LITERATURE REVIEW

2.1: Plastics

Plastics are a class of materials used worldwide for various applications. They are versatile and have many desirable properties that can be utilized for specific target applications. They are generally low-weight, durable, and have a low manufacturing cost compared to other materials.¹ Plastics are generally produced from petrochemical sources, meaning fossil fuels like oil and gas, and the derived product is a specific type of chemical polymer.¹ Due to their vast range of properties, relatively low cost, and easy accessibility, they are a desired commodity used worldwide daily.

The production of plastics has increased significantly over the past 50 years. It is estimated that 9200 million metric tons of plastic were produced then.² In 2019 alone, 368 million metric tons of plastic were produced, and if other alternatives are not found to help reduce this number, then the production is predicted to double in 20 years.² The sheer scale at which these materials are manufactured and sold is cause for concern, and change is needed. This is especially true within large industrial fields, such as the medical industry.

The medical industry is a heavy consumer of plastic products. Medical plastic waste is classified as “all plastic waste created by healthcare institutions, medical labs, and biomedical examination centers, and waste from small sources.”³ Medical plastic waste can consist of many products, such as intravenous (IV) bags, surgical tools, and even the medical gowns that doctors and nurses are mandated to wear. Not only are medical supplies made of plastics, but any product that comes into contact with any bodily fluid is considered waste. The United States Environmental Protection Agency (USEPA) classifies medical plastic waste as “a hospital or clinical waste that blood, fluids, or other contaminated objects have infected.”³ Therefore, any plastic product that

comes into contact with contaminants is considered waste. This aims to prevent the spread of disease and infections within a hospital setting.

Even though some plastics are used in waste applications, there are other applications within the medical industry where plastics won't have to be disposed of due to waste. Below is a chart that breaks down the global medical plastics market by application share.

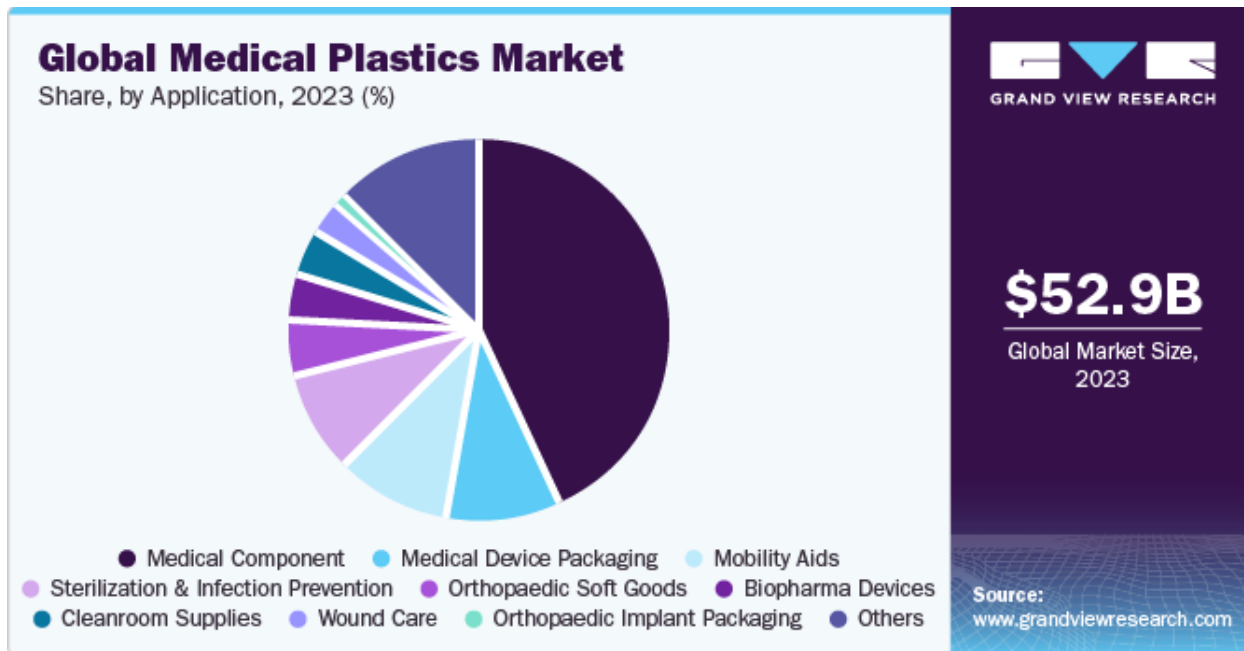


Figure 2.1: Global medical plastics market by share, by application, in 2023.⁴

Of the applications shown above, medical device components make up 40% of plastic applications. Due to the COVID-19 pandemic, the use of plastic medical components has increased significantly. These include personal protective equipment (PPE) devices such as gloves, facemasks, and gowns, all produced from plastic.⁴ Technological advanced medical equipment such as magnetic resonance imaging (MRI) scanners and ventilators were used much more frequently. Apart from medical components, many other plastic applications are used in the industry, as shown in the graph. These include medical device packaging, mobility aids, sterilization, infection prevention, and orthopedic implant packaging. These are just the significant

applications within the medical industry where plastic is used. More will come with the advancement of research and development around plastic usage.

The range of plastics used in a medical setting is extensive due to the variability each specific plastic can deliver. Some plastics are utilized more than others. In 2023 alone, the global medical plastics market size was estimated at around \$52.9 billion.⁴ This global revenue stream is expected to increase at a rate of 7.4% annually until 2030.⁴ The significant increase can be attributed to the increase in medical devices using common plastics and device packaging and the need for these devices for at-home healthcare. Besides the use of plastics within medical applications, other disposable items are also used. These can include catheters, surgical instrument handles, and even syringes.⁴ Below are some of the most commonly used plastics in the United States medical industry.

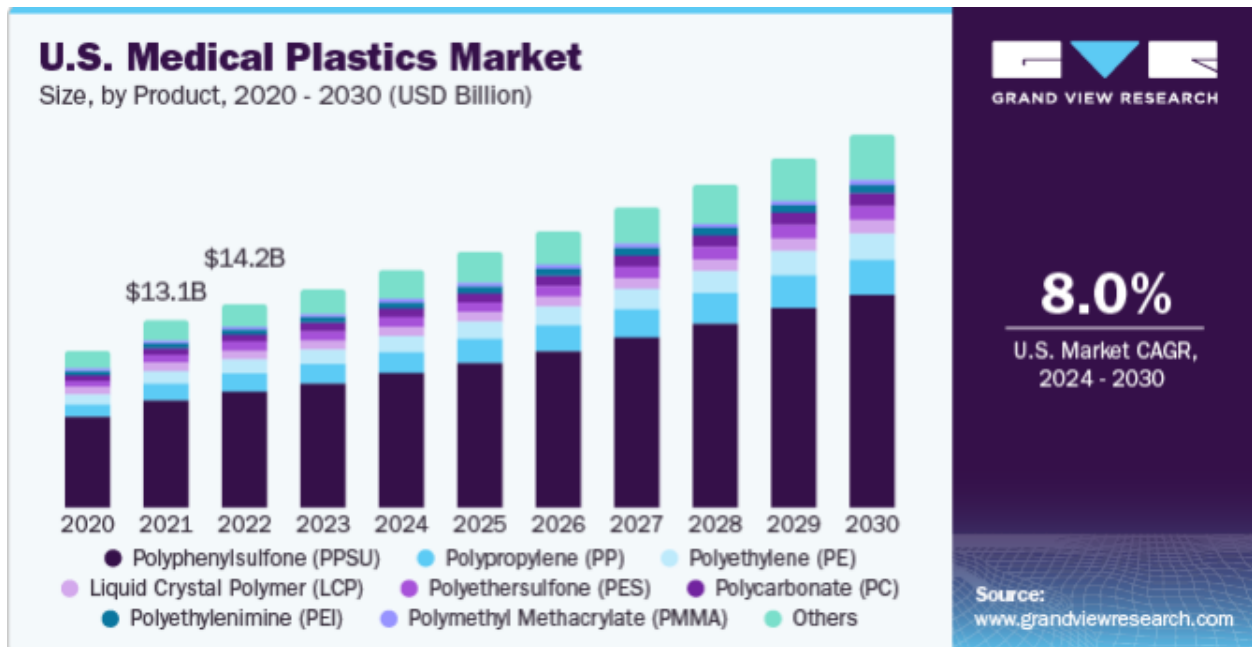


Figure 2.2: U.S Medical Plastics Market.⁴

From the graph, of the total \$52.9 billion generated in 2023, the United States composed over 25% of that entire market. The United States is heavily invested in the use of plastics within

the medical industry, and the graph shows that this number is expected to increase significantly over the next 6 years. The graph also shows the percentage of each specific plastic used within this industry. It is shown that polyphenylsulphone (PPSU) is generated the most, with polypropylene (PP), polyethylene (PE), and other polymers making up the rest of the list.

2.2. Plastic Properties

Many different specific properties of plastics can make them ideal for medical applications. Within the field of plastics, there are different categories in which each type can be organized. Two of the major types of plastics are thermosets and thermoplastics. “Polymers that undergo melting or softening upon heating and solidify when cooled are called thermoplastic polymers.”⁵ Furthermore, “thermoset polymers are usually polymerized or hardened upon heating and, once formed, are infusible and cannot be remolten or reformed.”⁵ The major difference is that thermoset polymers, or plastics, are irreversible once formed, while thermoplastic plastics can be reheated and remolded after the first cooling cycle. The chemical structure of each type is the cause of this. Thermoplastics are generally linear or branched polymers, so their bonding can be easily altered. Still, thermosets generally have crosslinked or networked polymers, which have much higher thermal resistance due to the nature of bonding.⁵ Thermoplastics, therefore, are generally used for short-term items like plastic bags, while thermosets are designed to last much longer, such as the plastic used for an MRI.

Within these, there are specific materials that have specific applications. Below is a table indicating the materials used as plastics, the trade names they are identified with, some of the major characteristics of each type, and the typical applications for which each type is used.

Table 2.1: Plastic material types, names, characteristics, and applications.^{6,7}

Material Type	Trade Names	Characteristics	Typical Applications
Polyethylenes	Fortiflex, ^{8,9} Hostalen ⁹	Chemical resistance, electrical insulating, tough, low strength	Plastic bottles, film wrapping
Polypropylenes	Fortilene, ⁸ Oleplate, ¹⁰	Resistance to heat, excellent electrical properties and fatigue strength, chemically inert	Syringes, plastic furniture
Polystyrenes	Dylene, ¹¹ Lustrex ¹²	Excellent electrical properties, relatively inexpensive, thermally and dimensionally stable	Styrofoam, food packaging containers
Polyesters	Duranex, ⁹ Ensitem ¹³	Excellent fatigue and tear strength, resistance to humidity and acids	Synthetic clothing, fruit containers
Fluorocarbons	Teflon, ¹⁴ Hostaflon ¹⁵	Chemically inert, excellent electrical properties, high- temperature resistance	Fishing line, high-temp heat pumps
Acrylics	Acrylite, ¹⁶ Plexiglas ¹⁷	Resistance to weathering, fair mechanical properties, good for light transmission	Glass substitute, water- resistant paint
Vinyls	Palvinyl, ¹⁸ Tecavinyl ¹⁹	Rigid, can be flexible with plasticizers, susceptible to heat distortion	Music records, plumbing tubing
Epoxies	Lytex, ²⁰ Epikote ²¹	Corrosion resistance, high mechanical properties, good electrical properties	Adhesives, marine sealants
Phenolics	Bakelite, ²² Micarta ²³	Excellent thermal stability, inexpensive, can be compounded with resins	Telephones, electrical fixtures

From the table above, some of the most common properties are excellent electrical resistance, chemical inertness, high-temperature resistance, and relatively low cost compared to other materials. Also, the table exemplifies the wide range of applications in which these polymeric materials can be used. For example, polypropylene-based materials can be used for syringes and plastic furniture, while polyesters can be used within synthetic clothing. The major characteristics of these materials are also used as the basis for material selection within the medical industry.

Specific properties must be considered when determining the best plastic for medical applications. First, the mechanical properties need to be particular to the target application. For example, suppose a product, such as an IV bag or tubing, requires much flexibility and elasticity while maintaining a relatively high mechanical strength. In that case, a commodity plastic such as polyvinyl chloride (PVC) is an option.²⁴ However, if a product requires high stiffness and strength, such as for an implant or dental instrument, a high-performance plastic, like polyetheretherketone (PEEK), would be selected.²⁴ Another vital property that must be explored is if the material needs sterilization. In a medical setting, if a piece of equipment comes into contact with the body, it must be sterilized. Sterilization is when a product's microbiological contaminants are inactivated, transforming the nonsterile medical devices into sterilized products.²⁴ One standard method of sterilization is steam sterilization. This process, also known as autoclaving, is taken out in an autoclave and consists of steaming the material at high temperature and pressure for a specific time. Following the process, the bacterium on and inside the products are neutralized, sterilizing the product. Therefore, any material needing steam sterilization must withstand high temperatures and pressures. Some examples of materials that can be selected are polypropylene, unplasticized PVC, high-temperature thermoplastics, and most thermosets.²⁴ Finally, determining the length at which a product needs to last is another essential characteristic that needs to be analyzed. Short-term devices such as gloves, gowns, or masks don't need to worry about the wear resistance of the product due to their high disposal rate. However, when designing a product to withstand a large amount of wear, selecting a material that can withstand loading for a prolonged period is essential. In this case, the chemical property that needs to be analyzed is the overall crystallinity of the material. Material can be amorphous, meaning that the collection of molecules has no order or is semi-crystalline, where the molecules can stack or align to form ordered crystalline regions.²⁴ A

high-wear resistance material, like high-density polyethylene (HDPE), is semi-crystalline. At the same time, polystyrene (PS) and PVC are amorphous and cannot withstand a prolonged wear period. These are just a few properties discussed during the plastic selection process, but other factors still occur.

2.3. Device Requirements

A strict process is required when seeking to market a medical device. First, the device must not be harmful to a patient during utilization. For example, in 2016, the United States Food and Drug Administration (FDA) banned powdered gloves. They deemed that this material posed an unreasonable and substantial risk of illness and injury when an individual was exposed to the powder that came from these gloves.²⁵ The FDA first approved powdered gloves, but once more research was done and they were found to harm patients, they revoked their approval and banned the products. Next, the materials have to match the application that they are intended for. For example, if a material needs to be sterilizable, then the property requirements of that material must be able to withstand a sterilization or autoclave procedure. Once the materials that are not harmful or toxic to individuals have been selected and match specific properties for the desired applications, they must seek FDA approval. There are three classes in which materials are classified: Class I, Class II, and Class III. Class I materials are considered low-risk devices, therefore having the least requirements for approval.²⁶ Class II materials are medium to moderate-risk medical devices requiring approval and general and special controls.²⁶ Class III materials are high-risk and generally life-supporting or life-sustaining materials that require general controls and pre-market approval.²⁶ Class III devices take the longest to reach approval, with caution in understanding all medical device properties. Without the approval of the FDA, medical devices will cease to be marketed.

The FDA also has another set of guidelines to be followed when introducing a new product into the medical market: the Current Good Manufacturing Practice (CGMP) guidelines.²⁷ These guidelines are in place to ensure proper design, monitoring, and control of manufacturing processes and facilities.²⁷ These guidelines must be strictly followed during any material manufacturing, or there could be a risk of a shutdown by the government. Another component of the FDA is the Generally Recognized as Safe (GRAS) Items and Materials.²⁸ These are any materials generally recognized by qualified experts as having been adequately shown to be safe under the conditions of their intended use.²⁸ Materials on this list are already pre-approved, which can help simplify the lengthy FDA approval process. When designing or implementing a new material or device for medical applications, it is important to consider these practices to succeed.

Even though some materials may not meet the FDA requirements for a medical device on their own, when combined with other materials, the new properties can be enhanced to meet the requirements. A perfect example of this is the chemical chromium. Chromium is found to be harmful and toxic to the body, but when formed into an alloy, such as a cobalt-chromium (Co-Cr) alloy, it can have beneficial and non-toxic properties.²⁹ These Co-Cr alloys are orthopedic devices for knee, shoulder, and hip prostheses.³⁰ When combined into an alloy with other products like Molybdenum, they can obtain properties like high Young's modulus, high corrosion resistance in body fluids, and good biocompatibility.³⁰ The alloy is just one example of an individual material that is insufficient for medical applications but provides a suitable alternative when combined. Furthermore, not all pre-approved materials can be approved when combined with another material. For example, hydrogen peroxide and vinegar alone are not toxic to the body. However, the combination of the two forms a highly corrosive acid. Overall, it is important to understand the

reactions of materials when designing products for medical devices due to their potential benefits or hazards.

2.4. Single-Use Devices

The Food and Drug Administration (FDA) defines a single-use device as one that is “intended for use on one patient during a single procedure ... and is not intended to be reprocessed (cleaned, disinfected/sterilized) and used on another patient.”¹³ The use of these products has increased significantly since the 1970s. Before introducing these short-term alternatives, most medical devices were made of rubber, glass, or metal, meaning they could be wiped down and sanitized, making them reusable.³¹ These devices were commonly over-engineered for their purpose, and the cost associated with buying and maintaining them was high. Also, these devices are generally a much cheaper alternative. Not only are they easily mass-produced, so cost is decreased, but the time and energy spent reusing and sterilizing continuous-use materials is saved with single-use devices. These single-use devices have been a popular additive within the medical industry since their introduction and will be utilized until an alternative option arises.

If left untreated, medical devices in landfills or the environment may remain there long. Depending on the type of plastic used, the degradation time for these plastics can range from a few years to hundreds of years. Below is a table demonstrating the length of time it would take for plastics to decompose within a landfill.

Table 2.2: Surface degradation rates and half-lives of specifically-sized common plastics.³²

Material	Experimental Thickness (um)	Surface Degradation Rate (buried landfill) (um/year)	Estimated half-life (buried landfill) (year)
Polyethylene Terephthalate	500	0	>2500
High-Density Polyethylene	10,000	1.0	250
Polyvinyl Chloride	10,000	0	>2500
Low-Density Polyethylene	100	11	4.6
Polypropylene	800	0.51	780
Polystyrene	20,000	0	>2500

Some troubling statistics are shown in this table. Granted, the displayed thickness values varied, but the surface degradation rate showed how the plastics would degrade over the year. LDPE showed the highest degradation rate, with 11 um/year; the polyethylene terephthalate (PET), PVC, and polystyrene (PS) displayed a degradation rate of zero and no estimated half-life time frame. These statistics exemplify how detrimental these plastics can be for the environment. If thousands of pounds of non-biodegradable plastic are put into the earth, it may never degrade and will be entrapped there forever. Finally, the values shown above also demonstrate how over-engineered single-use products are. Most of these products are used within a day but are designed to last thousands of years. For example, an IV bag is used until the liquid is emptied but is no longer used. According to the statistics above, it has the potential to last thousands of years when it is only used for one day. Alternative solutions must be made for these forever plastics, designed to serve their purpose, like current materials. Still, they can also be safely incinerated or degraded in a reasonable time frame.

There are different ways in which these devices can be disposed of besides landfilling. Some of the most common are incineration, autoclaving, or recycling. Incineration consists of burning waste products. Landfilling is when the waste is put directly into the ground, and recycling breaks down the material and uses it for another purpose. “In the United States, 49-60% of medical waste is incinerated, 20-37% is autoclaved, and other technologies treat 4-5%.”³³ Landfilling medical waste, however, is challenging because a law prohibits landfilling biohazardous waste. Therefore, only waste that isn’t deemed biohazardous or properly sanitized can be landfilled. Incineration is also another poor option for eliminating waste material. For example, one of the most common plastics used in the medical industry is PVC, but when PVC is incinerated, it releases chlorine gas and dioxins into the air.³³ These are components that contribute to acid rain and negatively impact air quality. Sterilization, on the other hand, is typically used when a material can be reused. This involves placing waste in direct contact with steam, with a temperature of at least 121°C for 30 minutes.³³ However, PVC, as well as other plastics, have a melting temperature within this range. Again, this is a poor method to treat this type of specific waste due to the vapors produced during the melting of these products.

Next, two methods could also be a solution: reuse and recycle. If medical devices that are disposed of, such as a cardiopulmonary bypass (CPB), are still operable, they could be donated for use in developing nations. In the United States, once the CPBs are used in practice, they are deemed hazardous waste and are discarded. However, the condition of these devices is still operable, and would only need to find a sterilization method before reuse. Recycling is another method that could also reduce the amplitude of products being incinerated or landfilled. The recycling process involves grinding PVC products into small, granular pieces and then heating these granules into liquid form to be remolded into a new product.³³ This process is once again challenging due to the

different variations of PVC, which are all compiled into one product. The product's irregularity makes it difficult to remake it into anything purposeful due to the combination of properties. Overall, the waste procedures for plastics, especially PVC, prove to be challenging in reducing the overall plastic footprint.

2.5 Alternative Materials

Recent research has shown that there are alternatives to plastics that maintain relatively the same properties but have much faster biodegradation time and are easier to dispose of overall. Different areas have been explored for various applications. There are bioplastics, biodegradable plastics, compostable plastics, and even adaptations of cellulose, which is the most abundant polymer on earth.³⁴ These alternative materials could answer the plastic waste crisis that is growing in severity every day. The current plastic materials are designed to last longer than their derived purpose. Due to their bioavailable background, some alternative materials can serve their purpose and degrade in a more applicable time frame.

Specific properties have to be proven before a plastic can be labeled biodegradable. They must be able to degrade under natural processes, contain low amounts of heavy metals, the material should not harm plant life, 90% of the material must be converted to CO₂ within 6 months, and 90% must be smaller than a 2x2mm mesh within 3 months of exposure.³⁴ On the other hand, bioplastics are made entirely from bio-based materials. However, not all bioplastics are classified as biodegradable. Studies have shown that bioplastics can have the same chemical compounds found in plastics when produced by eco-friendly materials, resulting in the same 400 years of degradation.³⁵ These bioplastics essentially make the same synthetic polymers made into common plastics. They are just derived from biomass derivatives rather than fossil-fuel derived. These materials may seem like a viable alternative to fossil-fuel-derived plastics due to their derivation

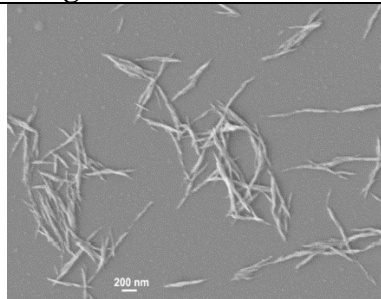
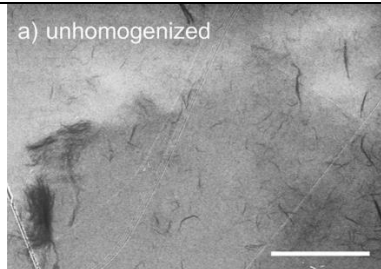
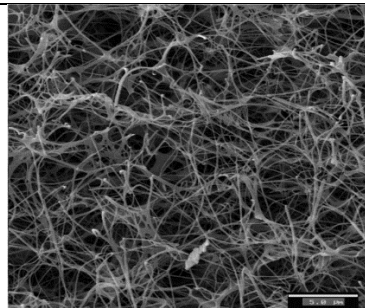
from natural materials like maize and plant oils. Still, they don't eliminate the long-term degradation issue. These materials are also more expensive than those synthesized with fossil fuels.³⁴ Finally, compostable plastics break down similarly to biodegradable plastics but decompose under industrial composting processes.³⁴ One of the more common types of compostable plastics is polylactic acid (PLA). These materials are biodegraded using an at-home composter or anaerobic digesting within a composting plant.³⁴ Using a composter for this material could then eliminate the waste generated by some common plastics.

Another common type of polymer that is used in industry is natural polymers. These types of polymers normally come from a plant or animal. Some common examples of plant-based natural polymers are starches, cellulose, and natural rubber. Starches are carbohydrates with a glucose monomer unit, which are then attached to a polymer chain through glycosidic bonds.³⁶ These polymers, or polysaccharides, are typically responsible for plants' energy storage. Some common starch derivatives are maize, rice, wheat, and potatoes; one typical application is pharmaceutical usage.³⁶ Cellulose is another very common material found in nearly all plant species. This material is the most abundant organic polymer on earth, "consisting of a linear chain of several hundred to over ten thousand beta 1-4 linked D-glucose units."¹⁶ The overall purpose of cellulose within plants is to provide structure to the cell walls. Some common applications of cellulose are for controlled drug release systems, film coating, and as a diluent/binder in pharmaceutical applications.³⁶ Finally, natural rubber is a common material used for many applications. It occurs naturally from a *Hevea Brasiliensis* tree in the form of cis-1,4-polyisoprene.³⁷ Although this material can be derived from other sources or synthetically produced, this is the most common source. Natural rubber is a versatile material, with applications ranging from car tires to lacrosse balls to even medical gloves for surgical applications. Overall, plants provide access to many naturally

occurring polymers, and the introduction of these into applications in which synthetic polymers are currently used could help diminish the use of non-biodegradable plastics.

Several natural polymers are derived from the animal kingdom. Some common types are alginate, chitin, and collagen. “Alginates, or alginic acids, are anionic polysaccharides that are linear, unbranched polysaccharides found in brown seaweed and marine algae.”³⁶ They are composed of two monomers, beta-D-mannuronic acid, and alpha-L-guluronic acid, linked through beta-1,4 glycosidic bonds.³⁶ Some alginate applications are stabilizers in emulsions, tablet binders or disintegrants, and drug delivery. Chitin is another common biopolymer derived from the skeletal material of invertebrates such as mollusks, annelids, and arthropods.¹⁶ Chitin has a similar structure to cellulose. However, the hydroxyl groups of the second carbon on the glucose units are replaced with an acetamido group.³⁶ Chitin can also be modified to form chitosan, an excellent drug-delivery agent. Finally, collagen is a biopolymer found in humans and animals and is the most prevalent structural protein in the human body.³⁸ There are 11 different types of collagen, with Type I being the most abundant. The fibers can be found throughout the body in tissues, muscles, and even bones. Due to its natural occurrence in the body, collagen has been researched as a natural material for tissue engineering applications. Overall, much research is being conducted on these materials, and the growth of applications will only increase in the future.

Table 2.3: Various cellulose nanomaterials.³⁹

Material	Production Method	Sizes	Images
Cellulose nanocrystals (CNCs)	Acid hydrolysis of cellulose fibers with sulfuric acid	3-35nm diameter 200-500nm length	 40
TEMPO-mediated cellulose nanofibrils (TCNF)	TEMPO-mediated oxidation	3-5nm width	a) unhomogenized  41
Bacterial Cellulose (BC)	Breakdown of sugar with the introduction of bacteria	2-micron length 3-4nm x 70-140nm cross-section	 42

Another specific set of natural materials that have gained research interest is cellulose nanomaterials. These materials are all composed or derived from cellulose, and their sizes vary along the nanoscale. First, cellulose nanocrystals (CNCs) are a unique form of nanocellulose, with sizes ranging from 3-35nm in diameter and 200-500nm in length. These materials are formed through an acid hydrolysis reaction of cellulose fibers using sulfuric acid. This reaction degrades amorphous cellulose regions, leaving a crystalline product.³⁹ Another common form of nanocellulose is TEMPO-mediated oxidation of CNF (TCNF). In this reaction, cellulose is put through an oxidation process in which a TEMPO group is attached to the cellulose chain. The

oxidated molecule is then mechanically degraded into fibers with a 3-5nm width.³⁹ Next, bacterial cellulose (BC) is unlike the previous two forms. Rather than breaking down previous forms of cellulose to a smaller scale, it uses bacteria to make nanocellulose strands. The process involves placing bacteria in a media containing a sugar source, and the bacteria will create cellulose in up to two weeks.³⁹ The dimensions are oriented in a twisting ribbon structure, with cross sections of 3-4nm x 70-140nm, with a length of more than 2 microns.³⁹ This procedure eliminates the risk of the material containing other wood byproducts, such as lignin and hemicellulose, which makes it ideal for biomedical applications.

2.6. Cellulose Nanofibrils

A final cellulose nanomaterial is cellulose nanofibrils, which have many different formation methods. These nanofibrils typically have a diameter of 5-50nm and a length of a few microns.³⁹ They can be produced through various mechanical treatments such as electrospinning, homogenization, grinding, and ball milling.³⁹ This material comprises pure cellulose, the most abundant natural polymer on earth, specifically derived from bleached softwood kraft pulp (BSKP). BSKP is derived from wood through a chemical process in which most of the hemicellulose is removed, and all of the lignin is removed. The pulp is then dried and formed into large sheets. To produce CNF, these sheets are first ground down in a large vat, and water is added to produce an accurate weight percentage. The resultant mixture is then fed into a high-shear dual-disc refiner. The refiner, shown to the right, has two plates, one stationary and one that spins at a high shear rate. When the cellulose fibers are



Figure 2.3: Dual-Disc CNF Refiner at the University of Maine Process Development Center (PDC).

placed under the shear stress produced by this refiner, the fibers start to fibrillate. Fibrillation is defined as the act or process of forming fibers or fibrils.⁴³ So, the larger cellulose fibers break down into smaller fibers as the high-shear process occurs, and these fibers are known as the cellulose nanofibrils. At the Process Development Center (PDC) at the University of Maine, they make a specific type of CNF that is 3% wt. CNF, with the rest being water and 90% “fines.” They define these fines as anything less than 200 microns in length.

Table 2.4: Known applications of CNFs.

Application	Beneficial Properties
Rheological modifier of mayonnaise	Decrease in starch and oil content, rheological stability, similar taste and feel. ⁴⁴
Structural enhancer in concrete	Mechanical property improvement, increased weather stability, increased hydrophobicity. ⁴⁵
Binding agent in particleboard and medium-density fiberboards	Mechanical property improvement and elimination of urea-formaldehyde resin (carcinogenic). ⁴⁶
Oxygen barrier	Efficient barrier properties below 65% humidity can replace current plastics used as oxygen barriers. ⁴⁷
Binding agent in low-density foams	Creates foam when mixed, microwave safe, binds fibers together. ⁴⁸
Coating for wood-particle food containers	Increased mechanical strength, excellent oil/grease resistivity, and biodegradability. ⁴⁹

CNFs have been used for a wide range of applications in many industries. One specific application has used CNFs as a rheological modifier in mayonnaise. The research team demonstrated how the starch and oil content could be decreased within mayonnaise, yet the rheological properties would remain the same with the addition of 0.75wt% and 0.42wt% CNF.⁴⁴ This enhancer could help alleviate some health concerns surrounding mayonnaise while keeping

the consistency, taste, and feel the same. Next, CNFs have also been explored as a structural enhancer in concrete applications. One team tested mechanical, freeze-thaw, and even water absorption properties. With the addition of CNFs, the tensile and flexural strengths improved, the freezing-thawing was enhanced to reduce overall cracking, and the concrete became more hydrophobic.⁴⁵ CNF enhanced the concrete's properties in this specific application, making it more weather-stable and increasing the mixture's overall mechanical properties. CNF has also been used as a binding agent for target applications. One research team at the University of Maine found that CNF effectively replaced urea-formaldehyde resin as the binding agent in particleboard and medium-density fiberboards.⁴⁶ Their study found that the mechanical properties of wood-flour boards were improved with the addition of CNF due to the strong linkage between the two.⁴⁶ Urea-formaldehyde resin creates carcinogenic emissions when formed, so their replacement can positively impact environmental health.

Cellulose nanomaterials have also been found to have an excellent oxygen barrier in dry environments (0% relative humidity) and can possess efficient barrier properties below 65%.⁴⁷ While they don't possess great moisture barrier properties, using cellulose nanomaterials as an oxygen barrier for various food applications can help reduce the plastic usage currently used as oxygen barriers.⁴⁷ CNFs are also a binding agent in creating low-density foams from thermomechanical pulp (TMP).⁴⁸ The addition of CNF allows the material to create a foam-like structure upon mixing, and microwave radiation can be used afterward to dry the foam.⁴⁸ These foams can help alleviate the amount of waste generated by petroleum-based foams, and microwave radiation can significantly reduce time and energy costs. Finally, CNFs have even been used as a coating for wood particle-based food containers.⁴⁹ The coating of the wood particles with CNF proves to have excellent oil/grease resistivity, increased mechanical strength compared to commercial food

containers, and pulp and poly-fluoroalkyls (PFAs) free.⁴⁹ Therefore, these containers have the properties to be successful alternatives to single-use, non-biodegradable plastic food containers.

Current research has been conducted at the University of Maine, and extensive research has been conducted on using CNF as a high-density material. They found that when heat is applied to the 3% wt. CNF solution, the material orients itself into a rigid high-density material when completely dried. The drying temperature ranges from 50-80°C, with overall structural porosity increasing as the temperature increases. The lab utilized a designed fire brick mold with 5 gallons of CNF capacity.⁵⁰ Fire bricks were chosen because they can wick the free-standing water out of CNF with capillary forced action. The mold with CNF is then dried at varying temperatures in a Wisconsin industrial-sized oven.⁵⁰ Once fully dried, samples were cut to size for their intended application or testing.

Various mechanical tests were conducted on the produced CNF material, all according to specific standards of the American Society for Testing and Materials (ASTM). As CNF is a relatively new material, an ASTM standard has not been designed specifically for it. With that in mind, standards were chosen based on the most similar material type. ASTM D695-23: Standard Test Method for Compressive Properties of Rigid Plastics,⁵¹ was chosen for compressive testing. ASTM D790-17: Standard Test Methods for Flexural Properties of Unreinforced and Reinforced Plastics and Electrical Insulating Materials,⁵² was used for flexural testing. Finally, ASTM D638-22: Standard Test Method for Tensile Properties of Plastics,⁵³ was selected for tensile testing.

Each test has specific guidelines, including specimen size, direction, and displacement rate. The heat drying method of CNF creates an anisotropic orientation of fibers, meaning that the fibers are not oriented in a specific direction or pattern. For compression testing, this means that the

material needs to be tested in 3 directions based on the drying method. Below is a diagram depicting this test's cutting methods and directions.

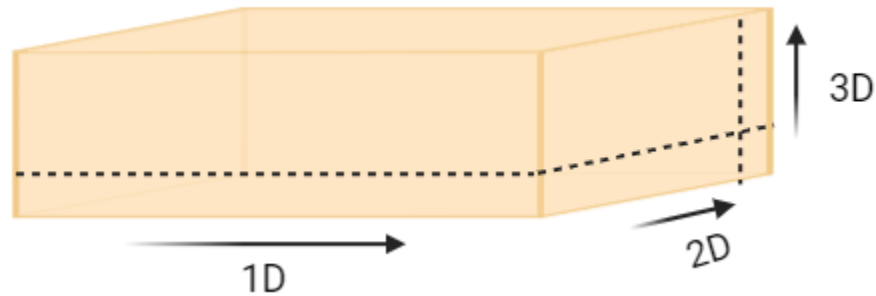


Figure 2.4: Original cutting directionality of CNF molds.⁵⁴

The arrows depict the direction in which each sample is cut along the mold. 1D samples are cut along the length of the mold, 2D along the height, and 3D along the width of the mold. For compression, CNF performed at 120MPa in the 1D, 130MPa in the 2D, and 220MPa in the 3D.⁵⁴ Based on the data, cutting the samples along the vertical direction was the most successful. For tensile testing, 1D showed a tensile strength of 43.69MPa, 2D had 28.43MPa, and 3D had 7.17MPa.⁵⁴ These results are opposite to the compression testing values, displaying weaker values in the 3D rather than in the other two directions. Finally, the flexural strength results were also opposite to the tensile results, with 1D having a flexural strength of 7.33MPa, 2D having 70.28MPa, and 3D having 104.64MPa.⁵⁴ All these values show that the CNF composite material can have relatively high mechanical strength, but it is highly dependent on the directionality of the sample and the type of testing conducted.

Due to its potential use in biomedical orthopedic applications, the biocompatibility, or cytotoxicity, has been tested. The main standard for testing this material was ISO-10993-5, the “Biological Evaluation of Medical Devices, Part 5: Tests for *in vitro* Cytotoxicity.” Due to the potential use as an orthopedic within the body, MC3T3 (mice pre-osteoblast cells) were selected

for testing. The cell viability of this cell line was found using an MTT method, and the viability was found to be 83.69%.⁵⁴ Also, the optical density (OD) average for the CNF material was 0.302. This value was a 70% reduction in viability compared to the blank control, meaning it is a nontoxic material.⁵⁴ While these results were nontoxic, some concerns arose during the MTT testing. The tested material wasn't permanently fixtured within the 6-well plate used, meaning there was high cell placement or viability variability.⁵⁴ Therefore, to better understand the material, the author suggested a new method or test before the results were conclusive.

CNF has many promising properties that could help alleviate the drawbacks of current materials. One specific application is in orthopedics. Current materials, like stainless steel, have a modulus of elasticity much higher than the surrounding bone, which can lead to stress shielding.⁵⁵ These implants cause the surrounding bone of the material to become weaker due to the increased stiffness of the metal. This can cause pain and may lead to revision surgery. Another newer material that can potentially be an alternative to metal orthopedics is a plastic called polyether ether ketone (PEEK).⁵⁵ This material has similar mechanical properties to titanium, is bio-inert, and can successfully be imaged with CT or MRI technologies.⁵⁵ However, these materials are difficult to manufacture and have poor osseointegration properties. CNF has properties similar to that of PEEK. However, CNF is composed of natural materials instead of fossil-fuel-derived methods. Previous studies have shown that CNF is also bio-inert, has a porous structure beneficial to osseointegration, and has properties similar to bone. With further research findings, CNF could become a natural alternative to PEEK and, with specific biological enhancers, can be an optimal orthopedic device alternative.

Another area for potential applications of CNFs in the medical field is the application of single-use devices. Current single-use devices, as mentioned above, are made of non-

biodegradable plastics. Adopting these plastics has generated enormous amounts of waste that require lengthy degradation times. High-density thermoset plastics, for example, possess higher mechanical strengths than thermoplastics, but most cannot naturally biodegrade. These high-density plastics are also derived from fossil fuels, a non-renewable material that contributes to greenhouse gases. CNF, on the other hand, is a material naturally derived from plants or trees yet still possesses high mechanical properties like some current thermosets. Furthermore, as these materials derive from naturally sourced cellulose derivatives, they have the potential to biodegrade naturally in a much shorter period than current alternatives. With the enhancement of specific mechanical properties for target applications, CNF materials could be a potential alternative to current single-use medical plastics.

2.7. Unknowns

Table 2.5: Unknown properties of CNF.

Property	Significance	Limitations	Solutions
Hydrophilicity	Needs to be controlled due to foreign body response in orthopedics	Water reuptake of dry material causes swelling and reduced mechanical strength	Crosslinking to reduce the breakage of hydrogen bonding
Internal strain	Material must be easily manufactured, uniform, and controllable	Current material possesses strains that cause curling of the molded material.	Implement a mechanical strategy called annealing to reduce strain.
Bioavailability	The material must be able to allow cell proliferation and differentiation to mimic human bone	Current CNF material is non-toxic. Cells live but don't expand or change.	Introduce materials that improve cell expansion or differentiation

Three current unknown property limitations of CNF must be resolved before CNF can be considered a suitable alternative to current medical device alternatives. The first is controlling the overall hydrophilicity of the material. Currently, adding water to CNF causes the material to uptake the water, causing the material to swell, which reduces the material's overall strength. If this material were to enter the body, the amount of swelling would need to be controlled, as the body undergoes a foreign body response by adding a new material. Furthermore, the body must respond to adding a foreign object safely and effectively. Currently, *in vitro* testing of CNF shows that osteoblast cells don't recognize CNF material as toxic. However, to further enhance CNF as a potential orthopedic alternative, the cell viability must be increased to allow cells to react normally. Ideally, this implant would act as a perfect replacement for bone. This means cell function within the implant would behave similarly to its interactions with bone. Finally, the internal strain of the material is a current limitation that must be resolved. When manufactured, the intense fiber alignment causes significant bending of CNF material. The internal strain of the material causes this bending. The bending imposes a potential setback for a future manufacturing process. Ideally, the material would be uniform, without bending, allowing for a permanently set material.

There are potential solutions that could alleviate some of these setbacks. First, the overall hydrophilicity of CNF could be reduced using a crosslinking agent. One study found that the overall hydrophobicity throughout the material increased when crosslinking starch nanocrystals.⁵⁶ While the properties and starch are not the same, crosslinking is a potential solution that could alleviate the overall hydrophilicity of CNF. Research has shown that some potential crosslinking agents are polyamide-epichlorohydrin (polycup), urea, and strontium chloride.⁵⁷⁻⁵⁹ Next, biological enhancers can help CNF become a more viable material. Hydroxyapatite (HA) and Bioglass are two materials that could have been previously found to increase the cell proliferation

and differentiation of materials.⁶⁰ HA is especially common as it is the natural mineral found in bone. Bioglass also possesses specific mineral content that allows osteoblast cells to differentiate and proliferate successfully.⁶⁰ Finally, a manufacturing process common in the manufacturing of metals is called annealing. This process generally uses heat as its main variation to aid in reducing the overall stresses of a material.⁶¹ To reduce the overall strain of CNF, this method could be adapted. The main component in CNF manufacturing is dewatering the material with heat. Therefore, as it is difficult for CNF to reach high temperatures, an annealing experiment could be designed using a wetting/drying process to alleviate the overall internal strains of the material. CNF, as a whole, is a promising material for its use in potential medical applications, but before its introduction into the field, these limitations must be answered.

CHAPTER 3: CROSSLINKING OF CELLULOSE NANOFIBRIL COMPOSITES

3.1: Introduction

In Chapter 2, extensive research was done on the current state of plastic usage and waste worldwide, some of the alternatives being produced to combat plastic production, and how CNF can be a viable alternative. In the upcoming chapter, various cross-linking strategies will be explored to try to reduce the overall hydrophilicity of CNF, which will help control the overall behavior of the material.

CNF has specific properties that allow it to be chemically versatile. It is hydrophilic, possesses high mechanical strength, and has moderate porosity in bulk. However, a solution needs to be found to improve the effectiveness of the material further, especially regarding hydrophilicity. Chemical crosslinking is a method that could help alleviate some of these property drawbacks. For example, when crosslinking within the molecule is increased, the pore sizes will decrease in individual volume, but the total volume of pores throughout the sample will increase.⁶² Polymer microbeads that are chemically crosslinked can provide an example of the potential benefits of this method. When these microbeads undergo crosslinking, their mechanical strength, stiffness, insolubility, and rigidity improve.⁶² While these methods are used specifically for microbeads, their effects are a profound example of how chemical crosslinking can enhance a material's properties.

Research has also been executed on the crosslinking of naturally occurring polymers. Chitosan, derived from chitin, is an example of a naturally occurring polymer utilized for its biocompatibility, biodegradability, and large supply.⁶³ Epichlorohydrin (ECH) is a crosslinking agent that was researched to help show how the properties of chitosan are affected when crosslinked. They showed that the strength of the chitosan fiber improved, the wet tenacity

improved, and when crosslinked in a wet state, the strength of the fibers was not degraded.⁶³ These property enhancements have the potential to significantly impact the potential applications of CNF.

Sharma, et. Al. analyzed the wet strength of CNF when crosslinked with polyamide-epichlorohydrin (PAE). The researchers found that when CNF was crosslinked with PAE, the overall wet strength was enhanced, but the biodegradability and recyclability were inhibitory.⁵⁹ They found that only the smallest amounts of PAE must be used as a crosslinker. This maximizes the effectiveness of the crosslinking while also keeping it biodegradable and safe.⁵⁹ These two characteristics are important in this case because they could be a biodegradable alternative to plastic and an orthopedic device.

It is also important to be aware of the degradation properties of polymers. When water is introduced, some specific polymers can degrade mechanically and chemically due to swelling in plasticization.⁶⁴ Water molecules can insert themselves into the polymer chain, causing the material to swell. This process can lead to the plasticization of the material and produce weaker mechanical strengths.⁶⁴ However, these studies were only tested on polymers alone, not crosslinking. While the chemical properties of these materials need to be evaluated independently, there could be a significant difference in properties after a crosslinking action.

It is important to understand the chemistry of crosslinked films made with CNF and PAE, or commercially as Polycup™, as well as bulk CNF with polycup when determining which method to test. When polymers are reacted with other materials, the polymer's entanglement is reduced near the surface.⁶⁵ The polymer's confinement and subsequent organization of the material cause the material to increase the number of possible cross-linking sites throughout the material. Below is a diagram showing the mechanism of crosslinking polycup with CNF.

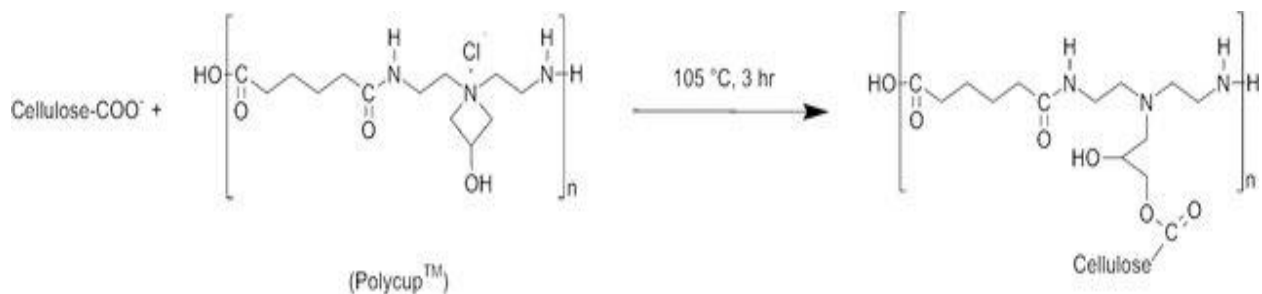


Figure 3.1: Crosslinking action of polycup and CNF.

Before this aspect of the project, several films were crosslinked with CNF to help determine the best temperature and percent of Polycup to use. The optimum crosslinking temperature is 70°C, and the best results were shown between 1.5-2.5% wt. polycup. 70°C was determined due to higher temperatures showing degradation of thin films during drying. Also, a previous study showed that between 1.5-2.5% showed the lowest water gain over time for thin film samples.⁵⁴ Therefore, for this experiment, the properties of CNF/polycup films were analyzed to help determine the overall effect of crosslinking on the composites.

3.2: Polycup

3.2.1: Bulk CNF Production

To start this experiment, bulk CNF scaffolds needed to be produced. 5 gallons of 3% wt. CNF was obtained at the process development center (PDC) at the University of Maine. This type of CNF contained 90% fines, meaning 90% of the fibers had a length of less than 200 microns. The CNF was mixed using a Hobart H600 mixer with a 60L bowl attachment at the Technology Research Center (TRC), located in Old Town, Maine. The Polycup was then added to the CNF in the mixer. A 1-foot diameter whisk was used to mix the solution at 124rpm for 5 minutes. After mixing, the solution was placed in a patented drying fixture, utilizing a capillary dewatering technique using porous fire bricks. The sample was dried at room temperature for 24 hours to allow for the removal of unbounded water. After about 24 hours, the top 6 bricks were removed, and

two bricks were placed on top of the CNF mixture to act as a downward force against the vertical internal strain during drying. The mold was then placed into a Wisconsin industrial-sized oven at 157°F (70°C). After 6 days of constant drying, the scaffold was completely dry. Repeated this process for 0% polycup, 2.00% polycup, 2.25% polycup, and 2.50% polycup.

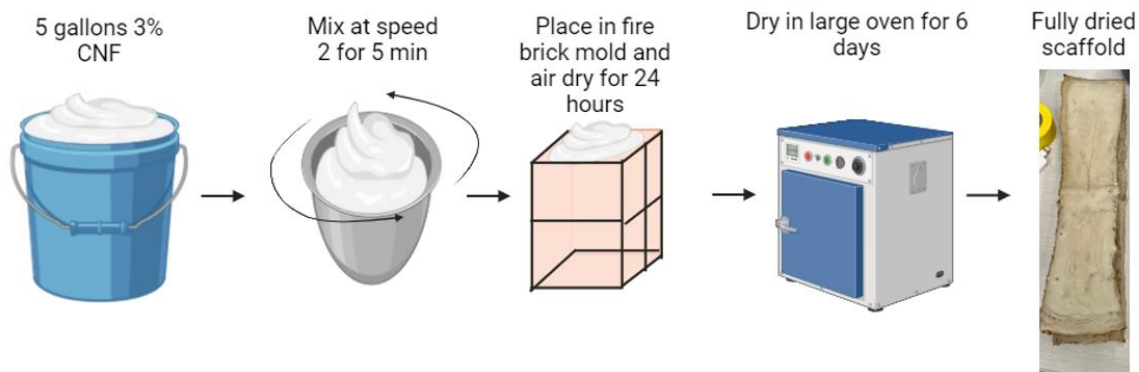


Figure 3.2: Bulk CNF production schematic.

Once removed from the oven, the scaffold was analyzed to determine if it was dried entirely. After drying, the scaffold had edges that weren't entirely uniform. A circular saw was used to make a rectangular prism with even height and width to resolve the uneven edges. Lengths were dependent on the extent of the uniformness of the mold. They were then cut vertically lengthwise along the prism with a circular saw at a thickness between 2-3mm. This thickness was chosen due to the overall pore sizes of the samples and the amount of material available. If the material were made thinner than this, the size of the pores would create weak spots during testing, which would skew the results. Also, a larger thickness would use more material than is currently available. The remaining slabs were cut widthwise at around 63.5mm per piece with the same circular saw. Then, to produce the final American Society for Testing and



Figure 3.3: Cross-section of a macroporous CNF sample.

Materials (ASTM) D638-22 dog-bone Type V shape, used a circular cutting bit in a custom jig to make the middle section of the dog-bone have a width of around 3.5-4mm shown in Figure 3.3. Once the molds were cut, they were placed into a large Ziploc bag. Desiccant packets were inserted with the specimens to remove excess moisture.

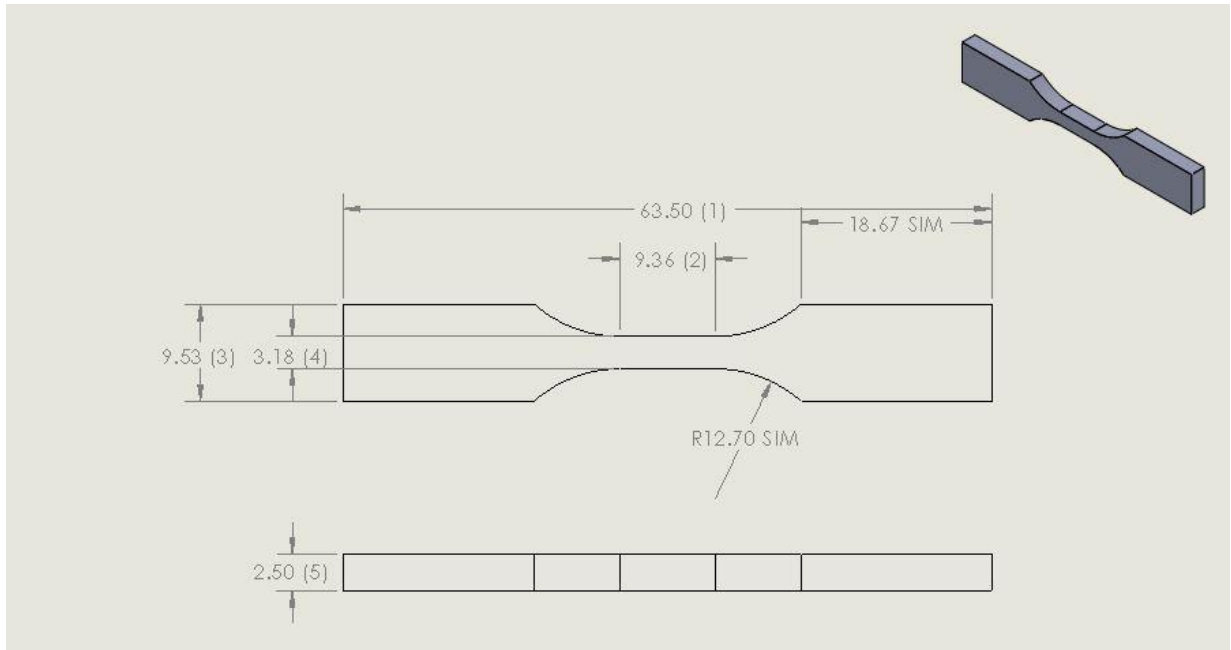


Figure 3.4: Schematic of Type V tensile testing sample, with dimensions from ASTM standard D638-22.

For flexural testing, the scaffolds were again cut vertically lengthwise along the scaffold into 4-5mm thick strips with a band saw. The samples were cut according to the dimensions outlined in the ASTM D790-17 standard. The dimensions of the rectangular samples were 20mm x 100mm. Once the samples were properly cut to size, they were placed in a Ziploc bag with a desiccant packet to ensure the material remained dry during storage. Below is a sketch depicting the dimensions of the sample.

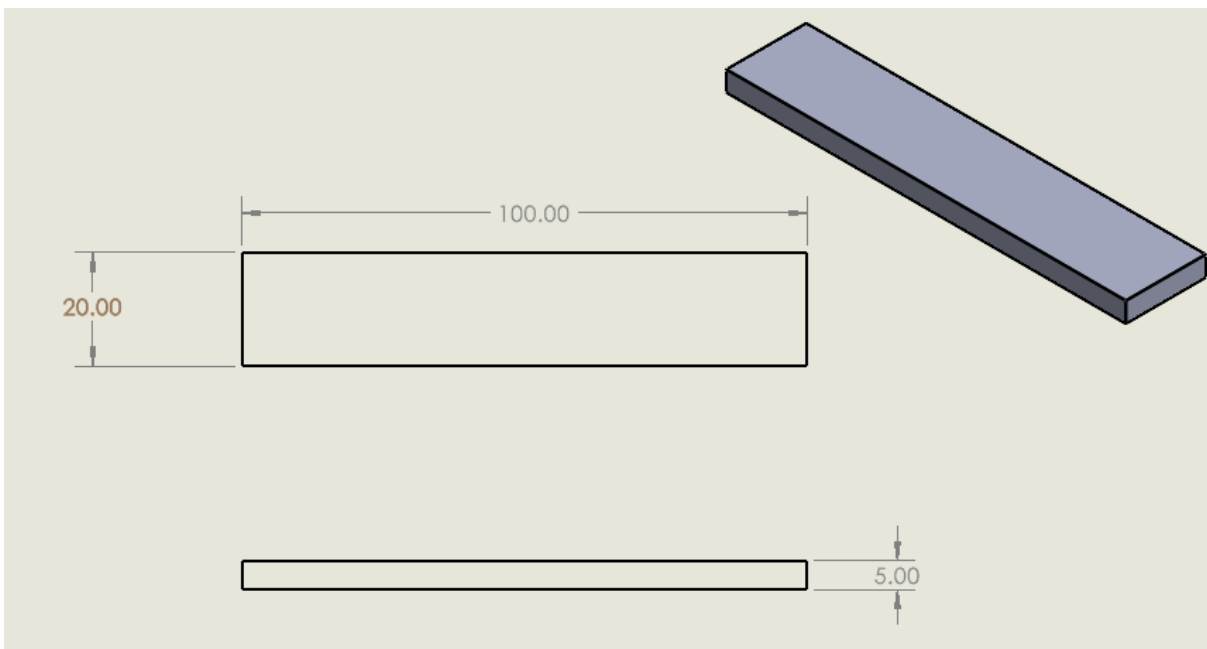


Figure 3.5: Schematic of flexural testing sample with dimensions from ASTM standard D790-17.

A primary goal of the cross-linking strategy was to try to reduce the overall water absorption of CNF. An experiment was designed to test the overall water absorption of the tensile testing samples at different time points and examine how water reuptake affects the material's mechanical properties. First, the mass of CNF samples was measured when they were completely dry. Measurements of the total length (1), length of mid-section (2), total width (3), narrow width (4), and thickness (5) of each piece were taken, as shown in Figure 8 and placed pieces of CNF into a 450mL of water at 37°C at varying periods: 30, 1 minute, 5 minutes, 10 min, 15 min, 30 min, 45 min, 60 min, 2 hours, 3 hours, 4 hours, 5 hours, and 6 hours. Each time point tested three tensile samples to ensure proper statistical data could be calculated. The mass of each sample was taken after the allotted time, and then a tensile test was performed following ASTM standard D638-22. Below is a diagram depicting the procedure for the water absorption testing.

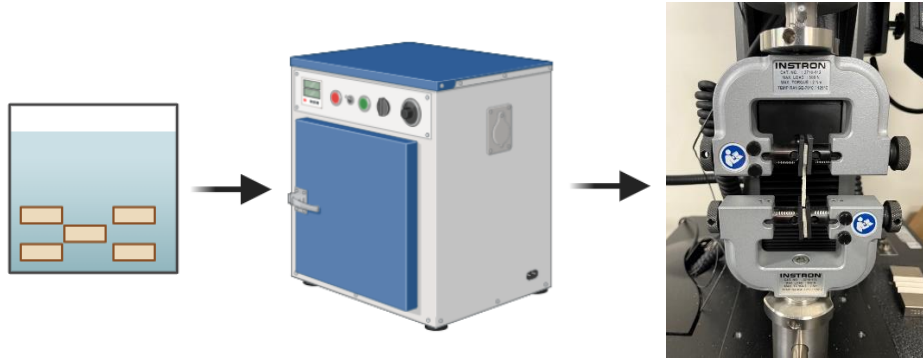


Figure 3.6: Water soaking in Fisher Scientific Oven (left) for absorption and tensile tests using Instron model 5942 (right).

The equation below calculated the samples' water absorption using mass. The mass was taken when the material was completely dry, and the final mass was taken after soaking for a specific time. The samples were also dried with a paper towel immediately following soaking to remove excess water that would affect the results.

Equation 1: Water absorption of samples.

$$\text{water absorption (\%)} = \left(\frac{m_a - m_b}{m_b} \right) * 100$$

m_a = mass after water absorption

m_b = mass before water absorption

3.2.2. Results

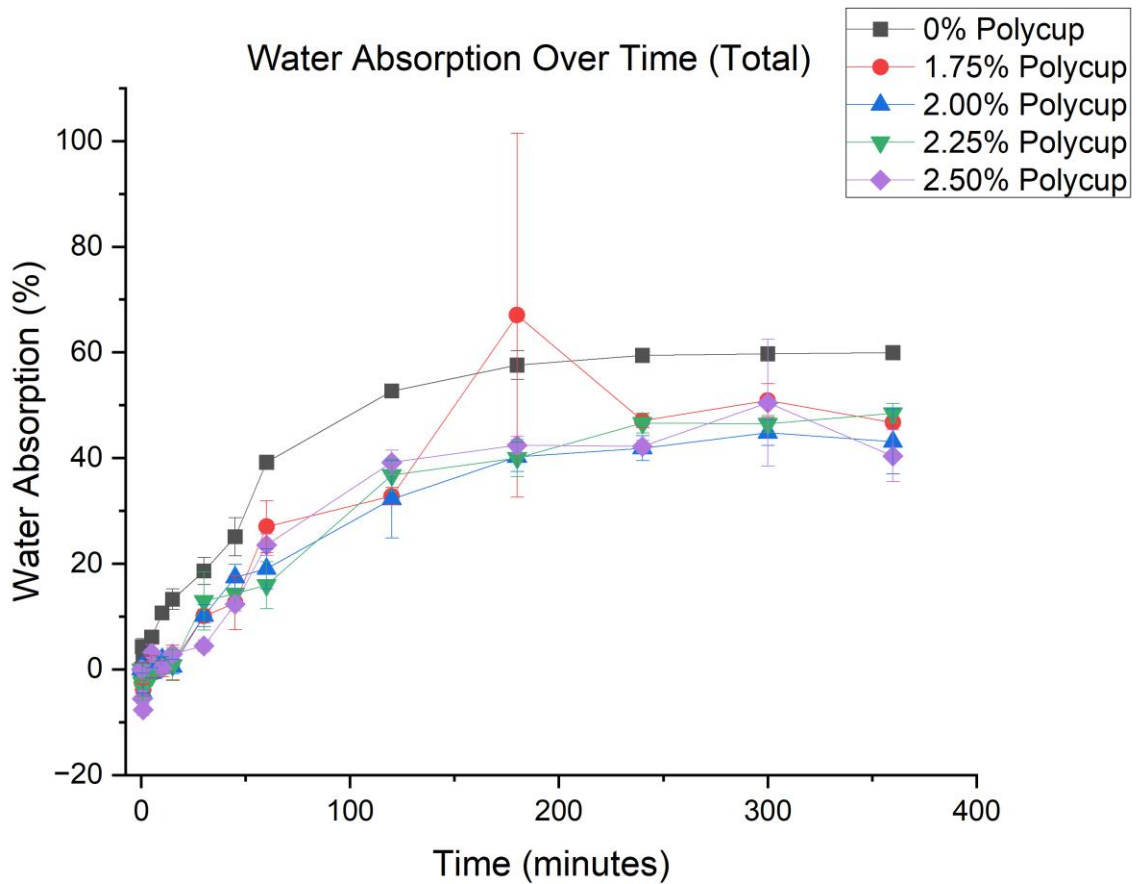


Figure 3.7: Water absorption rate over all time points for each polycup % by wt.

This graph exemplifies a common trend throughout all the samples. There was a sharp increase in water absorption rates between 30-180 minutes, which remained relatively the same for the last 180 minutes. The samples reached a threshold of water absorption where they didn't uptake any more water once that threshold was reached. In most of the data, the polycup samples remained relatively precise, with no major differences between samples. However, these examples had less water absorption than that of pure CNF. Throughout the entire length of water absorption, the pure CNF showed an increased absorption rate compared to all the polycup samples. This

proves that polycup produced a lower water absorption rate than pure CNF over 6 hours. A second graph was produced from minutes 0-60 to analyze the first hour more clearly.

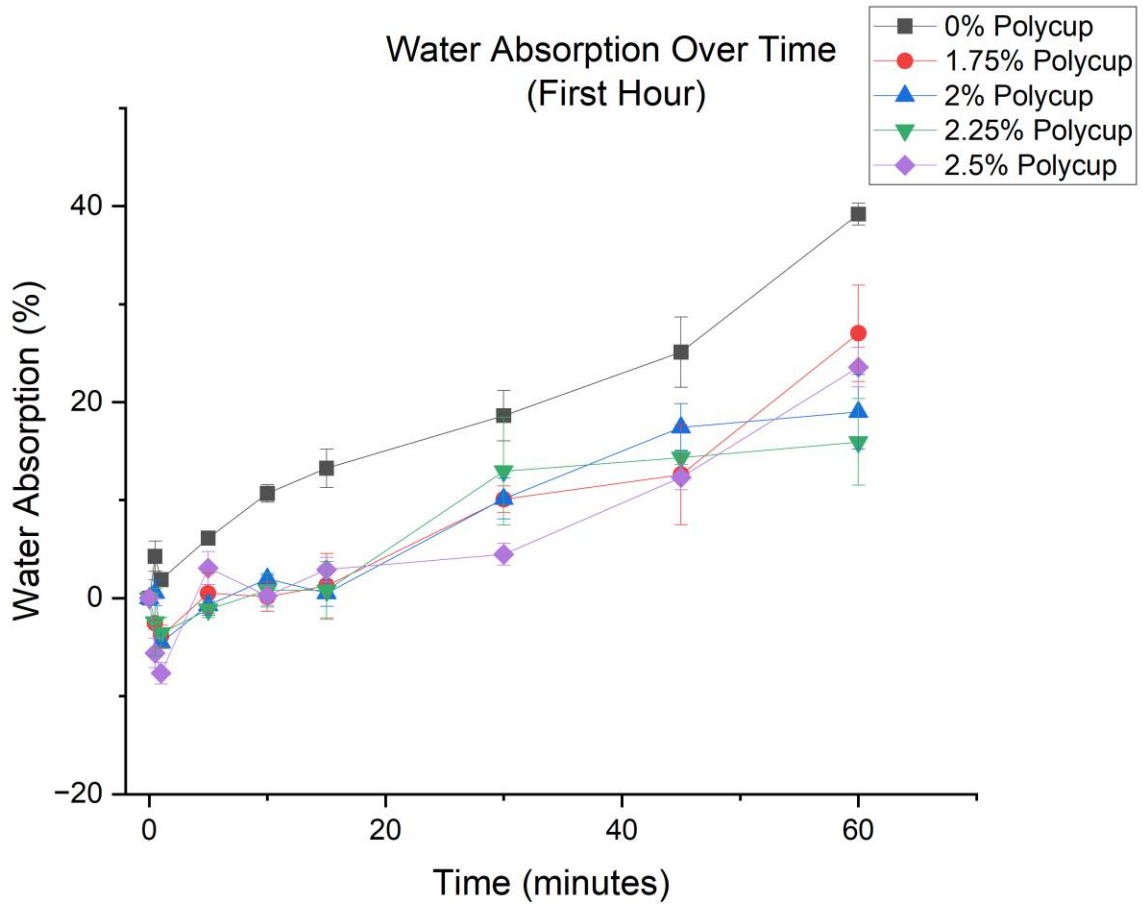


Figure 3.8: Water absorption of CNF samples with varying amounts of polycup over 1 hour.

Unexpected results were shown within the first 15 minutes. The samples tended to have a negative water absorption rate, meaning they lost mass within the first 15 minutes. A possible reason for this could be that the weaker, thinner parts of the dog bones were most likely absorbed and broken off before the sample was weighed. The method of patting the samples to remove excess water could have also contributed to the samples' mass loss. It is possible that some of the thinner residue left on the films was accidentally removed during this process. To resolve this, the

samples could be polished beforehand, or the cutting method could be revised to ensure no loose material was obtained. The lines slope sharply after the 15-minute mark for the rest of the first hour. This is the area with the highest increase in water absorption rate. After the 15-minute mark, the material appears to begin to absorb water. Further research needs to be done to determine why this is happening and what can potentially be done to prolong this change in water absorption. However, as shown in Figure 3.8, the Polycup appears to absorb less water over time, but the mass loss error needs to be resolved before conclusions can be made.

The expected results of the mechanical testing were that when compared to pure CNF, the polycup materials would mechanically degrade slower as water absorption time increased. The prediction was that as time went on, the CNF samples with polycup would absorb less water than CNF alone, which would directly correlate to its stronger mechanical properties over absorption time. As water is absorbed into the dog bones, the fibrils within the samples begin to swell, break apart, and absorb water. These factors directly influence a loss of mechanical strength when tensile testing is conducted. To determine the mechanical strength of these samples, an Instron 5942 machine was used. This machine was programmed to measure each trial's stress, strain, and Young's modulus. The input values were the thickness and the thin width of the sample. Two important variables in mechanical testing are mechanical strength and Young's modulus. As the Instron calculated these values for each sample, the overall triplicate for each time point was averaged, and the standard deviation was calculated. The values for the mechanical strength were then graphed below.

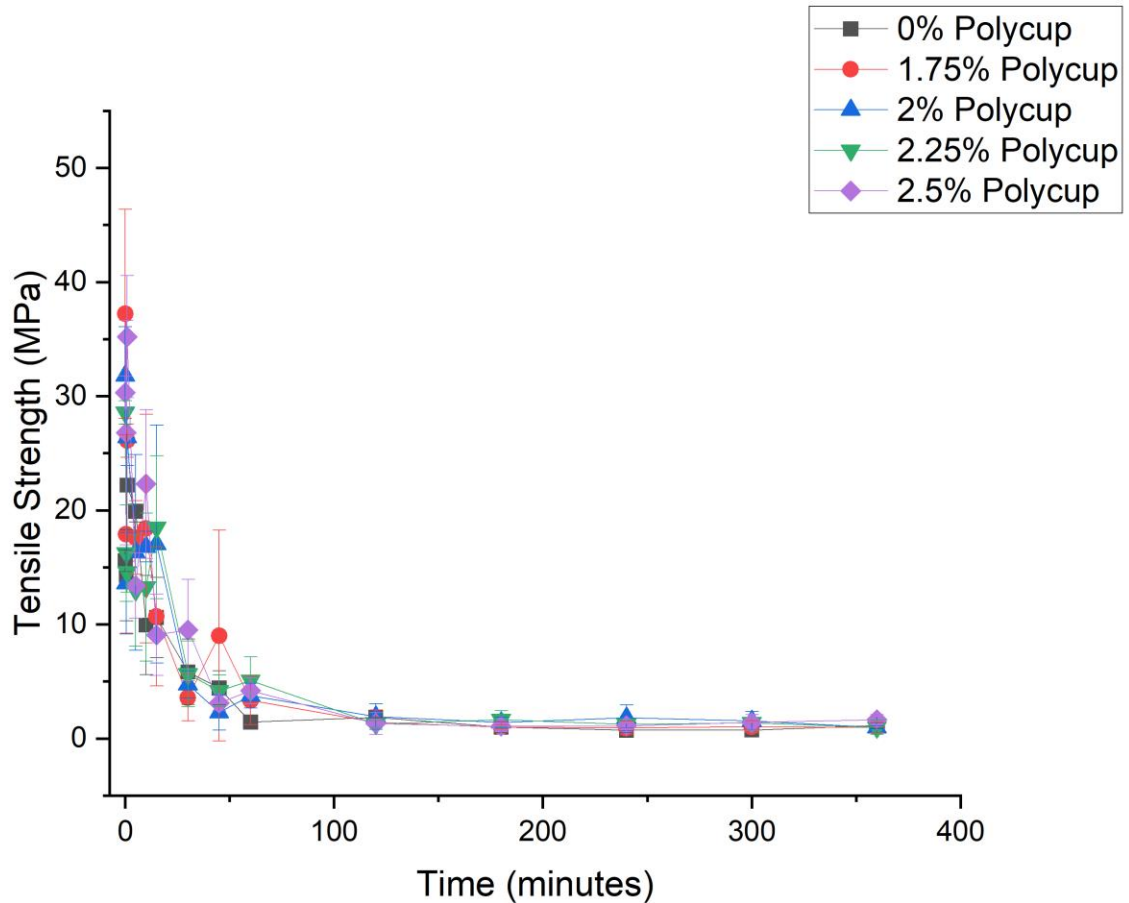


Figure 3.9: Tensile strength of bulk CNF with polycup over total water absorption time.

There is a common trend among all the samples. At the beginning of the water absorption, the dog bones exemplified relatively high tensile stress, yet throughout the first hour, they decreased significantly. Between 120-360 minutes, each material plateaued at the same stress amount. A threshold was reached at around the 120-minute mark, and after that point, the tensile stress remained relatively constant. While there are some common trends in this data, there doesn't appear to be a difference between the samples with and without Polycup. Next, the first 60 minutes of the testing are shown below to give a better view of the properties that occurred then.

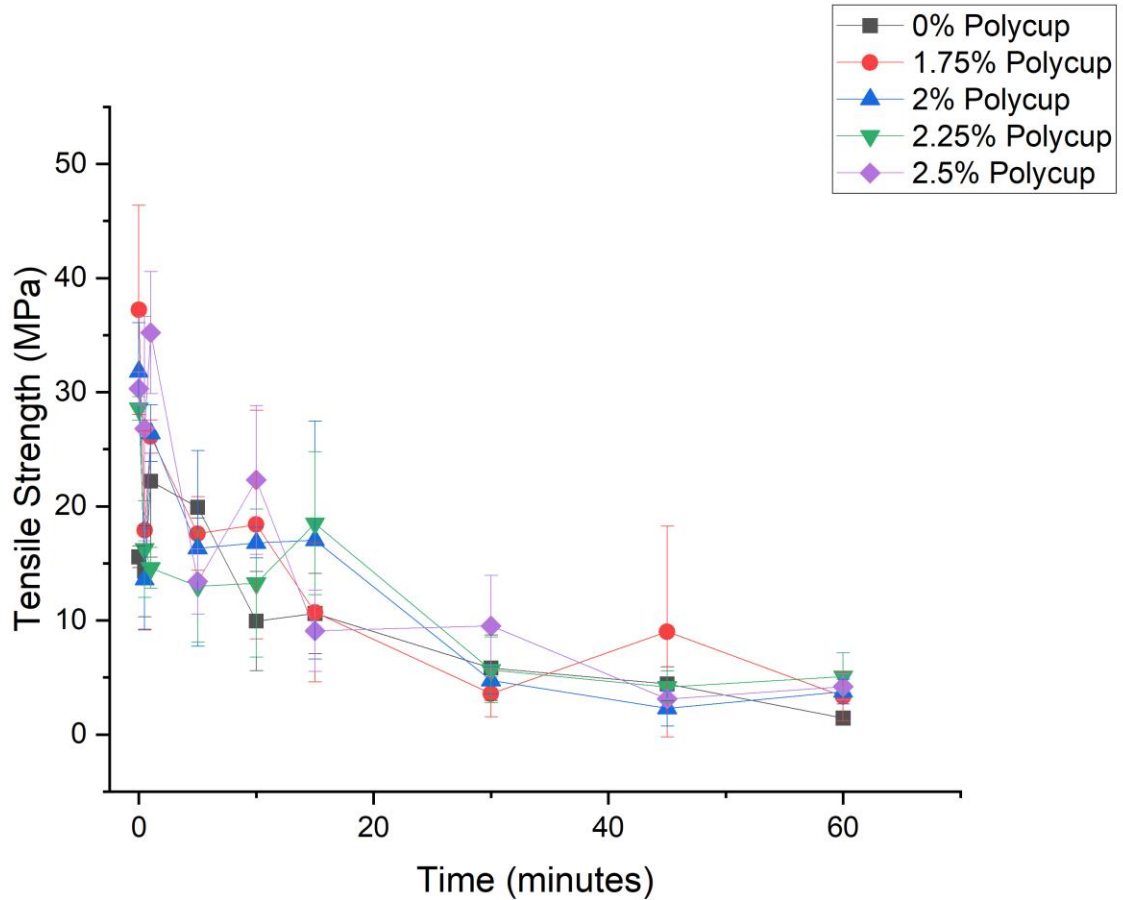


Figure 3.10: Tensile strength of bulk CNF with polycup over the first hour of water absorption time.

Overall, there isn't a large difference in change in stress over time of water absorption. All the trials tend to follow a similar trend, with a steep decline within the first 5 minutes of testing and another between 15-30 minutes. This is most likely explained by the initial effect of water upon the samples and a major change in mechanical strength sometime between 15-30 minutes. Also, these values are relatively low for the thickness of the CNF that is being tested. Rather than having a max strength value between 20-30 MPa, generally, it should be around 40-50 MPa. A cause of this is most likely due to the pore size compared to the thickness of the films. Before testing this material, it was expected that a thickness of 2-3mm would be an optimum size for

tensile testing. However, once the films were cut, it was observed that the pores were large in comparison to the size of the material. To minimize the effect of porosity on tensile strength, the thickness should be increased to 5-7mm, and the shape of the dog bone should be Type I, based on the ASTM standards. This would hopefully increase the mechanical strength and exemplify a better pore size ratio to sample thickness.

The expected results for Young's modulus calculations were very similar to that of the mechanical strength testing. It was expected that there would be high modulus during the first part of the water absorption testing, and then over time, it would most likely decrease. It was also expected that the pure CNF would show a faster decrease in modulus compared to the samples with amounts of polycup. The same procedure for calculating the average and standard deviation of the calculated values from the Instron is used below.

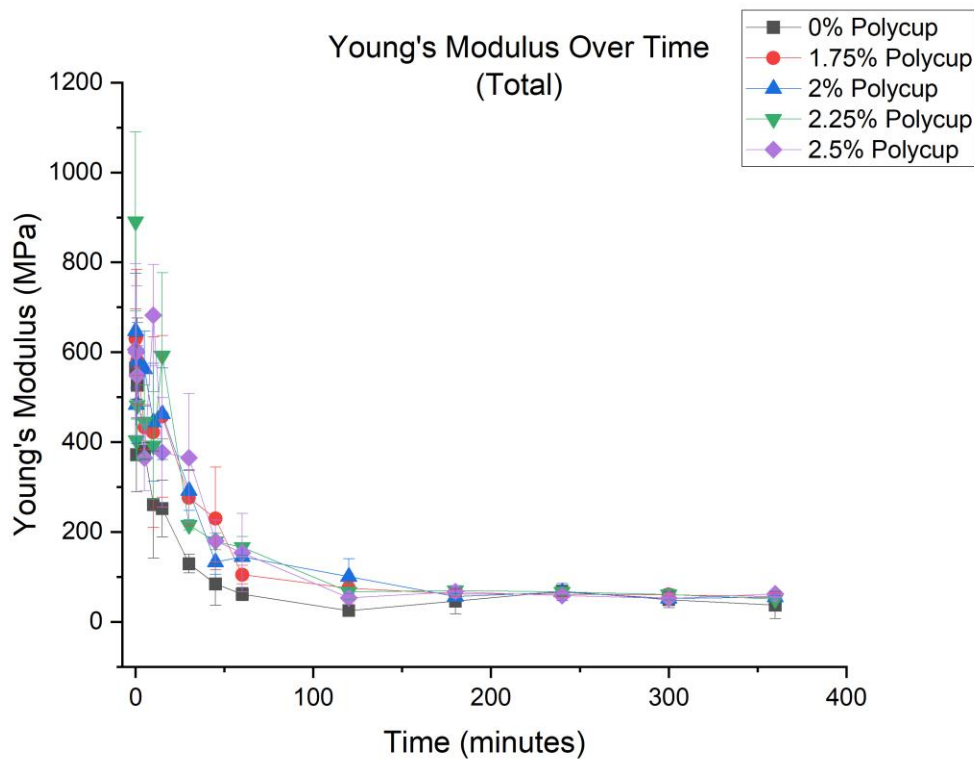


Figure 3.11: Young's Modulus of bulk CNF with polycup over total water absorption time.

From Figure 3.11, a negative trendline can be viewed. Initially, the values for Young's modulus were high, yet within the first hour, the values decreased drastically. After 120 minutes, however, the values, similarly to the tensile stress, began to plateau. Mostly, within the first 180 minutes, the polycup values were relatively similar, while the pure CNF obtained lower values than the rest. This exemplifies how the polycup is effectively reacting with the CNF to help produce a less hydrophilic product that is more resistance to mechanical degradation during the first 30 minutes. The graph was created below to better understand the effects during the first hour.

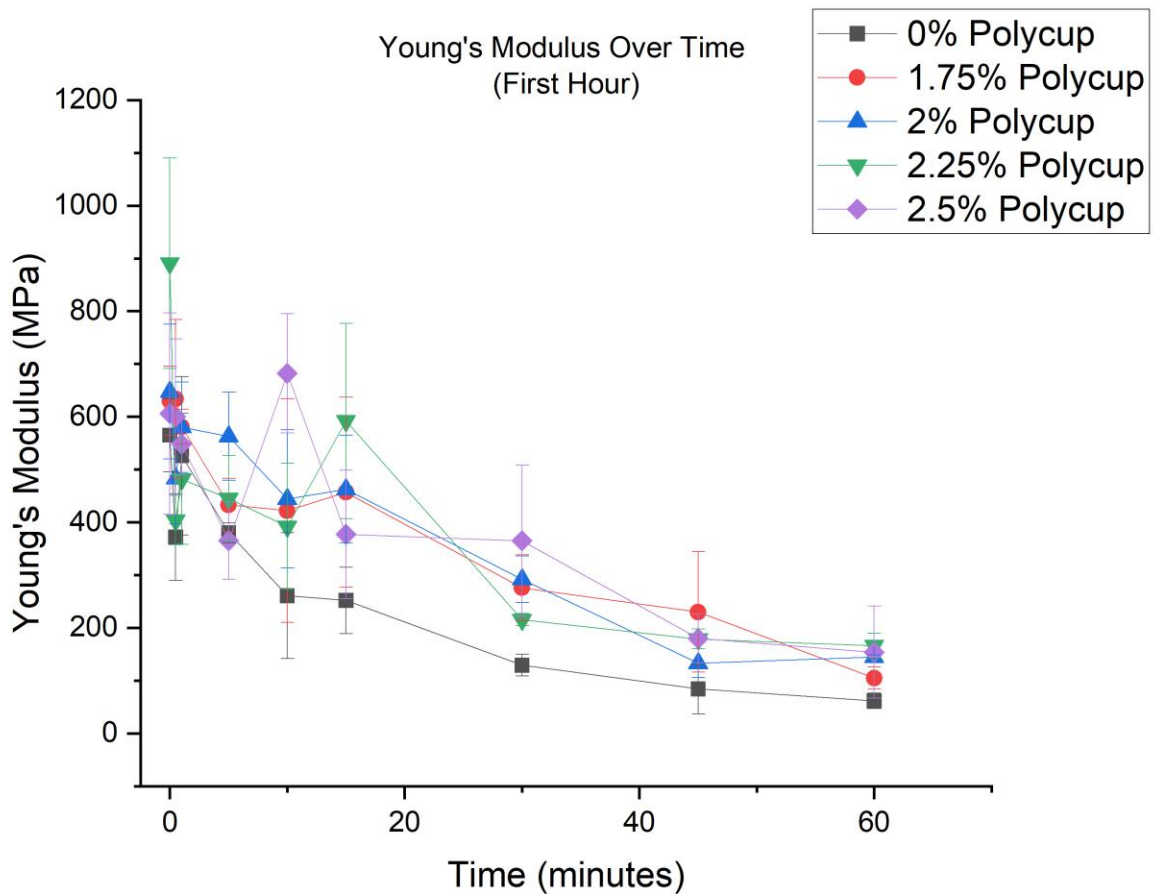


Figure 3.12: Young's modulus of bulk CNF with polycup over first hour of water absorption.

In Figure 3.12, it is shown that pure CNF decreases its Young's modulus values faster than that of the CNF materials with polycup in them. From about 5 minutes to an hour, it is shown that

it has a weaker Young's modulus when compared to the rest. However, it exemplifies the same trend. It has a decrease within the entire first hour, yet between 15-30 minutes, there is a larger decrease than the rest. Overall, throughout this mechanical strength data, it can be shown that the highest effect of hydrophobicity is shown within the first 15 minutes of water absorption. Then between 15-30 minutes, there is a sharp decrease in mechanical strength. This sharp decrease indicates that a large amount of water absorption occurs, negatively influencing the samples' mechanical strength. Finally, the overall modulus was lower than expected. Initially, the values were expected to be at least 1000 MPa, yet none of these values reached that amount. Again, the most likely explanation for this low value is the relative pore size in comparison to the thickness of the sample. Next time, a larger thickness will be used, which will require a larger Instron machine. It will also require a Type I ASTM tensile test. This new type of dog bone should create a more accurate representation of the mechanical strengths and the effects of water absorption based on polycup percentage.

In the next set of experiments, flexural samples were tested based on varying environmental saturation conditions rather than water-soaking times. From the data shown in the tensile testing trials, water fully saturates the material within a relatively short period. In this trial, flexural testing was done on the material at dry conditions, with equilibrium moisture content (EMC), and fully saturated. The dry condition entailed placing the samples in a dehydrator for 24 hours, then immediately placing them in a Ziploc with a desiccant packet to ensure no moisture uptake of the sample. To produce the EMC value, the samples were placed in an environmental chamber at 50% humidity for 24 hours. Finally, the samples were soaked in water for a period of 24 hours to represent full saturation. The samples also contained 0, 1, 2.5, 5, and 7.5% wt. polycup.

The samples were tested on an Instron model 5942 using 3-point bend testing attachments. The samples were tested in accordance to ASTM standard D790-17.



Figure 3.13: Flexural testing setup with 3-point bending attachment on an Instron model 5942.

The span width for the tests was 80mm apart, as shown above. The top attachment was forced down upon the material at a rate of 2mm/min. The program Blue Hill Universal was used to create stress/strain curves, measure force applied and displacement of material, and calculate mechanical properties. The materials were tested until failure.

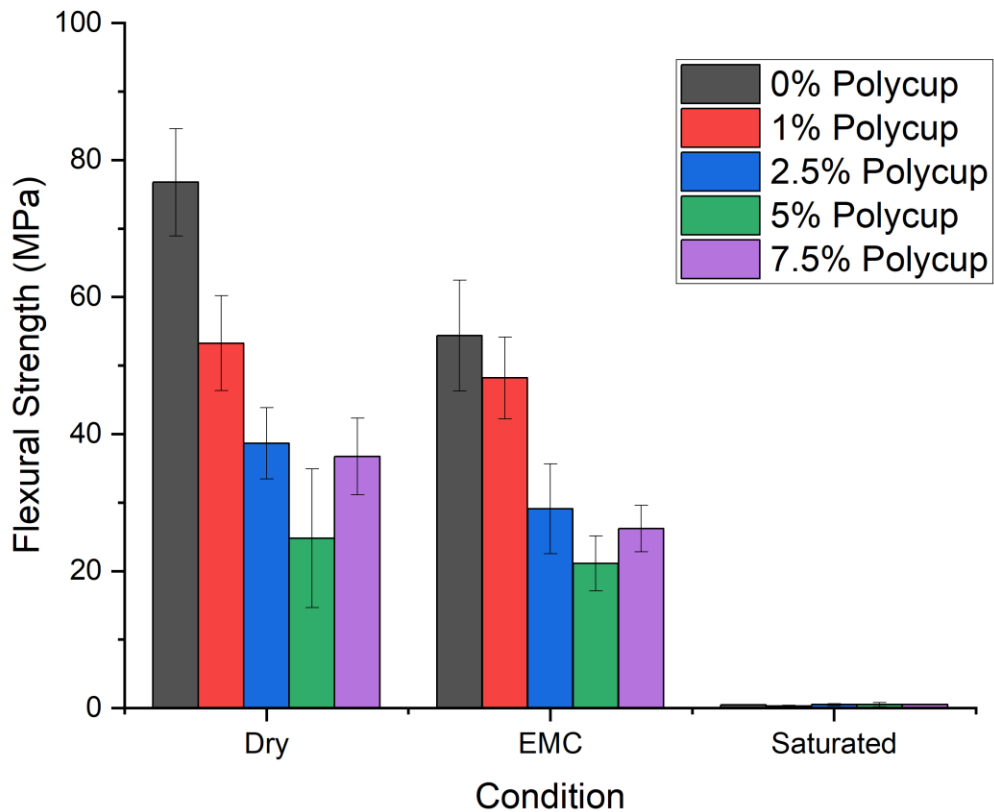


Figure 3.14: Flexural strength of CNF scaffolds with polycup across various saturation conditions.

When testing the flexural strength of these samples, it is prevalent that environmental conditions impact the strength of the material. Within most of the samples, increasing the saturation content of the material showed a negative impact on flexural strength. This can be seen especially when looking at the samples soaked in water for 24 hours. Those samples displayed a significant decrease in flexural strength values. When dried, the fibers create an interlocked network in which the material bonds to itself and creates an anisotropic structure. However, when water is introduced into the material, these bonds are interrupted, which causes the material to swell. These interruptions weaken the material, as shown in the figure above. Polycup was used to attempt to prevent the disruption of these bonds through crosslinking. However, introducing this

material proved to decrease the overall flexural strength of CNF. Polycup samples proved to have a decreased flexural strength value compared to the pure CNF sample.

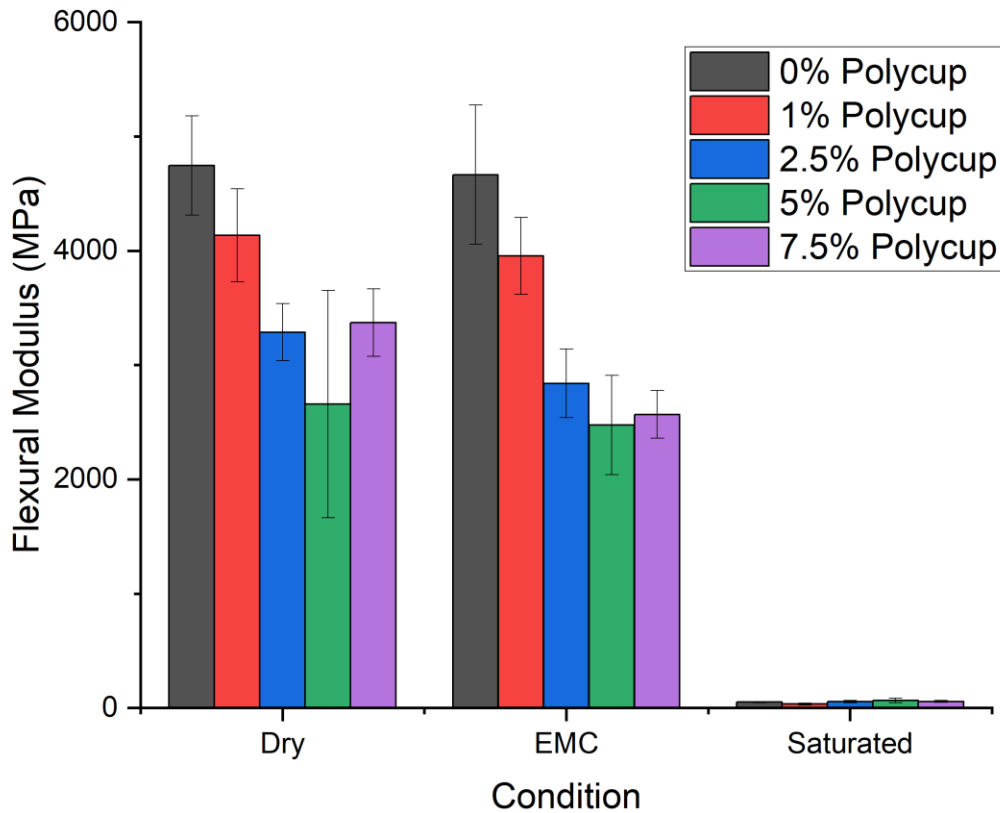


Figure 3.15: Flexural modulus of CNF scaffolds with polycup across various saturation conditions.

The flexural modulus was also examined for each material set. The results from this test can help determine a material's overall stiffness or elasticity. The stiffer a material is, the higher the modulus value will be. A lower modulus value means the tested material is more compliant and has a low stiffness value. Here, there is a similar trend to the flexural strength in which both the amount of polycup and the saturation negatively impact the modulus of CNF. For most

samples, the modulus value was decreased when polycup was introduced. This phenomenon can again be caused by the increasing porosity in the samples with polycup. Also, adding polycup did not increase the modulus of CNF when water was introduced. The modulus values decreased from an EMC environment, and then substantially decreased after fully saturating for 24 hours. Finally, adding Polycup displayed similar trends between the thin films and the bulk material. There was a negative effect in the mechanical strength values across both sample sets, but the water content still affected the material. While polycup was a promising material for its potential crosslinking properties, the drawbacks are too substantial to move forward with this product.

3.3: Urea

3.3.1: Thin Film Production

Before a material additive can be considered for long-term use within CNF, it is important to ensure the material properties are suitable for their intended purpose. To reduce material cost and time, thin films of CNF composites can be produced. These films typically have a thickness between 0.1-0.4mm. Rather than using around 5 gallons of CNF, with a week-long drying period, thin films utilize only 200g of CNF with a 48-hour drying period. These films possess properties similar to larger CNF products, yet they are more efficient when experimented with new materials. The process for creating thin films starts with obtaining 200g of CNF, followed by adding any necessary additives. The mixture is placed in a Kitchen Aid 6-quart mixing bowl and mixed at speed 2 for 5 minutes using a Kitchen Aid Professional 5 plus mixer. After mixing was complete, the mixture was placed on a fire brick and pressure was applied down onto the mixture with another fire brick, as shown below. The material was then dried at 60°C in a Fisher brand Isotemp oven for 48 hours.

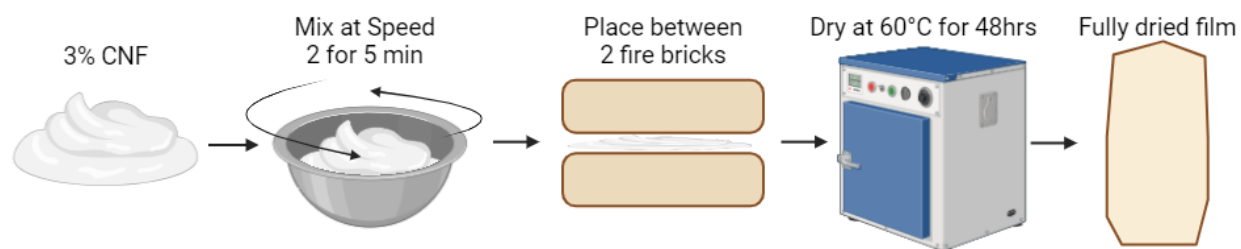


Figure 3.16: CNF thin film procedure.

To ensure that the urea was evenly distributed across the entire sample, a 10% wt. urea solution was created to add to the CNF slurry. Urea was used due to background research showing promising crosslinking and biocompatibility findings. Normally, 3% wt. CNF is used to produce these CNF materials. The addition of water, through the 10% urea solution, causes the material to dilute. To prevent this, a 6% wt. CNF slurry was made. There were two methods to make this type of CNF: vacuum filtrate 3% CNF to the desired wt. % or water down a higher wt. %. Due to the bond strength of 3% CNF with water, it was more time-consuming to remove water from the slurry. Therefore, 20% wt. CNF was obtained from the Process Development Center (PDC) at the University of Maine and watered down to 6% CNF. During the rewatering process, continuous stirring of the slurry was administered by the Kitchen Aid Professional 5 Plus mixer. The rewatering process took around 5 minutes of mixing at speed 2, in which the material was fully saturated with water.

The materials were prepared to make a CNF thin film using 10% urea solution and 6% CNF. The 10% urea solution was added to 100g of 6% wt. CNF based on calculated dry weight. For example, a normal thin film containing 200g 3% wt. CNF, the final dry weight will be 6g. When creating a 25% wt. urea film, the final dry weight will contain 2g dry urea and 6g CNF. The final dry weight of 2g is the equivalent of 20mL of 10% urea solution, added to 100g 6% CNF. To make the total concentration 200g 3% CNF, the excess amount of water that wasn't added through

the urea solution is added back into the mixture. Once 200g 3% wt. CNF is achieved with the desired urea, following the same thin film procedure for pure CNF films.

Once the thin films are created, they must be cut into size and dimensions according to ASTM standard D638-22. The standard states that any material less than 4mm must use Type V specimen dimension. These dimensions are the

same as in Figure 3.4. However, the thickness is typically between 0.1-0.5mm, depending on the sample's composition. The samples were cut using a Trotec Speedy 400 laser cutter to ensure the precision and accuracy of the sample dimensions. The standard also requires cutting

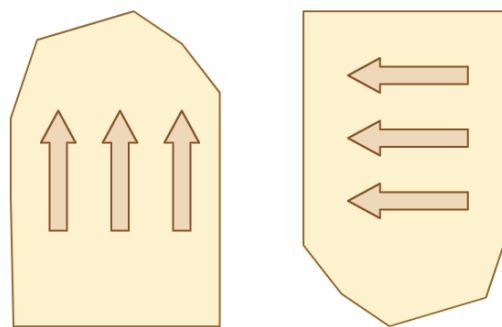


Figure 3.17: Cutting of CNF thin films in the 1D (left) and 2D (right).

alignment for materials with an anisotropic structure. With a material with unoriented fibers, the samples must be cut along the length and width of the film, as shown in Figure 3.17. These are labeled 1D, or 1-direction, and 2D, or 2-direction. 5 specimens were cut for each direction.

3.3.2: Results

Different temperatures and compositions were tested to determine the crosslinking ability of urea. The samples for urea were produced with 5, 10, and 25% wt. and dried at both 60°C and 80°C. 5 samples were created for each material type using the Type V design specifications according to the ASTM D638-22 standard. The Young's modulus and tensile strength for the thin film samples were calculated using the Blue Hill Universal program under the Instron 5942 model used for testing.

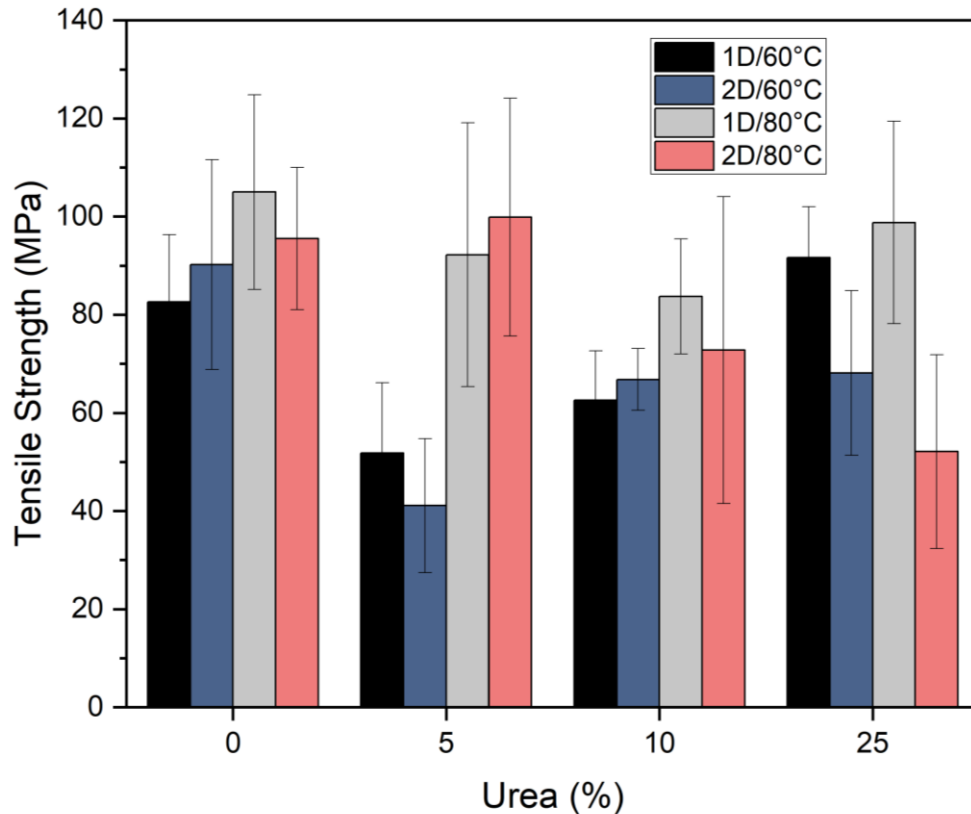


Figure 3.18: Tensile strength for urea samples in 2 directions at 60°C and 80°C.

Some interesting trends occurred in the graph above. The pure CNF samples proved to have the highest overall tensile strength across all the samples. However, some crosslinked urea samples had comparable strength values. The 80°C samples in each direction provided high strength values in the 5% urea material and both 1D samples in the 25% urea material. Furthermore, the 1D samples trended towards having higher strength values than the 2D samples. A reason for this increased strength could be that when urea is added to the CNF, the cellulose could have a fiber orientation along the material's long axis. More testing will have to be done to prove this, but it could explain the increased strength values. Overall, these values are better than the results found in the polycup samples. When polycup was introduced into CNF, the strength values displayed a noticeable decrease. However, some of the urea formulations initially appear to have a neutral effect on the strength of CNF and display similar strength values.

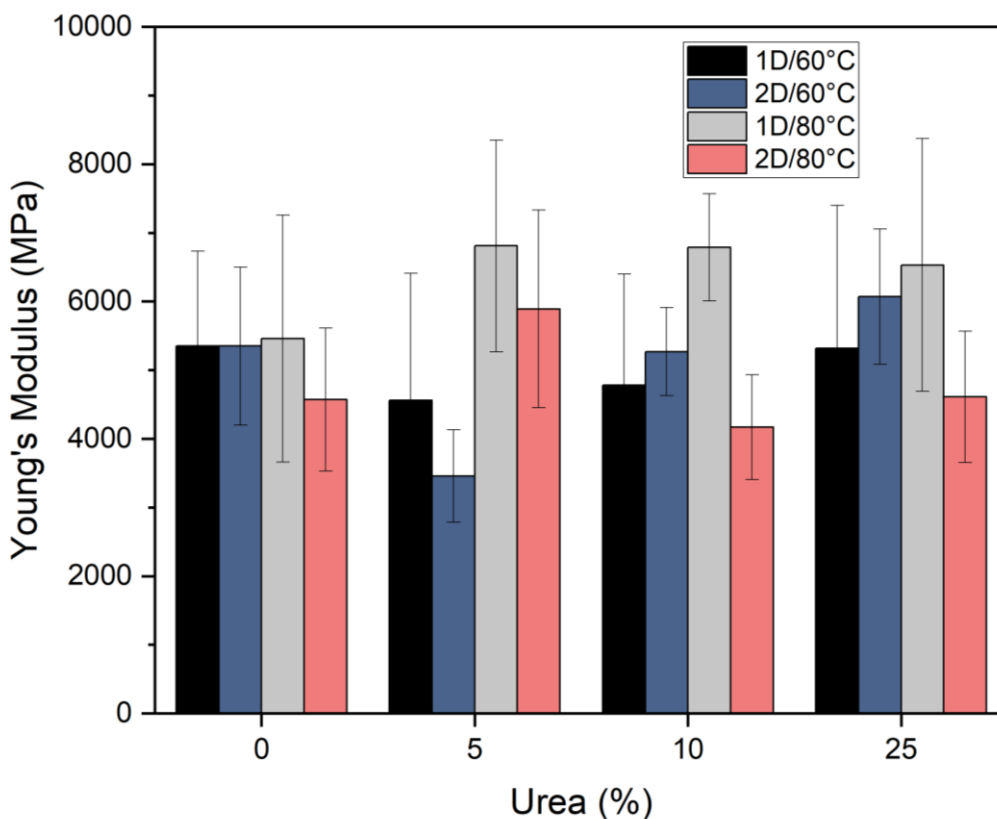


Figure 3.19: Young’s modulus for urea samples in 2 directions at 60°C and 80°C.

There were similar trends for the modulus values when testing the urea samples. Nearly all samples displayed a similar modulus value compared to the pure CNF. This is again an upgrade compared to the polycup samples, in which nearly all tested samples contained weaker modulus values than pure CNF. Furthermore, the 1D 80°C sample showed the highest modulus values across all the urea formulations. However, the 2D 80°C samples seemed to show the weakest stiffness values for most of the tests. Again, a possible reason for this happening could be the alignment of fibers along the long axis of the film when crosslinked with urea.

Specific variables needed to be tested to determine the impact of urea across CNF samples. First, the material's crosslinking action could have demonstrated alignment in CNF fibers along the sample, so the directionality of the films was first compared. Next, previous studies showed that a higher crosslinking temperature could positively impact the amount of crosslinking, so the

effect of temperature across films was also compared. To do this, the tensile strength values were compared across variables.

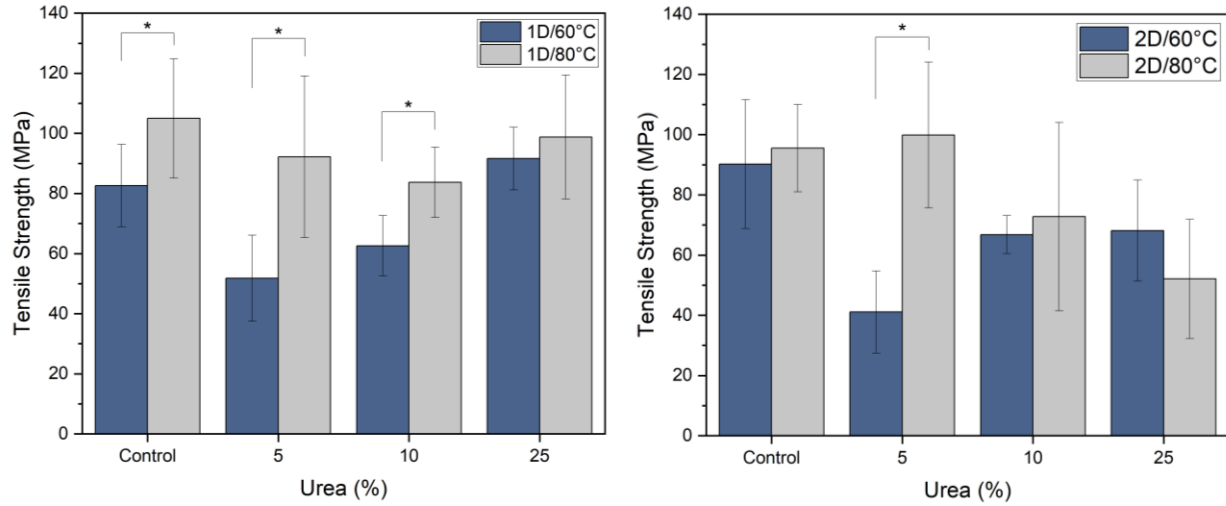


Figure 3.20: Tensile strength of urea samples compared against 60°C and 80°C in both the 1D (left) and 2D (right).

The data above portrays that the temperature was more important in the 1D than the 2D. For the 1D samples, only the 25% urea sample did not show a statistical increase in strength values compared to the others. For the 2D, only 5% showed a statistically significant increase in the 80°C sample. This data means that the increase in temperature positively impacted the strength of the films, which will be used moving forward.

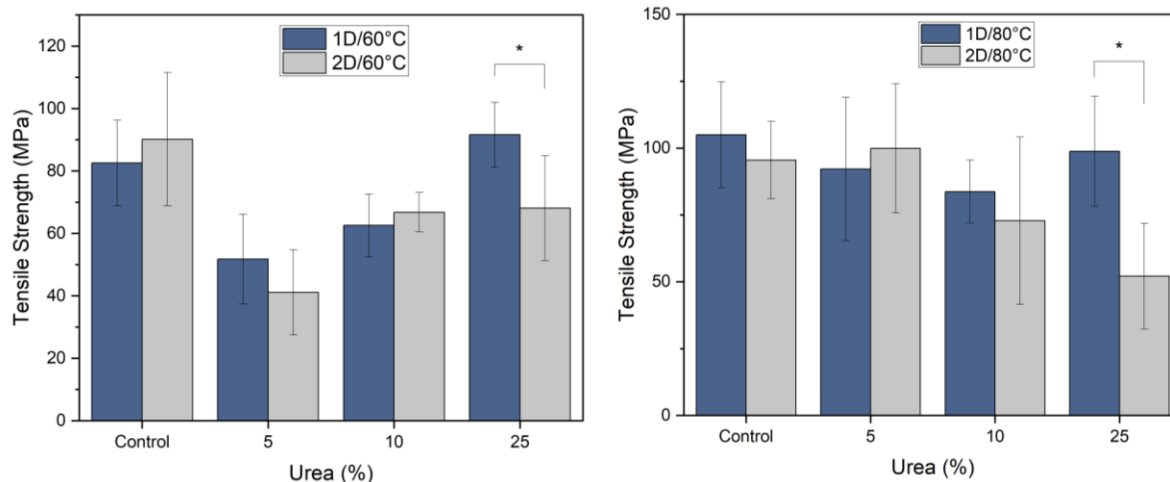


Figure 3.21: Tensile strength of urea samples compared against 1D and 2D in both the 60°C (left) and 80°C (right).

The data above shows that there was little impact of directionality across the urea concentrations. The only statistically significant difference between the directions across both temperatures was in the 25% concentrated samples for both temperatures. Therefore, a conclusion can be made that directionality is only important for higher concentrated samples. Overall, temperature impacts the mechanical strength of the CNF films more than directionality.

3.4: Strontium Chloride

3.4.1: Results

Strontium chloride was another crosslinking agent that was explored when added to CNF. Strontium chloride is easily soluble in water, so it could be evenly distributed within the CNF when added in its salt form. Therefore, the standard process for creating thin films was utilized. The films were produced with 5, 15, and 25 wt. % strontium chloride. After drying, the Trotec Speedy 400 laser cutter was used to cut the samples into the Type V, ASTM D638-22 standardized sample dimensions. The samples were again cut in the 1D and 2D. Once the sample sizes were properly cut, an Instron model 5942 was used to perform a tensile test on the samples following

the ASTM standard. Blue Hill Universal was used to create stress/strain curves to calculate the films' Young's modulus and tensile strength.

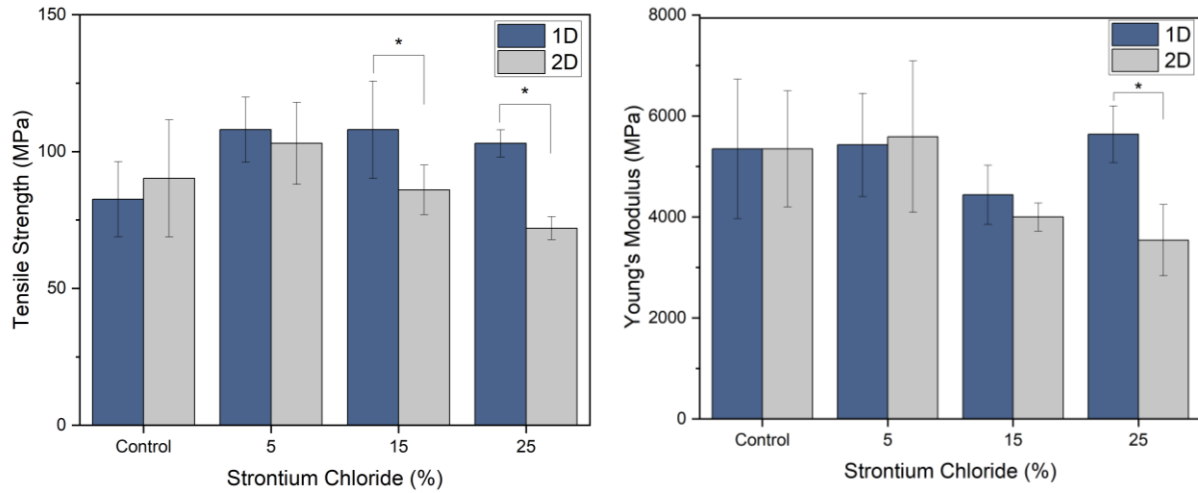


Figure 3.22: Tensile strength (left) and modulus (right) of strontium CNF films compared across directions.

The results for the strontium chloride films showed that the addition of the salt positively impacted the tensile strength, and also the modulus of CNF. In the 1D, all of the strength values were increased by adding strontium chloride, and the 2D samples only showed slight decreases. For the modulus, the 2D samples appeared to display a more negative trend when compared against the 1D. To test for the impact of directionality, a Mann-Whitney u-test was conducted. The results from this test showed that with increased amounts of salt concentration, the 1D samples showed a significant increase in both strength and modulus. This means that when using higher concentrations of strontium chloride, the directionality is impactful.

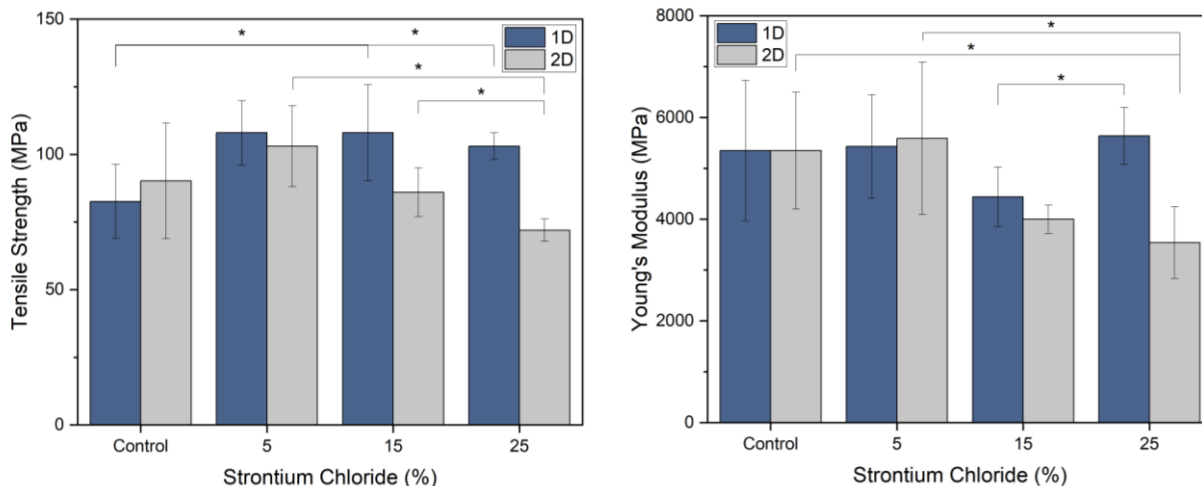


Figure 3.23: Tensile strength (left) and modulus (right) of strontium CNF films compared across wt. %.

Next, the strontium films were statistically tested across the varying weight percents to determine the impact of salt concentration on their mechanical values. For the strength values, the 1D samples significantly increased the overall strength of the CNF films. Also, the 25% strontium showed a statistically significant decrease in strength for the 2D samples. The modulus, however, was less affected by the impact of strontium. The differences mainly appeared with the higher salt concentration samples. Therefore, further experiments will utilize the lower concentration salt values, as they displayed better results overall.

Below is a comparison of the tensile strength at 5% concentration for all three crosslinking agents. It is shown that at the 5% concentration, the strontium films were statistically significant in both directions. 5% was chosen for comparison due to Polycup only having a maximum 7.5% formulation value. The data here proves that the addition of urea and strontium chloride positively affects the tensile strength of CNF films. While urea isn't as significant as strontium chloride, it still shows increased results. Moving forward, more experimentation will be done with these new crosslinking agents.

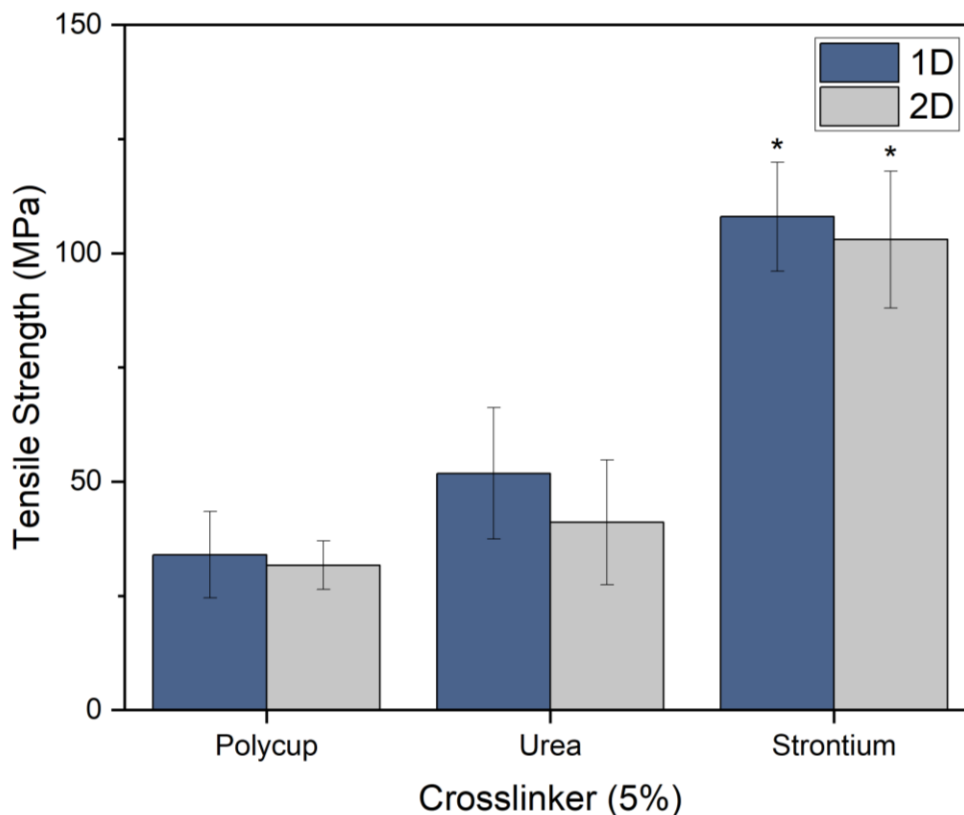


Figure 3.24: Comparison of tensile strength across all crosslinking agents.

3.5: Conclusions

Three different materials were tested to attempt crosslinking CNF to aid in reducing the overall hydrophilicity of the material. While early tests of polycup provided some promising results, the mechanical from the larger material proved that it harmed the mechanical properties of CNF. The flexural data for different environmental conditions showed decreased modulus and strength values after the polycup was added. Due to the decreased mechanical values, other alternatives were explored. Two crosslinking alternatives placed under initial thin film strength testing were urea and strontium chloride. Both were picked due to their potential crosslinking capabilities while acknowledging their impact on the body. For urea, the results showed that the 80°C films improved the tensile strength more than the 60°C films. Also, the directionality of these films did not impact the mechanical values. The addition of urea had less of a negative impact

overall than the polycup did. The strength and stiffness values were more consistent with pure CNF, an improvement from the polycup trials. Finally, the strontium chloride films improved the overall tensile strength of the CNF films. The samples cut in 1D all portrayed higher tensile strength values, and the 2D showed comparable results. The stiffness values for these films stayed consistent for 5 and 25% wt. in the 1D but decreased at 15% wt. Overall, the 1D testing proved to have better results in both the urea and strontium chloride samples, showing that directionality impacts the results of this material. Based on the positive initial strength testing results of both new materials, they will be explored as crosslinking agents with CNF. Further testing will require analyzing the wettability of the samples, cell viability, and the effect of environmental conditions on the material when compared to pure CNF. If these results are not ideal, other salts and crosslinking agents will be explored to try to reduce water reuptake into dried CNF.

CHAPTER 4: HOMOGENIZATION METHODS FOR CELLULOSE NANOFIBRIL COMPOSITES

4.1: Introduction

In Chapter 3, crosslinking strategies were explored to reduce the water reuptake of CNF materials after drying. Three potential crosslinkers were explored, urea, strontium chloride, and polycup. The polycup samples initially showed promise in their strength and water absorption properties, but further testing showed a substantial mechanical strength reduction. Therefore, two other materials, urea and strontium chloride, were used in as crosslinking agents when added to CNF. Initial tensile testing results showed that strontium chloride increased the overall tensile strength of CNF, while urea remained consistent in the original CNF tensile properties. Both of these materials will be explored and tested in the future to determine the extent of crosslinking and its impact on CNF properties. The upcoming chapter will explore the homogenization of materials added to CNF composites.

Based on prior results conducted by the Mason Lab, CNF by itself is a non-toxic material with it being around 84% viable. While this value enables further research to be done on the material, this project aims to increase this number closer to the maximum viability of 100%. When searching for materials to use for their potential in orthopedic applications, it is important to look at the components, structure, and composition of bone. Bone is comprised of about 60% hydroxyapatite, 30% proteins such as collagen, and 10% water.⁶⁶ Hydroxyapatite (HA) is a calcium phosphate-based mineral responsible for the bone's strength and stiffness.⁶⁷ Conversely, Collagen is responsible for creating a framework for the hydroxyapatite particles and provides elastic properties to the bone.^{6,7} Since both of these components are already in bone they were

immediately proposed as materials to boost the cell viability of CNF. As CNF already possesses a fibrous interconnected network, HA was first selected for experimentation over collagen.

Recently, HA was synthesized using a carefully designed process in the Mason Lab.⁶⁸ When producing this material, many tests were run to determine the procedure's effectiveness. They found that the HA produced contained the same properties as synthetic HA and HA found in the body.⁶⁸ During the procedure, manufacturing processes were explored to determine how to get the most effective size distribution of particles. They utilized a milling machine and experimented with different milling media sizes and overall milling time. The best formulation tested was produced using a mix of large and small media and was milled for 4 hours.⁶⁸ This type of HA was selected for use as an additive to CNF to improve cell viability.

When inserting a solid material into another material, it is important to ensure that it is distributed evenly throughout the sample. Materials that are unevenly distributed can produce inaccurate data measurements, which can lead to false conclusions and interpretations of the material. When producing thin films of CNF with HA nanoparticles, there were visible indications that the material was unevenly distributed. Some areas on the material appeared to have higher concentrations of HA than others. Figure 4.1 shows visible clumping of the material, with some areas having higher amounts of HA than others.



Figure 4.1: CNF thin film with 15% HA untreated.

One strategy to distribute HA evenly is fully dissolving the material in water. However, research shows that HA can be dissolved, but it is a difficult process with temperatures nearing 1000°C.⁶⁹ Other options include chemically modifying the material or solution, adjusting the solution's surface charge, or simply suspending the material in solution. Chemical modification was avoided to keep the material content consistent. Therefore, an experiment was proposed to suspend HA particles in solution before their insertion into the 3% wt. CNF slurry.

4.2. Methods

During initial HA/CNF sample testing, the thin films produced showed HA material that was not completely distributed. Initially, several techniques were used to improve dispersion. The first technique was using a 45-micron sieve, letting only the small particles pass through. However, clumping was still apparent in the films after they went through the sieve. The next idea was to add water to the HA and let it saturate for 24 hours. The saturation method was improved from the previous methods, and the next steps were to see which mixing methods provided the best results. Two main controls were used for this experiment: no-treatment and sieving. The treatment methods involved placing the HA in water to create a 10% wt. solution and then testing the effect of different mixing methods. The HA material was added directly into the solution for the no-treat method. The HA was placed through a 45-micron sieve to reduce the number of large particles for the sieving method. The material types were then mixed by blending, hand-stirring, and sonicating for five minutes. For the blending test, Ninja Pro System 1100 was used. The material was placed in the mixer for 5 minutes at the lowest speed setting, around 1100-1200 rpm. A QSonica sonicator was used at around 70% power for the sonication method. The total sonication time was 5 minutes, but the method was paused at 2.5 minutes to allow the solution to cool. Finally, the hand mixing was done with a scoopula in a beaker for 5 minutes. After mixing for each method, the 10% HA

solution could be added to the CNF. This was consistent with the procedure explained for adding the 10% wt. urea solution above.



Figure 4.2: No-treat HA mixing methodology for thin film CNF composites.

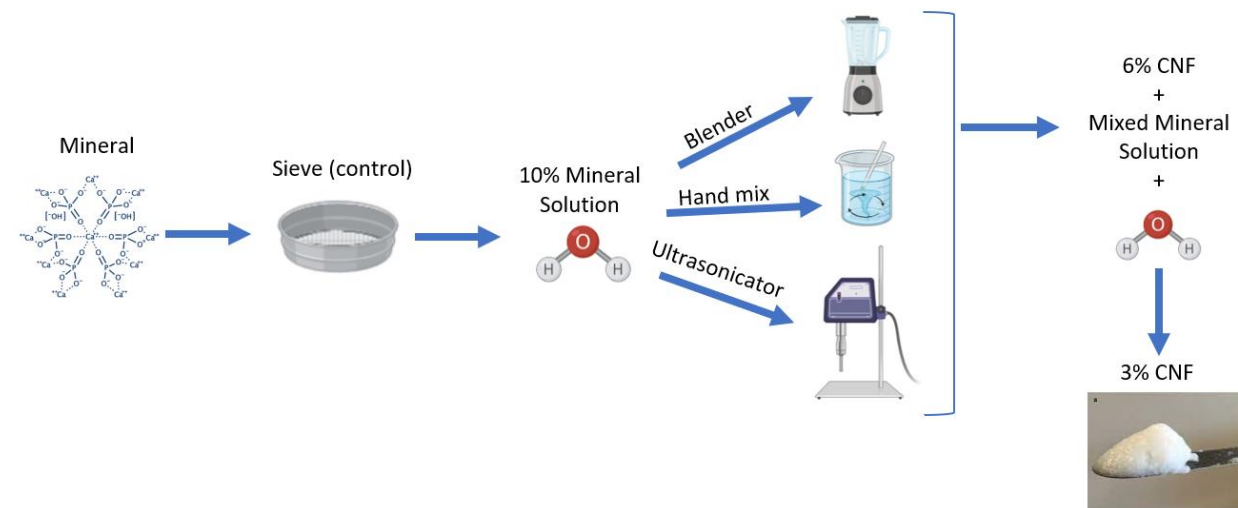


Figure 4.3: Sieved HA mixing methodology for thin film CNF composites.

4.3. Results

The HA was mixed into CNF with 5, 15, 25, and 50 wt. % for each mixing condition. A tensile test was the initial method used to test the mechanical strength of these thin film composites. The ASTM D638-22 standard was followed when designing this tensile test. Samples were created according to the Type V sample specifications outlined in this standard. For these samples specifically, they were cut by hand using scissors to the desired shape. At the time of production, the Trotec Speedy 400 laser cutter could not be accessed, so the samples were cut using this method. As these samples were also anisotropic, the materials were cut in the 1D and 2D, as shown in Chapter 3. The samples were tested using an Instron model 5942, with the Blue Hill Universal program generating stress/strain curves to calculate Young's modulus and tensile strength of each sample. 5 samples were tested for each different material type of HA.

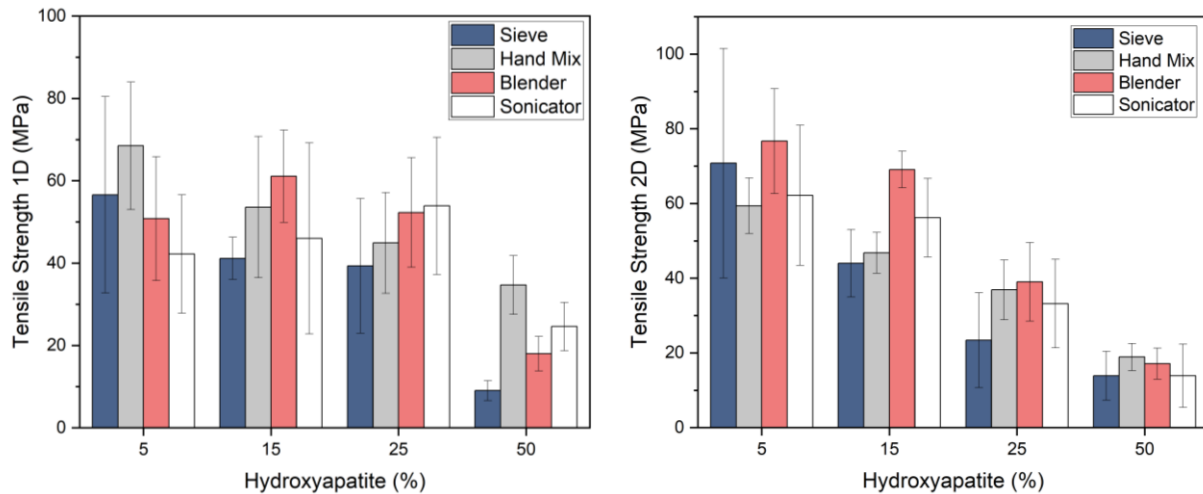


Figure 4.4: Tensile strength sieved CNF films with HA in the 1D (left) and 2D (right).

There are some common trends from the graphs above. For each direction, the overall tensile strength decreases with the increase of HA, with 5% mainly consisting of the highest strength and 50% with the lowest. Initially, it was hypothesized that increasing mineral content would help increase the material's overall strength. However, the data shows that this is not the

case. When HA is introduced into the material, the bonding between the cellulose and HA disrupts the overall highly fiber-oriented structure, producing a weaker product. Also, the graphs display that the strength of the hand mix, blender, and sonicator samples are generally higher than that of the sieved samples. When samples are evenly distributed, the uniformity increases the overall strength. With samples that aren't evenly distributed, however, there tend to be weak points in the material where there is a congregation of one material type, which can cause decreased mechanical strength values. These hypotheses are true for this material. The sieved samples appeared to have a lower distribution of HA particles throughout the film, directly correlating to the material's tensile strength. The other three methods, which incorporated suspending the HA in water, showed increased dispersity throughout, which again directly correlated to the strength of the material.

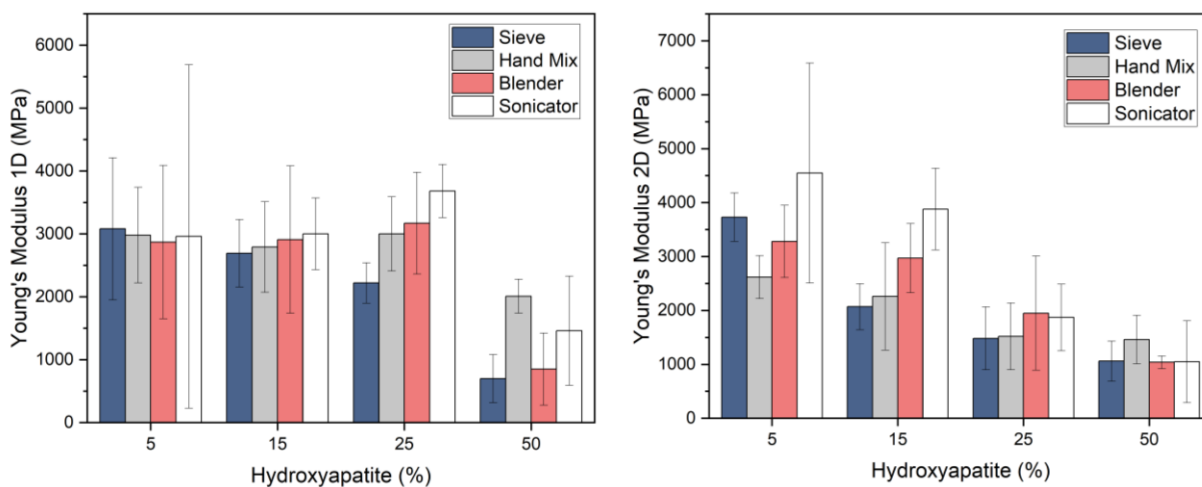


Figure 4.5: Young's Modulus of sieved CNF films with HA in the 1D (left) and 2D (right).

The Young's modulus values above depict similar trends to the tensile strength data. The modulus mainly decreased with the increase of HA content; the sieved samples generally displayed lower modulus values than the rest, and there was a slight variation between the two different directions. Again, the integration of HA into the CNF material decreases the material's overall stiffness due to the disrupted highly integrated network. Also, the anisotropy of the material

appears to have a similar impact in both directions. Next, the samples that used the same mixing methods without sieving are shown.

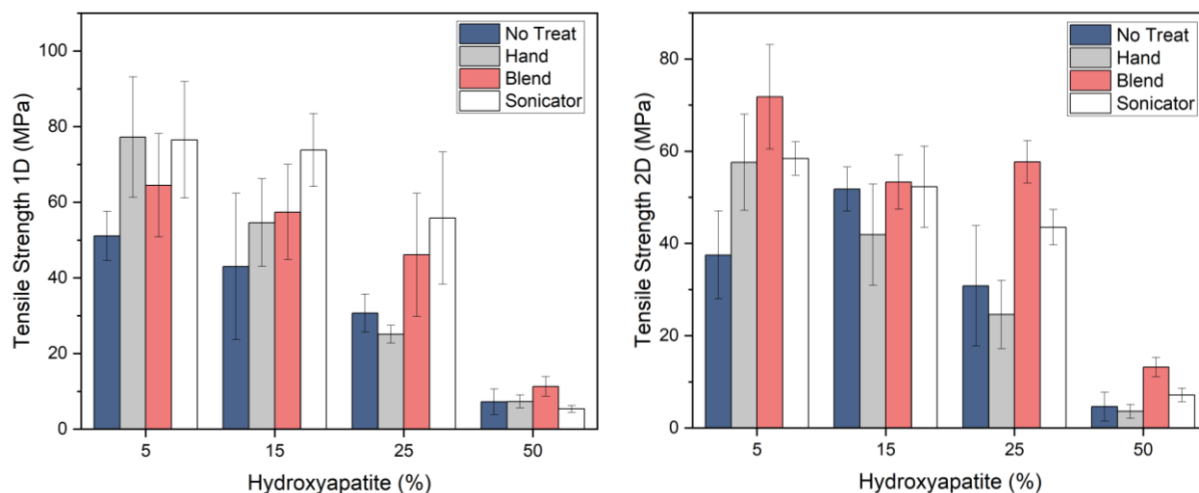


Figure 4.6: Tensile strength of no-treat CNF films with HA in the 1D (left) and 2D (right).

The trends from these graphs are similar to the sieved samples. The no-treat samples mostly had a decreased tensile strength when compared to the pre-saturated samples. Also, the overall tensile strength of the samples decreased with increased HA content. Again, the integration of the HA particles into the CNF fiber network negatively disrupts the overall tensile strength of these materials.

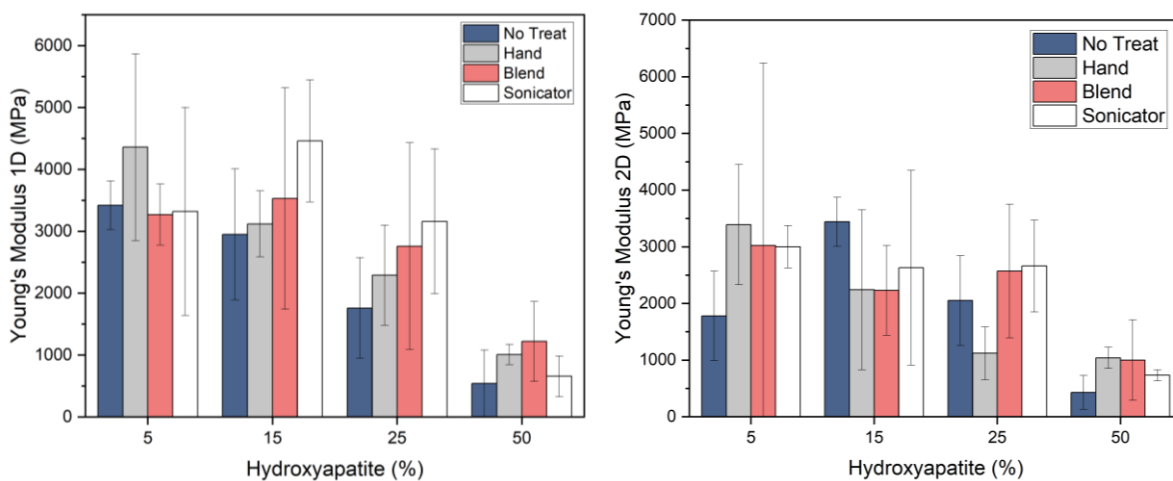


Figure 4.7: Young's modulus of no-treat CNF films with HA in the 1D (left) and 2D (right).

The results from these samples displayed similar trends to the sieved samples. The overall stiffness of the samples decreased with higher mineral content added to the CNF material. Also, the no-treat samples again mostly showed lower stiffness values across both directions when compared to the pre-saturation samples. Finally, there isn't any conclusive trends across the two directions of the material.

Finally, statistical analysis is essential in determining if a material is statistically significant or different from each other. It was important to first compare the impact of sieving against no-treat. This initial test can show how the initial dry impact of sieving portrays. Next, it was important to compare the pre-saturated mixing methods against each other. This test can provide information on if there is any difference in mixing methods between the three. Finally, it was important to test the impact of the sieving before the HA was placed into the water. This can show if sieving is a necessary step in the pre-saturation process. A Mann-Whitney u-test using Origin Pro was used to generate p-values. The points on the graph below with a * symbol represent p-values that are less than 0.05, meaning the two material types are statistically significant.

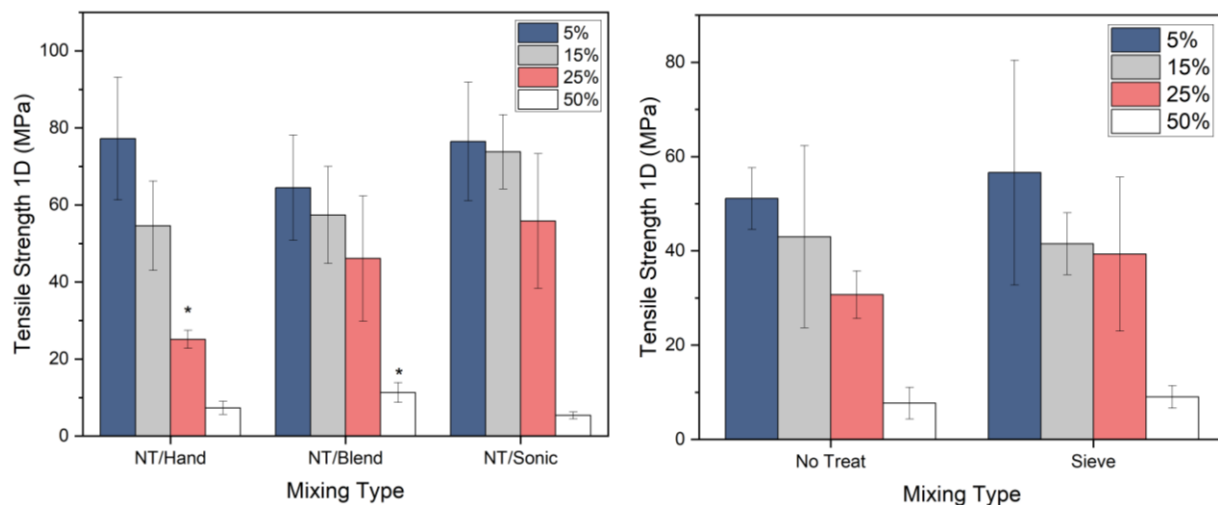


Figure 4.8: Statistical analysis of saturated mixing types (left) and pre-saturation (right).

It was decided that the values for tensile strength 1D for all the sample methods should be compared. It was assumed that a comparison between one set of data would correlate with the rest of the data. In the graphs, NT represents no-treat. The tests were conducted by testing the same weight percents across different mixing methods. For example, 5% NT/Blend was tested against 5% NT/hand. It was found that there were only two points that were statistically significant from the pre-saturation methods. The 25% NT/hand sample was significantly less than the other two methods, and the 50% NT/Blend was significantly higher than the other methods. Due to the low values from the 50% samples, moving forward only 5-25 wt. % will be used. Based on mechanical data, any of the three pre-saturation methods can be used in lower HA concentrations. In the next graph, there were no points in which there was a statistical significance between the no-treat samples and the sieved samples. Therefore, either one can be used moving forward.

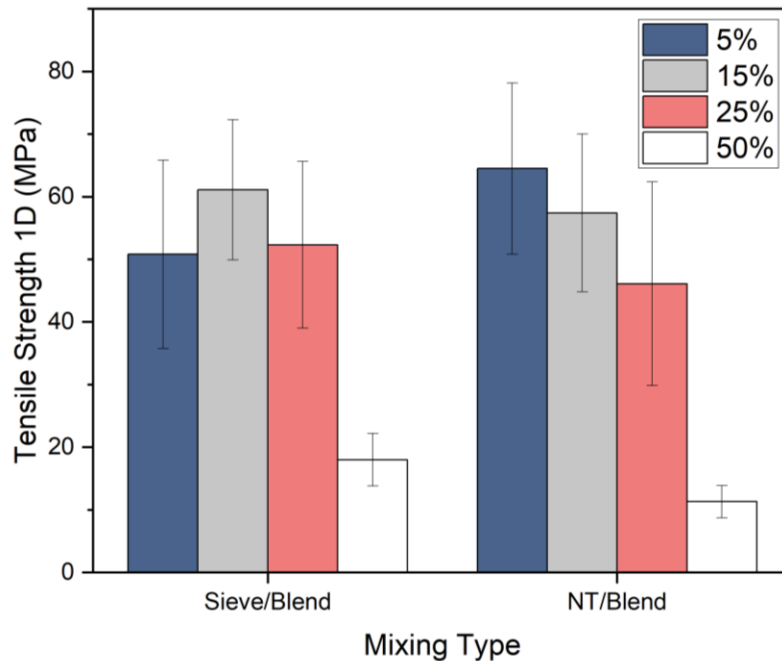


Figure 4.9: Statistical analysis of sieve vs no-treat blended mixing types.

The graph above shows that when the samples were tested between the same wt. % of blended samples that were and were not sieved prior to saturation, there was no statistical significance across all samples. This means, that after the HA particles are saturated, there is no positive or negative effect of sieving. Therefore, either method could be used with to mix HA into CNF.

When examining the impact of altering the overall composition of a material, it is crucial to examine the material changes at the macro-scale and micro-scale. This means exploring how the material is changed based on what the eye can see, or the macro-scale, and examining the material at a small size scale that the eye can't depict, the micro-scale. There were immediate alterations in the physical composition when looking at the material with the naked eye.

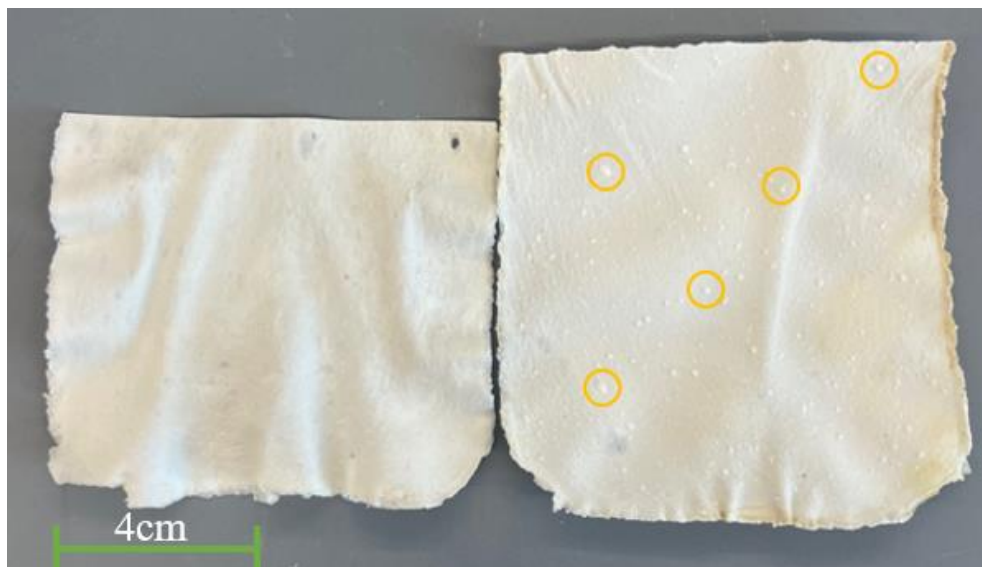


Figure 4.10: 15% HA/CNF thin film portions with HA treated by blending (left) and left untreated (right).

From the image above, there are visible distribution differences between the sample with HA treated with suspension and blending and with HA that was left untreated. Both samples contain the same amount of HA, however, there are visible portions of the untreated film where

HA has congregated, while the blended film shows a white color throughout. The consistent color that is present in the blended film proves that there is a higher dispersion of HA particles throughout the film when compared to the untreated film at a macro-scale. However, further imaging must be conducted at the micro-scale before the distribution increase can be confirmed.

Scanning electron microscopy (SEM) was used to image CNF/HA composites. Each method and material type were imaged at varying optical zooming intensities. The purpose of this imaging was to determine the overall dispersion of HA into CNF material at the micro and nanoscale. Two images best showed the difference in dispersion of HA: 50% blended vs. 50% no-treat.

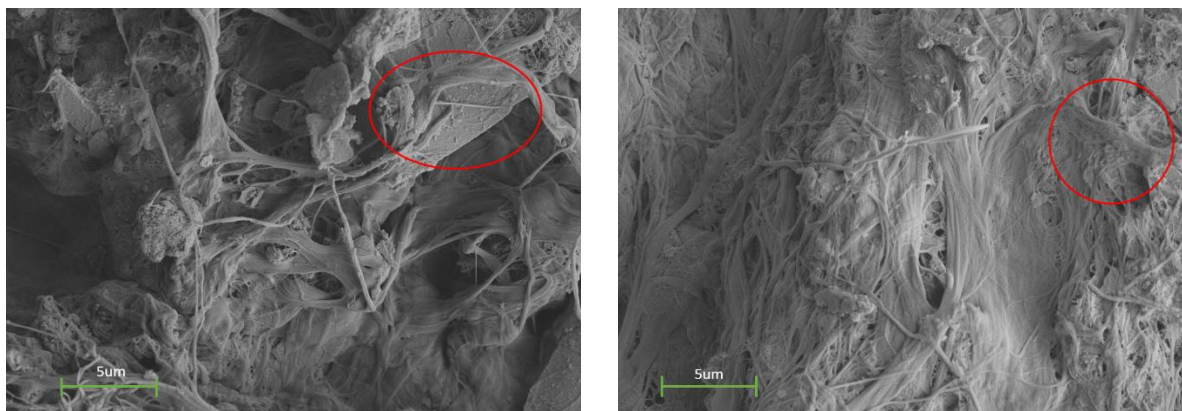


Figure 4.11: 50% HA/CNF blend-mixed film with a 4x SEM image (left), and a 50% HA/CNF untreated film with a 4x SEM image (right).

On the left side is a 4x SEM image of a CNF film containing 50% HA and was made using the blender mixing method. On the right, is another 4x SEM image of a CNF film, but this image is of a film that contains untreated HA. Throughout the film, there are unorganized CNF fibers in an anisotropic orientation, but there are also areas that contain HA minerals. The two specific areas of interest are in red. It is important to note that these images were taken randomly and were not selected based on their quality. On the left, smaller individual HA particles are bonded to a

cellulose fiber. On the right is an area in which there are HA particles that have conjoined and bonded to each other. These images exemplify how the change of HA integration within CNF plays a role in the overall distribution of the mineral. When first suspended in water and mixed with a blender, there seems to be better dispersity overall than when left untreated, as shown in the picture.

Now that the process for distributing HA into CNF composites has been solidified, large-scale composites can be produced using a similar method. It is important to keep previously used techniques consistent when processing these large-scale composites. Samples were made with 0, 5, 15, and 25% wt. HA. Due to material restrictions, 50% was withdrawn from experimentation. The total amount of CNF used for these composites is 5 gallons. To follow the same procedure used to incorporate HA into CNF, 2.5 gallons of 6% CNF would need to be produced. However, due to material restrictions and processing difficulty, the decision was made to first make a gallon of 3% wt. CNF with all of the total HA necessary, and then mix that gallon with 4 gallons of pure 3% wt. CNF. To do this, the required amounts of HA for each sample were placed through the 45-micron sieve and then placed in a 10% HA solution. $\frac{1}{2}$ gallon of 6% wt. CNF was diluted from 20% wt. CNF. The required HA solution was added to the $\frac{1}{2}$ gallon of CNF, as well as any remaining water necessary to reach 1 gallon 3% wt. CNF/HA slurry. The CNF/HA slurry was then placed in a 5-gallon bucket, and the remaining 4 gallons of CNF were filled on top. This ensures that the correct amount of CNF is added to make the composite. The 5 gallons are then placed in the 60L bucket of the H600 Hobart Mixer, mixed at speed 2 for 5 minutes, and then placed in the fire brick mold. The samples were left to air dry for 24 hours, and then dried at 70°C for 6 days until fully dried.

After the composites were fully dried, samples were ready to be prepared. Due to the dimensions of the dry material, samples can only be cut in two directions: 1D and 2D, as shown below.

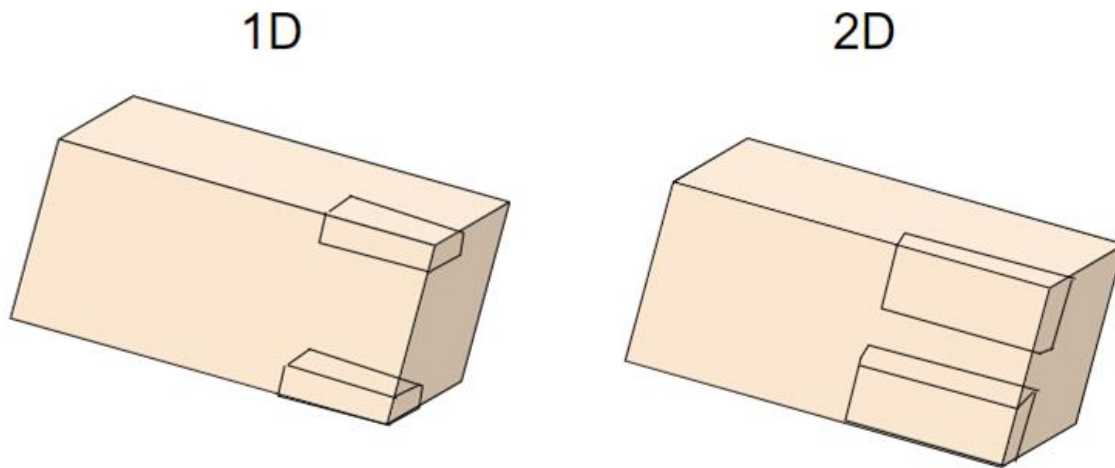


Figure 4.12: Cutting directions of new CNF molds.

To start, the edges of the material had to be cleaned and made even. Rather than using a circular saw to clean up the edges an end mill was utilized. Once the edges were cut evenly, the samples were prepared according to the ASTM D790-17 standard. The sample dimensions were cut in the 2D direction, and they were 100mm long, 20mm wide, and 4-5mm thick using a band saw. They were cut in the 2D due to prior tests resulting in the highest values.⁵⁴

Another set of CNF/HA composite scaffolds were created for the compression samples, = this time utilizing a new cutting method. Rather than using an end mill to clean the uneven edges of the material, a custom-made jig was used to accurately cut the samples using a band saw. Once the edges were even, the compression samples were cut according to ASTM D695-23. The samples were cut in the 2D direction and were 25.4mm long, 12.7mm wide, and 12.7mm thick.

5 samples were produced for each material type. The samples were tested using an Instron model 5942, using the 3-point bending attachment. The span width for the material was 80mm. The downwards component was forced onto the material at a rate of 2mm/min. The stress and strain curves of the material were generated using the program Blue Hill Universal, and the flexural modulus and strength were calculated.

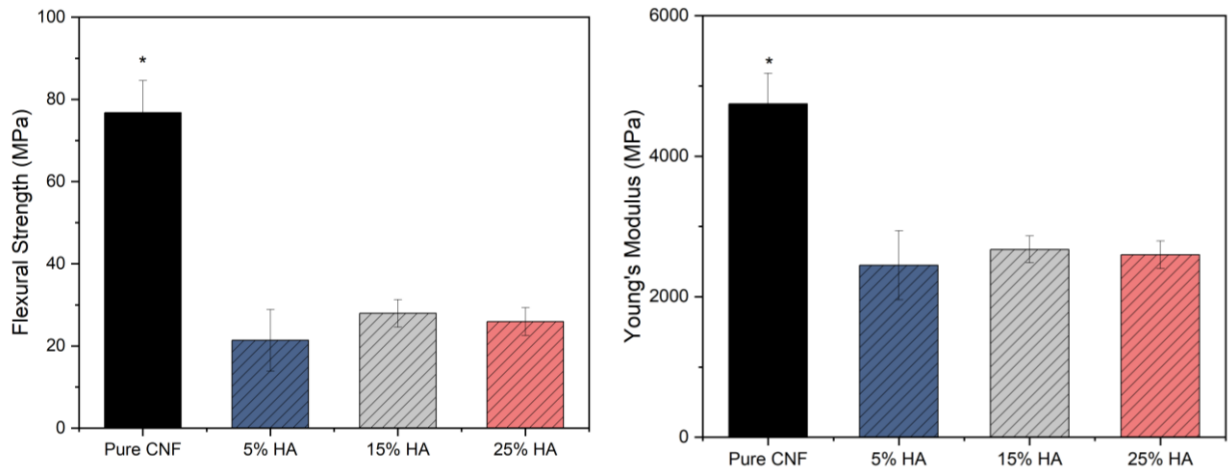


Figure 4.13: Flexural strength (left) and modulus (right) of CNF/HA composites.

The graph demonstrates that there was a significant decrease in flexural strength with the addition of HA. Pure CNF performed much better than the HA composites and was statistically significant from the rest. The HA added appeared to weaken the highly bonded CNF and failed at a much lower rate. This could be caused by an increase in porosity of the material or weaker bonding due to the HA disruption of fibers. Similar trends were seen for the flexural modulus values. The pure CNF modulus value was much higher and statistically significant when compared against the composites with HA. The addition of HA decreased the overall stiffness of the material. Again, this decrease could be attributed to the weakening of overall fiber bonding due to the disruption caused by the HA nanoparticles.

For compressive testing, 5 samples were created for each material type, ensuring that the top and bottom sides of the material were flat. An Instron model 5882 was used to perform the

compression testing, with the compression attachment consisting of a rigid, flat, circular bottom plate, and a top, flat, circular top plate that can be forced down into the material. The 5882 model was used for this test due to the higher load cell. Following the ASTM D695-23 standard, the downward displacement rate was set to 1.3mm/minute. Load and displacement rates were calculated during the test using the Blue Hill Universal program, which helped determine the compressive strength and modulus of the materials. For the HA materials, they didn't follow a normal compressive curve. Rather than breaking when the compression value reaches its peak, the material instead reaches a peak and begins to increase in strength. The material compounding within itself causes this spike, and once the material starts to increase in strength a second time, the trial is ended.

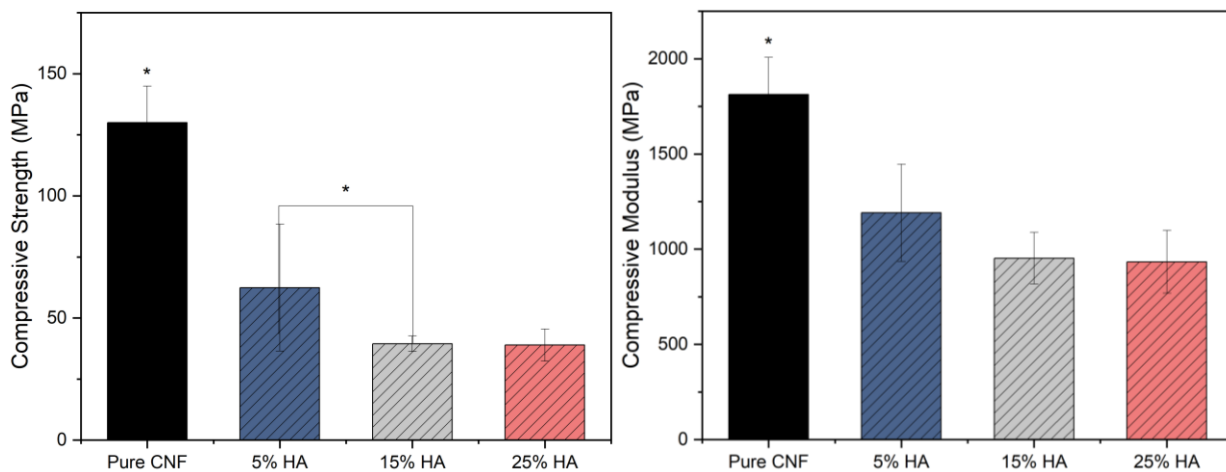


Figure 4.14: Compressive strength (left) and modulus (right) of CNF/HA composites.

The compressive testing followed a similar trend to the flexural testing shown above. When the bulk material with HA was tested, there was a statistically significant decrease in both the compressive strength and modulus. Also, the 5% and 15% HA samples both proved to be statistically significant from each other. Again, a common reason for this could be that the HA is harming the tight material orientation of the CNF fibers.

4.4: Conclusions

The findings of this experiment showed varying results. First, the newly proposed method for incorporating HA nanoparticles into the CNF proved to be successful. The overall increase in dispersion into the HA was prevalent when looking at the macro and micro-scale material. The tensile strength also appeared to portray better results with the methods in which the HA was pre-saturated in water. However, with these promising results, when the HA composites were compared against pure CNF in both flexural and compressive testing, there proved to be a statistically significant decrease in both the strength and modulus for both tests. The decrease could be contributed by the increase in porosity throughout the material, or the interruption of the tight anisotropic behavior of the CNF fibers could have decreased the strength and stiffness of the material. Therefore, while there remain questions to be answered on the cell viability increase of this composite, the decrease in strength and stiffness of the material is concerning, and different options need to be explored.

CHAPTER 5: CELLULOSE NANOFIBRIL COMPOSITES WITH BIO-ACTIVE GLASS

5.1: Introduction

In the previous chapter, the incorporation of a mineral, hydroxyapatite, into CNF was explored. Initially, there was incomplete dispersion into the material, but a method was developed to increase the overall dispersion of particles. While the method of incorporation proved successful, the addition of HA into the CNF harmed the material's mechanical properties. Both the flexural and compressive strengths and moduli were significantly decreased with the addition of any amount of HA. HA was initially explored as an additive for its biocompatibility characteristics, as it is a mineral found in bones. While experiments are ongoing to test the bioavailability of a CNF/HA composite, the decrease in mechanical properties requires other materials to be explored. A candidate for replacement is the use of bioactive glass (Bioglass).

Bioglass is a set of mainly silica-based materials showing good bone and soft tissue biocompatibility.⁷⁰ One particular set of Bioglass is the 45s model, which contains 45% SiO₂, 24.5% Na₂O, 24.5% CaO, and 6% P₂O₅. One study found that when 45s Bioglass was added to marrow cells, these cells differentiated into osteoblast-like cells and also formed a large amount of mineralized tissue.⁷⁰ The addition of Bioglass within these cell lines promoted both cell growth as well as differentiation. Another study found that when compared against the 58s and 63s Bioglass compositions, the 45s displayed higher osteoinduction activity, increased alkaline phosphatase activity, and biomineralization.⁷¹ The 45s material type also displayed the most negative zeta potential, which can explain the increase in these cell values.⁷¹ Of all the Bioglass material sets, the 45s is the most effective in replicating *in vivo* properties of bone. The use of it has proven to proliferate, differentiate, and mineralize cells, all actions that occur *in vivo*.

Therefore, the 45s Bioglass material will be combined into a CNF scaffold and the mechanical strength will initially be tested, followed by an examination of its impact on osteoblast cells.

5.2: Methods

Bioglass is another mineral-like material, so the previous HA method was applied to produce Bioglass films and scaffolds. When initial mixing was conducted, visible clumping of the material occurred. However, the overall dispersity visually improved when the Bioglass was first put into suspension and then added to the CNF. Thin film samples were made with 0, 5, 15, and 25 wt. % 45s Bioglass, using the previously described mineral addition method from Chapter 4. Large scaffolds were also created at the same weight percent using the large scaffold mineral addition method described in Chapter 4.

When preparing samples for mechanical testing specific ASTM standards were followed. For flexural testing, ASTM standard D790-17 was used. The CNF/Bioglass materials were cut into 100mm x 20mm x 4-5mm tabs. 5 samples were created for each formulation. To cut the samples, a band saw and a custom-made jig were used to cleanly create the correct sample sizes. ASTM standard D638-22 was used for the tensile testing samples, and the samples were produced into a Type V sample size, as shown in Figure 3.4. The thin film samples were used for this test, and the thin nature of the material required that the Type V size must be selected. After the films were produced, a Trotec Speedy 400 laser cutter was used with the program Ruby to accurately cut the thin film samples to the correct dimensions.

5.3: Results

The first mechanical test conducted was a tensile test of the thin film CNF/Bioglass material. This test followed the instructions provided by the ASTM D638-22 standard. Ten Type V samples were prepared for each sample set, five in the 1D and five in the 2D. An Instron model

5942 was used for the test. Blue Hill Universal was used in collaboration with the machine to create stress/strain curves to calculate the tensile strength and Young's modulus of the films.

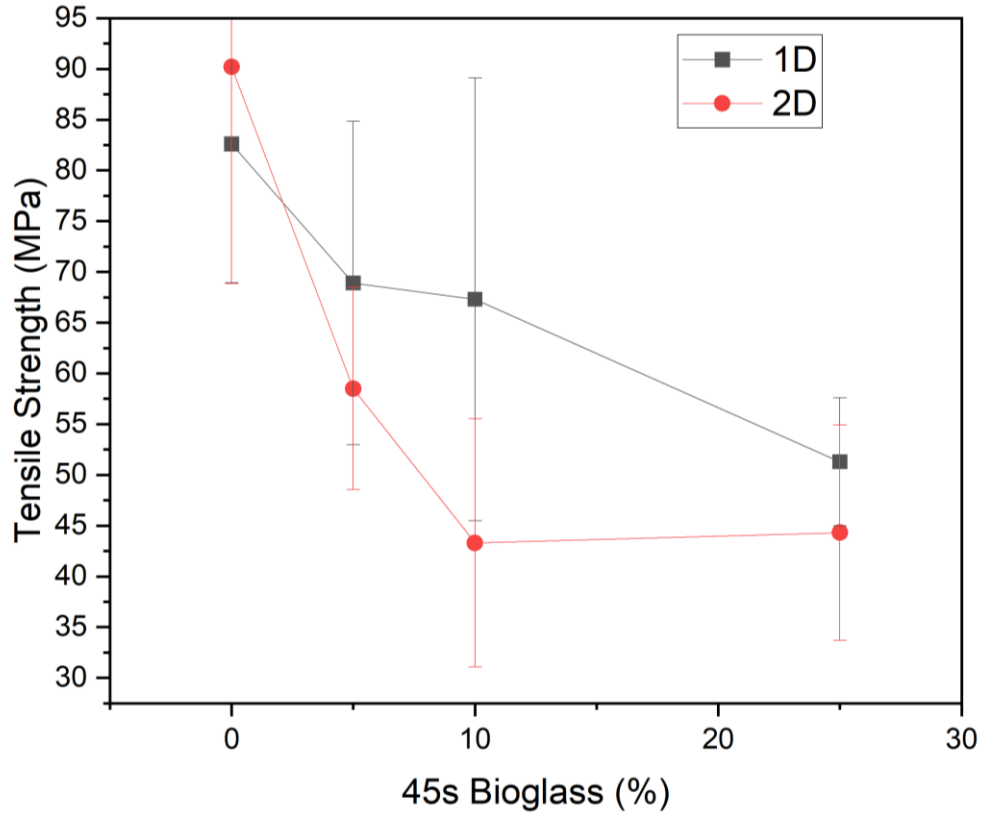


Figure 5.1: Tensile strength of Bioglass/CNF films.

The results from the tensile test portrayed some common trends. The addition of 45s Bioglass decreased the mechanical strength of CNF overall in both directions. As the amount of Bioglass increased within the films, the tensile strength also decreased. A possible reason for this reduction could be due to the interruption of the tightly bound cellulose fiber network with glass fibers. It is assumed that the glass fibers bound themselves to the cellulose fibers, which prevented them from binding to each other, thereby reducing the tensile strength of the material. Finally,

other than the pure CNF sample, the 2D samples had a lower tensile strength when compared the 1D. These results indicate that directionality impacts the mechanical values of these samples.

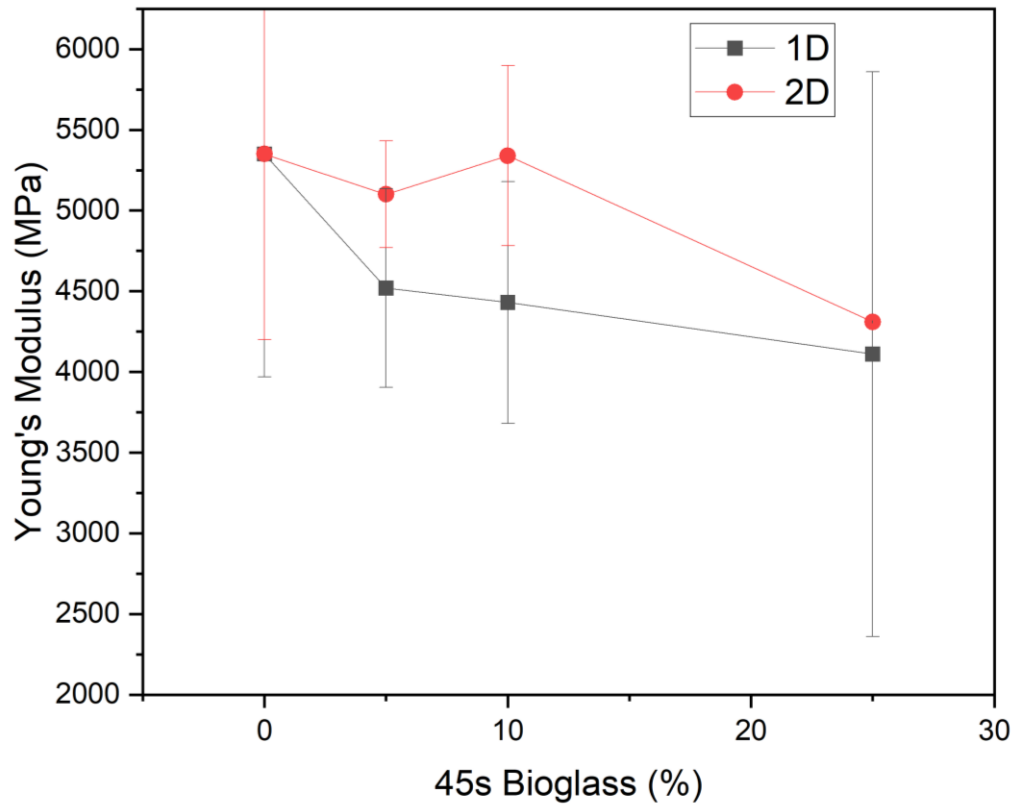


Figure 5.2: Young's modulus of Bioglass/CNF films.

The modulus values for the 45s Bioglass films with CNF showed somewhat opposite trends from the tensile strength results. First, the 1D samples showed a decreased stiffness when compared to the 2D samples. While the difference between them is not large, it is interesting that the samples with higher strength values show a lower stiffness. This again shows that directionality impacts the mechanical properties of CNF films. Also, the stiffness values had a more gradual reduction in values when Bioglass was added. The difference between pure CNF and the samples with Bioglass was less than that of the strength values. Overall, the results from this tensile test show that while there is a reduction in tensile strength values when Bioglass is added more data is

required to determine if this is a viable material. Therefore, larger molds will be manufactured, and a flexural test will be conducted.

The flexural samples were created using the previous bulk material preparation method discussed in Chapter 4. The formulations were 5, 15, and 25% wt. 5 flexural samples were created for each formulation. The test was conducted in accordance with the ASTM D790-17 standard. The tests were conducted on an Instron model 5942, using Blue Hill Universal to calculate the flexural modulus and strength values. The displacement rate of the flexural 3-point bending test was 4mm/min. The samples were tested until failure.

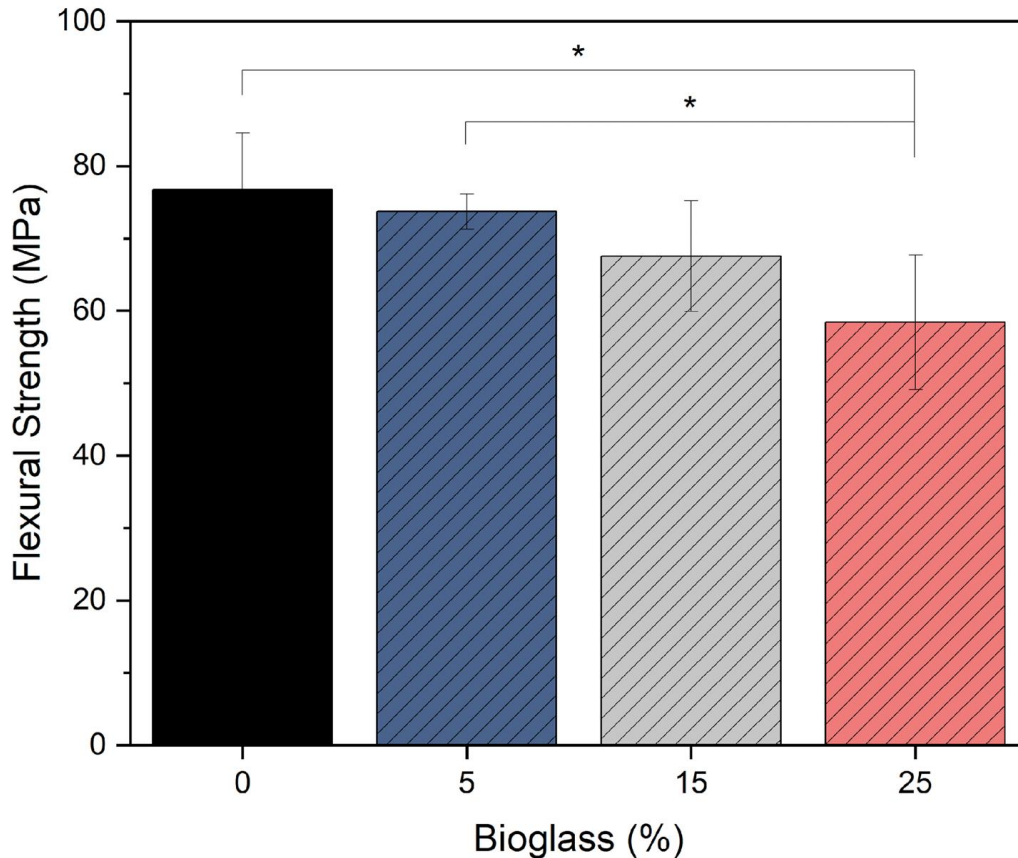


Figure 5.3: Flexural strength of 45s Bioglass/CNF composites.

The results from the flexural testing of Bioglass showed promising results. Compared to the HA samples, the Bioglass showed higher flexural strength when added to CNF. Even though

the strength values decreased with an increased amount of Bioglass, the decrease was less substantial than that of HA. For example, for the 5% sample of HA, the flexural strength was 21.38 MPa, and the Bioglass samples had a strength value of 73.71 MPa. The difference in strength is just over 50 MPa, a considerable increase. When compared to the value of CNF, the HA samples showed a difference of around 55 MPa, while the Bioglass only decreased the strength by around 3 MPa. This difference shows that the Bioglass samples impacted the flexural strength much less than that of HA, satisfying the purpose of this alternative material. Also, the only sample that was statistically significant was the 25%, showing a significant reduction compared to the 0 and 5% samples.

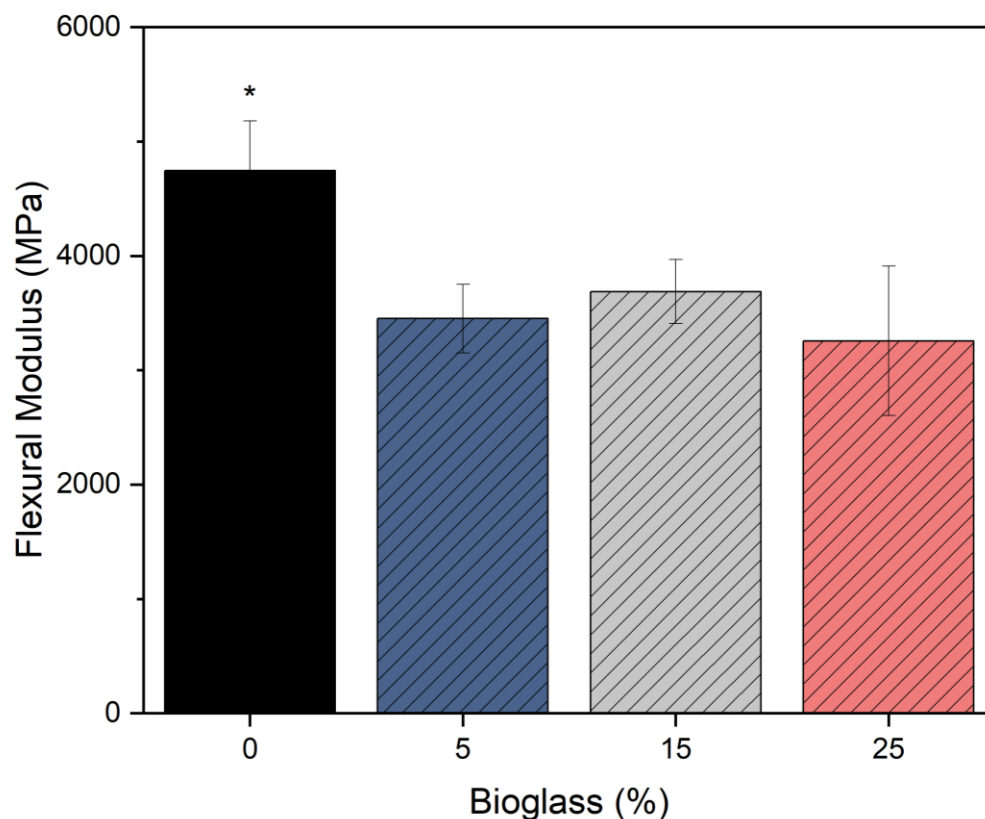


Figure 5.4: Flexural modulus of 45s Bioglass/CNF composites.

The results of the flexural modulus values of the Bioglass showed a reduction in stiffness across all samples. The addition of the Bioglass disrupted the overall internal structure of the

material, which decreased its stiffness. Furthermore, the three Bioglass samples all displayed a significant decrease in stiffness when tested using a Mann-Whitney u-test. While these numbers are significantly less than the pure CNF sample, the flexural strength values show promise. Also shown below is how the flexural strength of the Bioglass samples compared against the HA samples tested in Chapter 4.

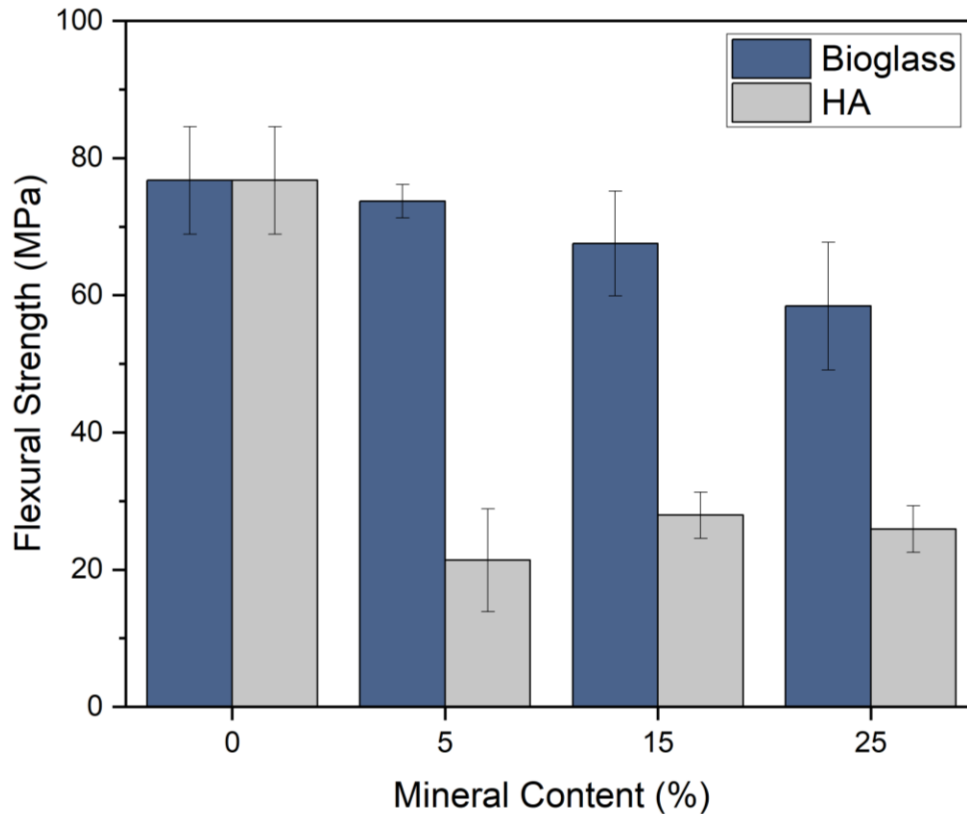


Figure 5.5: Comparison of Bioglass and HA flexural strength with CNF.

The flexural data shown above exemplifies the large difference in mechanical strength between CNF with Bioglass and HA. All of the Bioglass samples tested with CNF were not only closer in strength to pure CNF but much larger than the HA samples. This graph represents the success in mechanical strength of CNF films with Bioglass compared to HA.

5.4: Conclusions

The addition of Bioglass into CNF composites was a promising study. Initially, Bioglass was not dispersed into the CNF material, but using the method found in the previous chapter, the material was thoroughly dispersed throughout. Values from the initial tensile test of thin films showed that the mechanical strength was somewhat consistent with the values of pure CNF. The difference was close enough that further testing was appropriate. Large-scale samples of Bioglass were then manufactured to test the flexural strength and stiffness of CNF when Bioglass was added. When HA was tested with the material, there was a significant decrease in mechanical strength and stiffness. However, the addition of Bioglass proved the opposite. The values obtained from the Bioglass testing showed substantial increases in both stiffness and strength compared to HA/CNF composites of the same wt. %. The close relation in both stiffness and strength of Bioglass/CNF composites proves that Bioglass could be a suitable alternative to attempt to increase the overall bioactivity of the material. Further cell viability testing will be required in the future, but these initial results are promising.

CHAPTER 6: STRUCTURAL ANNEALING OF CELLULOSE NANOFIBRIL COMPOSITES

6.1: Introduction

In the previous chapter, Bioglass was explored as a potential alternative to hydroxyapatite. The main purpose of this experiment was to determine if there was a material that could increase CNF bioactivity, like HA, but also maintain similar or better mechanical properties to CNF. The results showed that Bioglass had a much higher stiffness and strength when compared to the HA samples. These results make Bioglass a promising additive for CNF, and further cell viability testing will be done to determine if it increases the overall bioavailability of CNF.

While the bioactivity of CNF is an aspect of interest for potential orthopedic applications, there are still concerns about CNF as a material that need to be answered. One is controlling the overall internal strain of the material. The material automatically curls irregularly when CNF is fully dried at high temperatures. Curling is prevalent along the long axis of the material, 1D, as well as along the edges. When designing materials, the material must remain a consistent shape throughout its lifetime to make it a reliable and stable material. Some common strategies in the manufacturing industry can reduce the overall internal strain of a material. For some metal and glass manufacturing, an approach called annealing is commonly used. An annealing procedure typically involves repeated heating and cooling of a material. This experiment aims to create a more enhanced crystalline structure within metals.⁷² An enhanced crystalline structure allows the surface to increase in uniformity, allowing it to become flatter and more consistent.

The time needed to heat and cool is important during an annealing process. Each specific material has a maximum temperature value, and all particles of the solid randomly arrange themselves in the liquid phase.⁷³ After they become arranged, the heating method, using a heat

bath, is slowly cooled to allow for the arrangement of particles in the low-energy ground state of a corresponding lattice.⁷³ The temperatures and rates are carefully considered and calculated to ensure that the optimum level of organization is achieved.

A modified strategy is necessary when applying this method to CNF. The properties of CNF are different than most metals. Rather than having a lattice-like arrangement of molecules, the CNF structure contains an anisotropic arrangement of cellulose fibers. Also, the assembly process of the material consists of dewatering the material at relatively low heat, rather than through a process that involves melting and reforming with high temperatures. Instead of using temperature to increase the motion of atoms, like in a metallic lattice, the accessible fibrils will be rehydrated, increasing internal fibril mobility similarly to atoms in a metal. This aims to attempt to create a tighter and more organized internal structure of CNF. The tighter organization is expected to increase the mechanical strength of the material while weakening some of the strains brought upon the material.

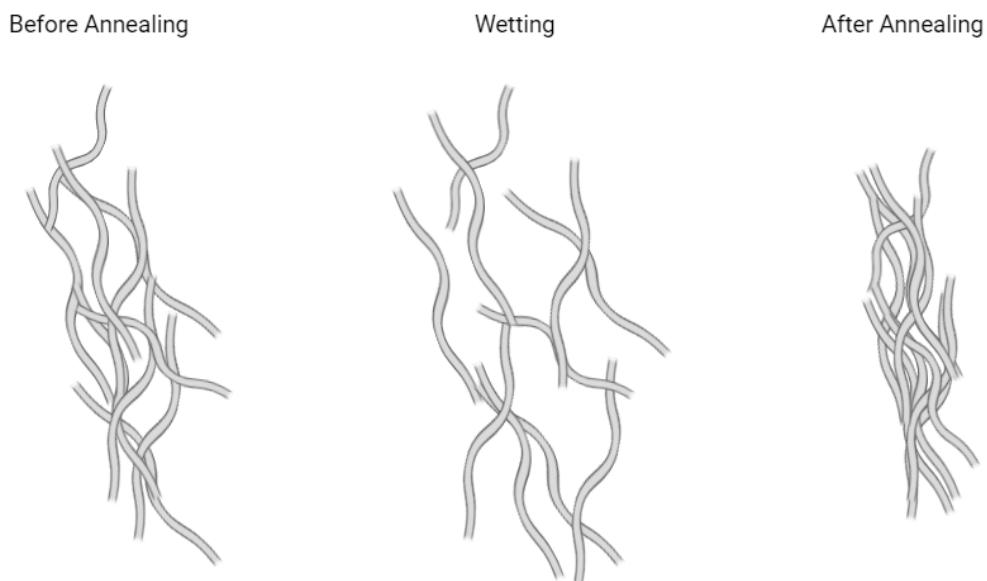


Figure 6.1: Representation of CNF fibers' expected behavior through annealing cycle.

6.2: Methods

This experiment used the bulk CNF mold preparation described in Chapter 3. Pure CNF was dried at 70°C for one week. Larger scaffolds were chosen rather than thin films because the larger samples had higher structural integrity when soaked. The samples were cut using a bandsaw into 100mm x 20mm x 4-5mm, following the ASTM D790-17 standard. The annealing procedure put the samples through wetting and drying cycles. One annealing cycle consisted of soaking a fully dried CNF sample at 37°C for 6 hours and redrying at 60°C for 18 hours. The temperature of the soaking cycle was selected to simulate the body temperature at 37°C. 6 hours of saturation time was chosen based on the soaking study from Chapter 3. Initial testing showed that samples became fully dry after saturation within the remaining time of the 24-hour cycle. The samples were dried between 2 fire bricks to prevent strain of the samples. Samples were placed through 0, 2, 4, 6, and 8 annealing cycles to determine the most effective cycling amount. 5 samples were manufactured for each set.

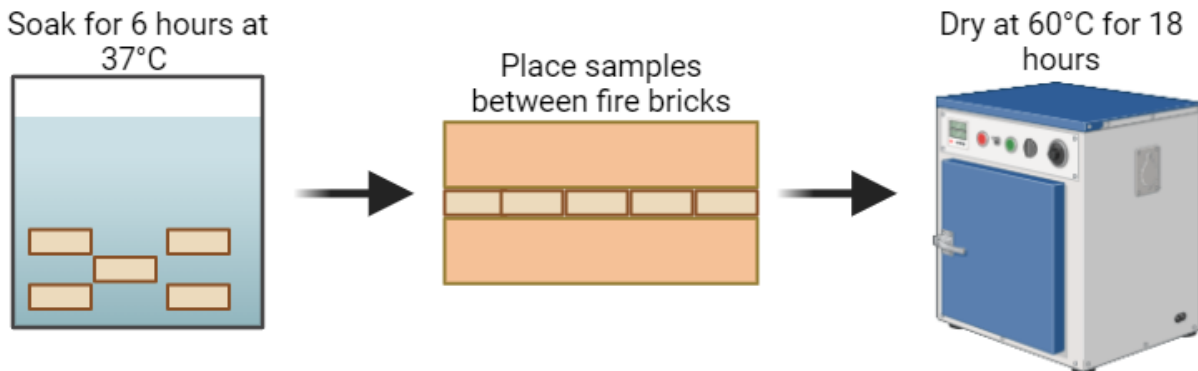


Figure 6.2: Procedure for 1 annealing cycle.

To determine the effect of annealing, the mass, volume, and density were all measured before annealing and after their last drying cycle. The assumption was that the samples would decrease in volume because of a tighter fiber alignment. Once all measurements were made, the

material's flexural strength was determined. Desiccant packets were used to prevent humidity uptake until testing.

6.3. Results

Each sample was tested using a 3-point bending test, following the ASTM D790-17 standard. An Instron model 5942 was used with a Blue Hill Universal program to determine each sample's flexural strength and modulus. The displacement rate of the test was 4mm/min, and the samples were tested until failure.

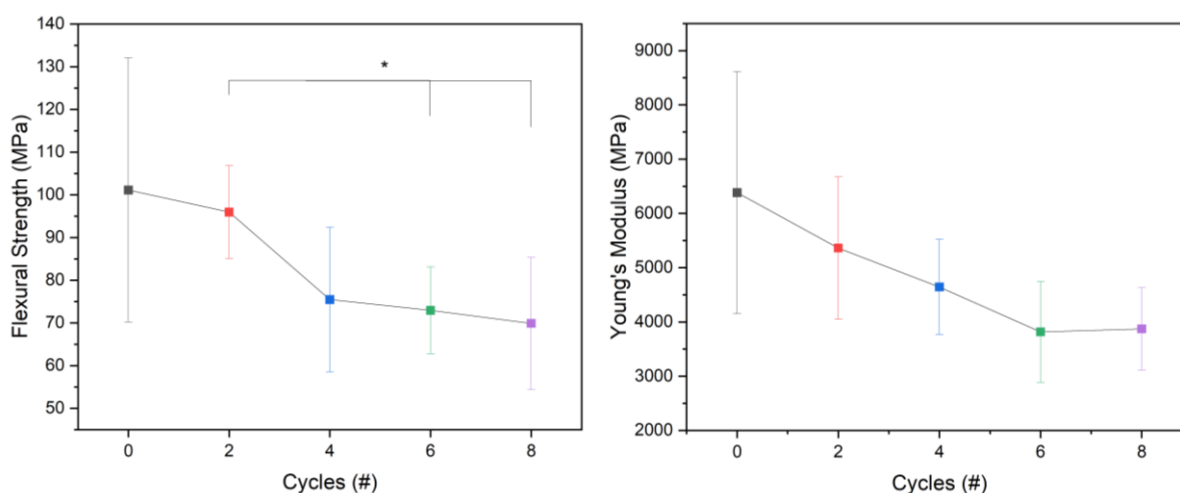


Figure 6.3: Flexural strength (left) and modulus (right) of 70°C pure CNF across increasing annealing cycles.

Some interesting observations were found when increasing the number of annealing cycles. As the number of cycles increased, the samples appeared to expand along the drying direction of the samples. The samples were cut in the 2D direction of the bulk mold. A sample cut in this direction is parallel to the drying of the material. In the bulk material drying mold, the material mainly decreases in size in the vertical direction. When the material is thoroughly dried, layering of the material can be observed in this direction. The samples in Figure 6.4 depict this layering.

On the far-right sample, the white lines along the length of the material symbolize the layering that occurs during drying. This sample came from the 2-cycle sample set, while the other two came from the 6-cycle sample set. It is observed that these layers begin to expand and separate from each other as the number of annealing cycles increases. The layer expansion correlates directly with the results from the flexural test. As the number of cycles increases, the material expands, leaving gaps that weaken the strength of the material overall. A Mann-Whitney test was used to determine the significance of the data next. The values for

flexural strength for cycles 6 and 8, when compared to cycle 2, were the only statistically significant value sets. A similar trend occurred for the flexural modulus data. As the number of annealing cycles increased, the material's stiffness decreased. The stiffness decrease is caused by the widening of the samples along the layers created by drying. While the amount of material is not reduced, the disconnectedness of the structure is reduced as more gaps are formed. No statistically significant values existed between the number of annealing cycles and the flexural modulus.



Figure 6.4: 6-cycle samples with observed expansion (left, middle) and 2-cycle sample (right).

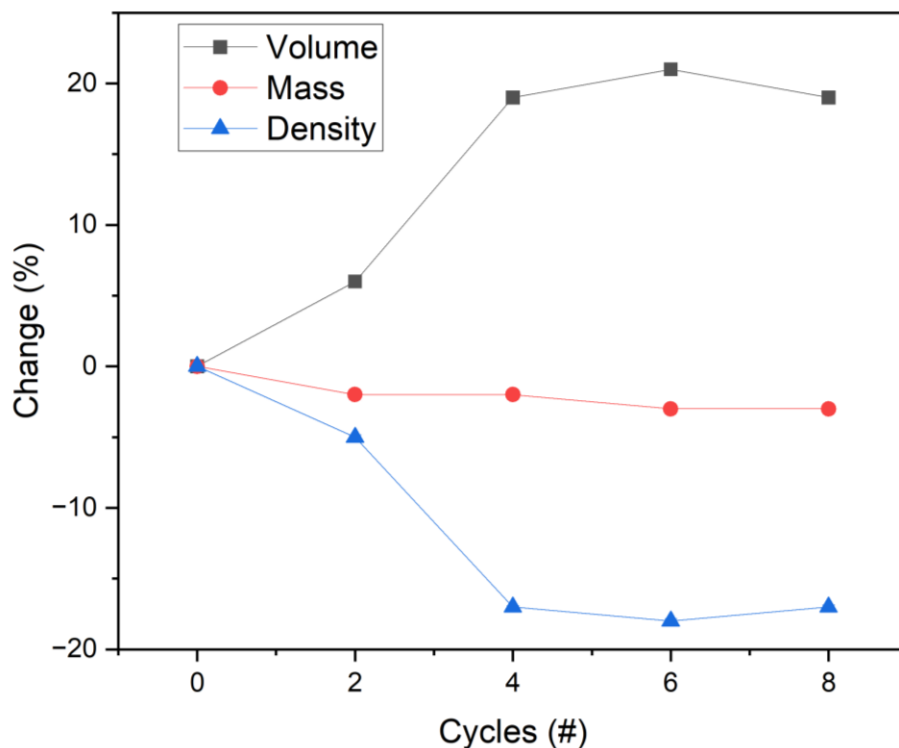


Figure 6.5: Volume, mass, and density changes across increasing annealing cycles.

As the annealing cycles increased, the volume increased, the density decreased, and the mass slightly decreased. The increase in volume was mainly due to an increase in the width due to the expansion of the material. Next, due to the mass staying relatively consistent, the density change decreased significantly due to the increase in volume. The mass and volume were expected to decline slightly, keeping the density relatively consistent. The materials did not behave as expected, with a slight collapse in the structure as the internal strains were “relieved” with cycles.

The results of this experiment were altered due to the cutting and drying method, leading to the design of a new process that considers the expansion behavior of the CNF material. This promising approach, which involves altering the drying temperature and cutting direction, could significantly enhance the understanding of material behavior. Based on prior results, it is expected that the porosity of CNF will decrease as the drying temperature decreases, opening up new possibilities for material engineering.⁵⁰ Therefore, samples were created at 60°C and 50°C. It is

expected that when the porosity is decreased, the expansion of the material will also decrease with fewer expansion areas. The samples were cut in both the 1D and 2D of the bulk molds. The 1D samples were cut perpendicular to the vertical drying direction. Instead of cutting the material with the layers appearing along the width of the samples, the layering will be along the thickness. This change is expected to decrease the material's expansion due to the reduction in layer presence. The same procedure was followed from the initial annealing test for 50°C samples in the 1D and 2D, 60°C samples in the 1D and 2D, and 70°C in the 1D.

6.4: Results

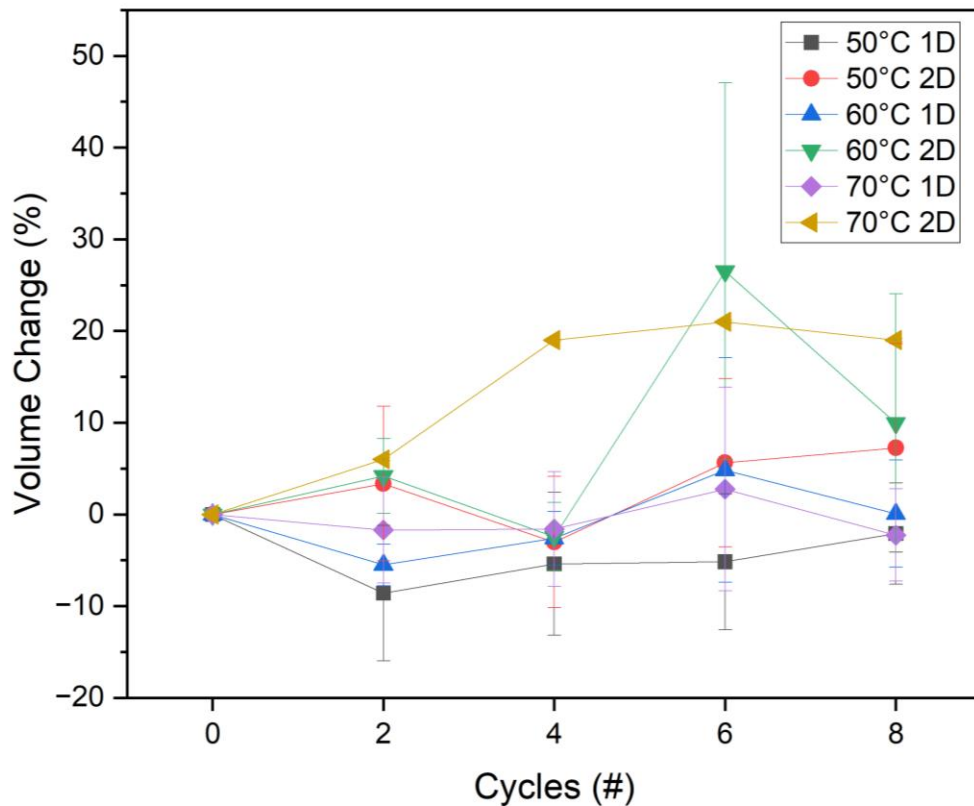


Figure 6.6: Volume change for differently manufactured CNF across increasing annealing cycles.

The volume change for each material type varied. Based on the graph's trends, the 2D samples experienced an increased volume as the amount of annealing increased. These results were expected from the previous trial. The layering action that occurs during drying impacts the

structure of CNF as it is placed through annealing. As annealing occurs, these layers permanently separate and expand from each other, causing an increase in the overall width of each sample. The data also suggests that the decrease in temperature also impacts these results. The decrease in temperature increases the overall drying time, decreasing the speed of volume reduction. This reduction appears to have affected the overall separation of layers during annealing. Finally, the 1D samples displayed reduced volume, the opposite of the 2D samples. This trend was predicted, as the act of annealing appeared to produce a tighter network of fibers, reducing the overall volume of the material.

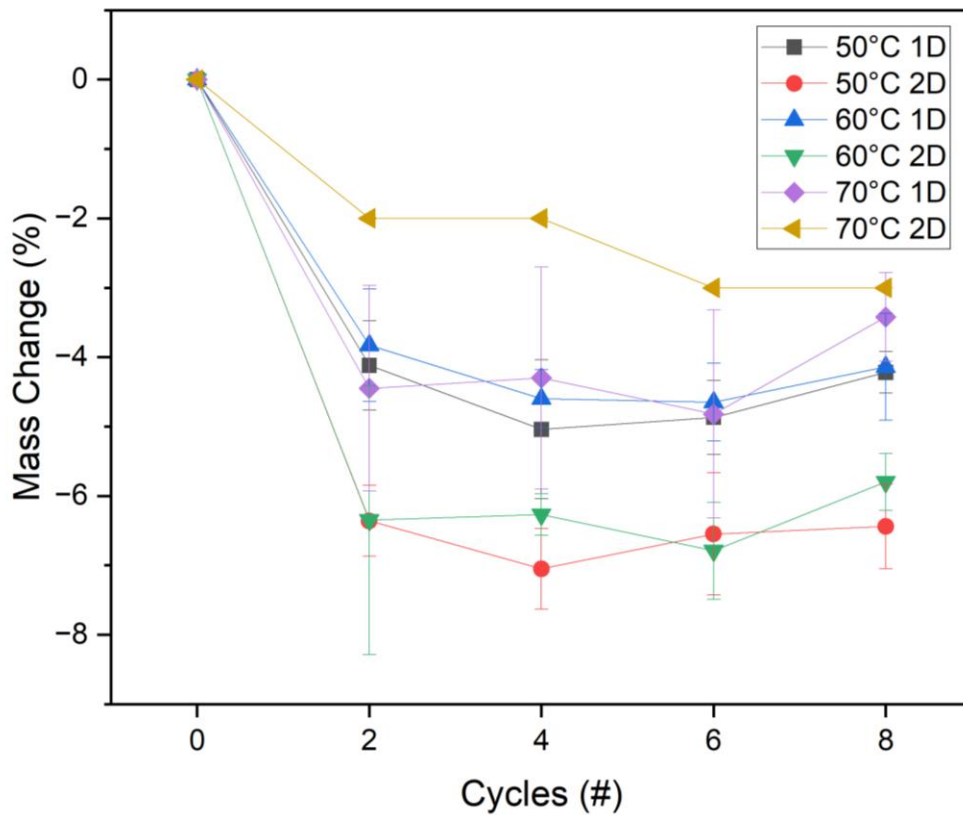


Figure 6.7: Mass change for differently manufactured CNF across increasing annealing cycles.

The mass trends were similar across all different manufacturing types of CNF. A potential reason for the decrease in mass could be the residual material lost during sample manufacturing. When the samples are initially cut, loose residual material remains along the outside of most

samples. When these samples were introduced to water, these pieces of loose material separated from the rest of the tightly bound solid, decreasing the sample's overall mass. It is important to note that the volume does not affect the change in mass. The addition or reduction of pores into the material, which changes the volume, incorporates air into the material, which has negligible mass. Therefore, the changes in mass are due to a loss of material during soaking.

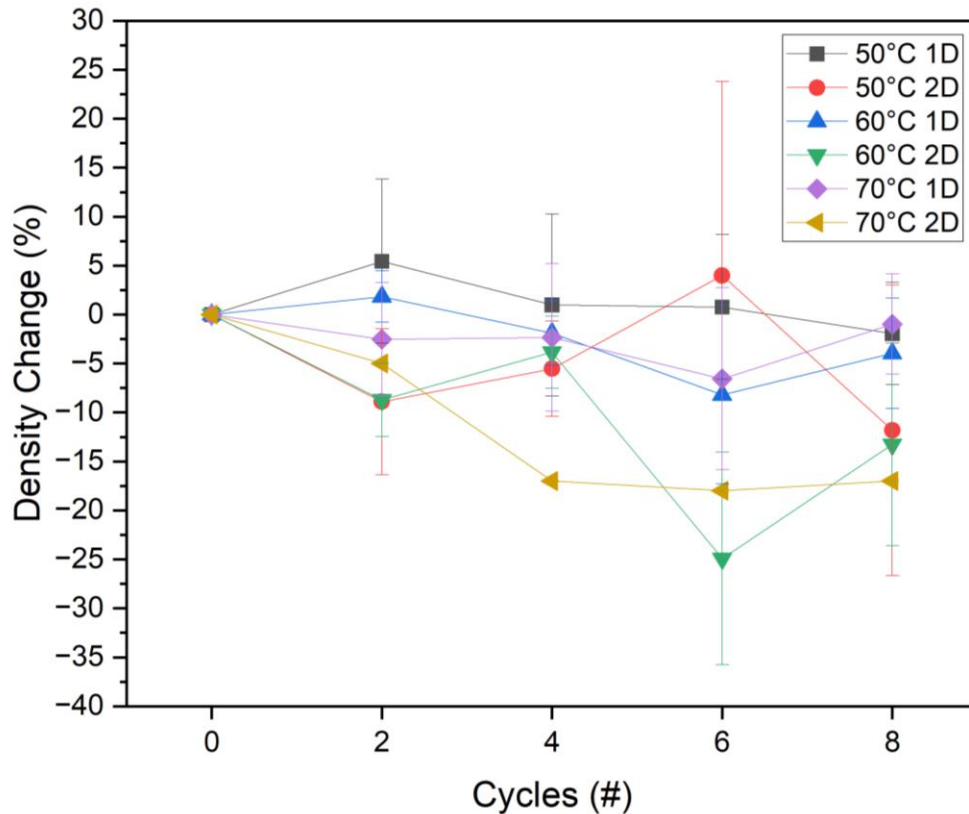


Figure 6.8: Density change for differently manufactured CNF across increasing annealing cycles.

The change in density data displayed varying results. Initially, the density of the material was expected to increase after annealing occurred. The assumption was that the volume would decrease and the mass would stay relatively the same. Instead, there was a wide range of volumetric changes, with most 1D samples displaying a decrease in volume and 2D the opposite. Furthermore, the mass decreased across all sample sets rather than remaining similar to the initial values. These data variations caused irregular density changes across all different material sets.

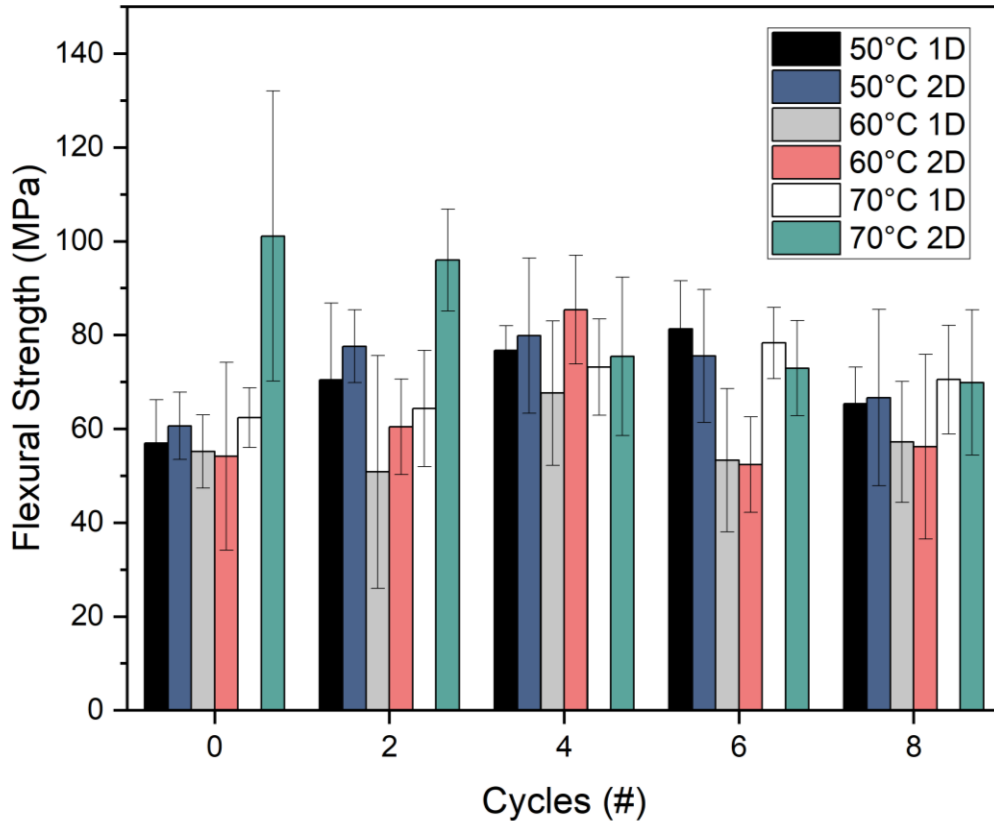


Figure 6.9: Flexural strength of differently manufactured CNF across increasing annealing cycles.

The data from this graph displays interesting results. Based on the material set at hand, three different variables can affect the flexural strength of CNF material. Therefore, a 3-way ANOVA test was used through the origin program to determine the effect of each variable set on each other. The results found that when comparing the directionality of the samples together, that directionality was statistically significant. When comparing the temperatures against each other, the data was statistically significant. When comparing the number of cycles against each other, the data was statistically substantial again. There was no statistical significance when comparing how the direction and temperature affect each other. However, there was a statistical significance when comparing the temperature and direction to the number of cycles. However, when comparing the three together, there was no statistical significance. This means that when all three variables are

combined against each other, there is no additional impact on the strength values. Next, the flexural modulus of the samples was tested. While the results from the statistical test show these results, there doesn't appear to be any major trends in this data. The only major trend shown is that the 70°C 2D sample decreased over time, and it was relatively one of the higher-performing samples. Therefore, while the statistical test showed variation, the overall results were inconclusive.

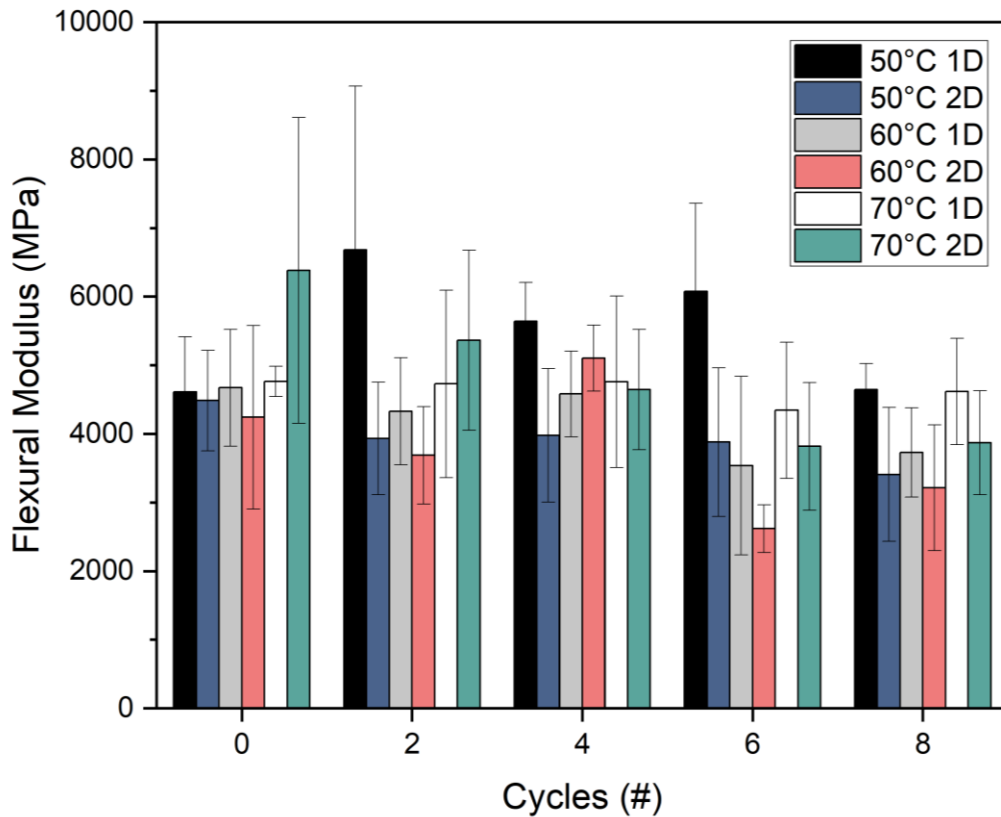


Figure 6.10: Flexural modulus of differently manufactured CNF across increasing annealing cycles.

The data from this graph show varying results. A three-way ANOVA test was used to determine the statistical significance of each data set. The results showed that the direction, temperature, and cycle were all statistically significant when compared against each other. Next, when comparing the temperature sets to both directions and the number of cycles, the results were statistically substantial again. However, the data was not statistically significant when the

directionality and cycling amounts were tested against each other. Finally, when the three variables were compared against each other, the data was not statistically significant. This means that when compared altogether, the three variables did not impact the significance of the modulus values from what was already compared. While the results from this statistical test show differences, there are no major trends across the data. One trend that can be seen is the 50°C 1D samples showing a relatively higher stiffness value compared to the other samples. However, due to the varying results shown across this test, no major conclusions can be made.

6.4: Conclusions

The annealing cycles showed varying results. When examining the changes in mass, density, and volume, it seemed as if the only trend that followed a similar trend across methods was the changes in mass for each sample. Each sample had a negative mass change after annealing occurred. Next, the volume increased for the 2D samples and remained consistent or negative for the 1D samples. These values were initially predicted due to the reduction in layering from the 1D sample section cut. The density values showed inconclusive results. Initially, the density was thought to decrease with increased annealing cycles. However, the reduction of mass throughout and the variability of the volumetric changes provided inconclusive results from the density. If the trial were reconsidered, an initial “washing” phase would rinse off the excess material remaining from cutting to reduce mass loss and provide more conclusive density results.

A statistical test from the mechanical testing data showed that each variable individually impacted both the modulus and strength results. However, when looking at trends across the entire graph, there were few conclusions that can be made. Therefore, moving forward, different studies will need to be done to determine how to reduce the overall internal strain of CNF material.

CHAPTER 7: CONCLUSIONS

7.1: Summary

Plastics worldwide are used for a wide range of daily applications. These materials range in material types and have versatile mechanical and chemical variability. One specific industry that has widespread adoption of plastics is the medical industry. This industry uses plastics for long-term use, like technologically advanced medical machines, and for short-term usage, like IV bags and tubing. These short-term devices are typically referred to as single-use devices. They are usually designed to last 100s years while generally only being used within 24 hours. The high usage of these materials, along with their long-term degradability, have posed concerns for the future waste procedures of these products. Therefore, a product with properties similar to these materials must be found but degrades much quicker than current devices.

CNF has been considered a potential biodegradable alternative to current medical plastics. The wide range of properties allows it to be altered for specific target applications. While many properties can be suitable for these applications, some questions must be answered before further development. This thesis aimed to analyze these complications and formulate solutions further to enhance the research and understanding of this material.

In Chapter 2, an in-depth look into the field of plastics was explored. The global usage and waste procedure of common plastics were analyzed, as well as the different purposes of these plastics. Single-use devices were defined, especially for their recent adoption within the medical industry. The waste complications for these products were discussed, and alternative materials were considered. CNF arose as a potential biodegradable alternative material due to its similar, yet versatile, properties. The current research on this material was summarized, and the possible complications were mentioned.

Chapter 3 aimed to find a suitable crosslinking option to alleviate the impact of water absorption into CNF. When water is introduced into CNF, the material becomes swollen and weak. Three crosslinkers were found as potential additives to reduce the rehydration properties: polycup, urea, and strontium chloride. Polycup showed initial promise in its ability to reduce the overall water absorption of CNF, but further investigation proved that it negatively impacted the desired mechanical properties of the material. Urea and strontium chloride were then initially explored as suitable crosslinking agents. Tensile testing of urea/CNF thin films showed minimal negative impact when urea was introduced. Furthermore, the strontium chloride films showed a positive trend, increasing tensile strength and stiffness values after introduction. Overall, both these materials show promise as potential crosslinkers from initial testing.

Chapter 4 initially focused on increasing the cell viability of CNF but soon found that dispersing the HA evenly into the CNF was another challenge. When HA was first introduced to CNF without prior treatment, visible clumping and a lack of dispersion occurred. Various pre-treatment methods were explored, and a suitable dispersion method of HA nanoparticles into CNF was found. Based on mechanical testing as well as micro and macroscopic imaging, it was determined that pre-saturation of the HA material prior to being introduced into CNF proved successful. Various other mechanical tests were conducted on HA/CNF material, which found that the addition of HA negatively impacted the mechanical strength of CNF material.

In Chapter 5, the bioavailability of CNF material was further explored with a material called Bioglass. Research has been done on this material, showing that it is excellent at promoting cell proliferation and differentiation. Before work can be done to determine the cell viability of the material, the mechanical strength properties had to be explored. HA proved to have potentially suitable cell viability properties, but the negative impact on the mechanical properties required

new materials to be explored. The mechanical testing from Bioglass was much improved compared to the HA samples. The strength values were more similar to pure CNF across all formulations of Bioglass than those of HA. Therefore, the transition to Bioglass had an initial positive impact, but further cell viability testing must be performed before making efficient conclusions.

Chapter 6 aimed to reduce the material's internal strain through an adapted annealing method. This method entailed putting CNF material through several different fully saturating and then thoroughly drying cycles. Initial results showed that the cutting direction significantly impacted the post-annealing structure of the CNF. Rather than create a tighter network of fibers, the layers of CNF that were produced during drying expanded in size and created weaker material overall. The directionality and drying temperature were then explored to determine if a variation in these methods could yield better results. The results for flexural modulus and strength showed that when compared statistically, the manufacturing method does impact the results. However, across the entire data set there were few major trends that can be seen. Therefore, the data shown through the annealing cycles was inconclusive, as there was no major impact across the different variables.

8.2: Future Work and Recommendations

To further enhance the properties of CNF for their potential use in various medical applications, further work must be completed. First, the mechanical properties of both urea and strontium chloride need to be explored. Initial testing suggests that both materials can positively affect mechanical properties from a thin film tensile test. However, the scalability of these materials and flexural and compressive testing have not yet been tested. If the positive trends continue throughout these tests, the water intake of these materials within CNF will be further tested to determine the crosslinking extent. If initial results prove that they can successfully reduce

the overall wettability of the material further cytotoxicity trials will need to be conducted to determine if they can be suitable for medical implications.

The results from the initial Bioglass mechanical testing proved to be promising. Cell viability testing will need to be conducted on Bioglass/CNF composites to determine if adding this material can increase the overall cell viability of CNF. Other options can be explored if Bioglass does not promote cell proliferation or differentiation. Two materials already proven to have suitable mechanical properties with CNF are strontium chloride and urea. The cell viability of CNF with these materials could also be tested to determine if they are sufficient for increasing the cell viability.

The results from the annealing study proved to be mainly inconclusive. Moving forward, other options should be explored to reduce the overall internal strain of the material. One potential manufacturing method that could provide promising results is inverting the CNF mold during drying. In the drying process, there is a time point where the material can be moved without structural degradation but is also not completely dry. At this point, the sample could be inverted to counteract the upward internal strain. Another option could be to ensure the mold is completely dry and lock the fibers in place by placing the fibers in liquid nitrogen. While potentially financially impactful, this method could help prevent the fibers from straining after fully drying. Finally, there could be an enhancement to the fire brick drying mold. Currently, the only pressure applied to the material is gravity in the vertical direction. If the other two directions also could vary with time, it could create a final product that is more uniform in size and could also prevent strain from occurring throughout the material. Overall, the manufacturability of CNF proves to be a challenge currently, but adaptations to the manufacturing method could produce better, more uniform results.

There are still many other considerations before introducing this product to the market. Depending on the particular device, FDA regulations for medical devices must be tested and considered. In terms of using this material as an orthopedic implant, the future direction is to finalize *in vitro* testing of CNF composites and then conduct *in vivo* testing within animals, followed by clinical trials. Regardless of the potential application, the overall production of CNF must be increased. Currently, production of this material is in an early pilot scale. If commercialization of CNF is to occur, specifically for medical applications, the size and scale of CNF production must be increased to fit those needs. CNF's properties make it a candidate material that can be used throughout various commercial applications soon.

REFERENCES

1. Hopewell, J., Dvorak, R. & Kosior, E. Plastics recycling: challenges and opportunities. *Philosophical Transactions of the Royal Society B: Biological Sciences* **364**, 2115–2126 (2009).
2. Walker, T. R. & Fequet, L. Current trends of unsustainable plastic production and micro(nano)plastic pollution. *TrAC Trends in Analytical Chemistry* **160**, 116984 (2023).
3. Kumar, A., Pali, H. S. & Kumar, M. A comprehensive review on the production of alternative fuel through medical plastic waste. *Sustainable Energy Technologies and Assessments* **55**, 102924 (2023).
4. Medical Plastics Market Size, Share & Growth Report, 2030. <https://www.grandviewresearch.com/industry-analysis/medical-plastics-market>.
5. Desidery, L. & Lanotte, M. Polymers and plastics: Types, properties, and manufacturing. doi:10.1016/B978-0-323-85789-5.00001-0.
6. materials-science-and-engineering-8th-edition-callister : Hritik : Free Download, Borrow, and Streaming : Internet Archive. https://archive.org/details/materials-science-and-engineering-8th-edition-callister_201910/page/n623/mode/2up.
7. Plastic Trade Names - Industrial Plastic Supply, Inc. <https://iplasticsupply.com/home/trade-names-trademark-brand-plastic-material/?cn-reloaded=1>.
8. Solvay | A Pioneering Chemical Company. <https://www.solvay.com/en/>.
9. Engineered Materials and Solutions | Celanese. <https://www.celanese.com/about-us/engineered-materials>.
10. Omico Plastics, Inc. | Custom Blow Molded Plastic Manufacturer | Kentucky. <https://www.omicoplastics.com/>.
11. Home - ARCO. <https://www.arcoplastics.com/>.
12. Shaping a world where the plastic products vital to our lives are even better tomorrow than they are today. <https://www.novachem.com/>.
13. High performance plastic solutions | Ensinger. <https://www.ensingerplastics.com/en-us>.
14. Plastic-Craft | Teflon Virgin Natural Sheet | Chemical Resistant. <https://plastic-craft.com/teflon-virgin-natural-sheet/>.
15. Hostaflon TFM(tm) PTFE. <https://www.plasticsnet.com/doc/hostaflon-tfntm-ptfe-0001>.
16. Evonik – Cyro | Plastic Materials. <https://www.plastic-materials.com/evonik-cyro/>.
17. Atoglas. <https://www.semiconductoronline.com/doc/atoglas-0001>.

18. Pal Group | Western Canada's most reliable packaging distributor and custom plastics manufacturer. <https://palgroup.ca/>.
19. High performance plastic solutions | Ensinger. <https://www.ensingerplastics.com/en-us>.
20. Lytex - Quantum Composites - Knowde. <https://www.knowde.com/stores/quantum-composites/brands/lytex>.
21. EPIKOTE Resins. <https://www.westlakeepoxy.com/en-gb/brand/epikote>.
22. Home - Union Carbide Company. <https://www.unioncarbide.com/index.html>.
23. Home - Norplex-Micarta. <https://www.norplex-micarta.com/>.
24. Plastics in Medical Devices: Properties, Requirements, and Applications - Vinny R. Sastri - Google Books.
https://books.google.com/books?hl=en&lr=&id=X3crEAAAQBAJ&oi=fnd&pg=PP1&dq=properties+of+plastics+for+medical+applications&ots=qI48_IDkZy&sig=8enNjpB23cQhcEqP2JUZUnUd5UI#v=onepage&q&f=false.
25. Medical Device Bans | FDA. <https://www.fda.gov/medical-devices/medical-device-safety/medical-device-bans>.
26. Overview of Regulatory Requirements: Medical Devices - Transcript | FDA.
<https://www.fda.gov/training-and-continuing-education/cdrh-learn/overview-regulatory-requirements-medical-devices-transcript>.
27. Current Good Manufacturing Practice (CGMP) Regulations | FDA.
<https://www.fda.gov/drugs/pharmaceutical-quality-resources/current-good-manufacturing-practice-cgmp-regulations>.
28. Generally Recognized as Safe (GRAS) | FDA. <https://www.fda.gov/food/food-ingredients-packaging/generally-recognized-safe-gras>.
29. Mavrogenis, A. F., Papagelopoulos, P. J. & Babis, G. C. Osseointegration of Cobalt-Chrome Alloy Implants. *J Long Term Eff Med Implants* **21**, 349–358 (2011).
30. Neacșu, I. A., Nicoară, A. I., Vasile, O. R. & Vasile, B. Ș. Inorganic micro- and nanostructured implants for tissue engineering. *Nanobiomaterials in Hard Tissue Engineering: Applications of Nanobiomaterials* 271–295 (2016) doi:10.1016/B978-0-323-42862-0.00009-2.
31. Reuse of Single-Use Devices: Understanding Risks and Strategies for Decision-Making for Health Care Organizations A White Paper by Joint Commission International. (2017).
32. Chamas, A. *et al.* Degradation Rates of Plastics in the Environment. *ACS Sustain Chem Eng* **8**, 3494–3511 (2020).
33. Wisniewski, A. *et al.* Reducing the Impact of Perfusion Medical Waste on the Environment. *J Extra Corpor Technol* **52**, 135 (2020).

34. Babaremu, K., Oladijo, O. P. & Akinlabi, E. Biopolymers: A suitable replacement for plastics in product packaging. *Advanced Industrial and Engineering Polymer Research* **6**, 333–340 (2023).
35. Kershaw, Dr. P. J. Biodegradable Plastics & Marine Litter. *United Nations Environment Programme (UNEP)* 1–38 (2015).
36. Gajre, V. (& Kulkarni,). Natural Polymers-A comprehensive Review. *Article in International Journal of Research in Pharmaceutical and Biomedical Sciences* (2012).
37. Natural Rubber - Shinzo Kohjiya - Google Books. <https://books.google.com/books?hl=en&lr=&id=SwBNDwAAQBAJ&oi=fnd&pg=PR1&dq=natural+rubber&ots=SkNo6Bl88L&sig=WHrvzFpEpTIC0puJVwY89JToURY#v=onepage&q=natural%20rubber&f=false>.
38. Gentleman, E. *et al.* Mechanical characterization of collagen fibers and scaffolds for tissue engineering. *Biomaterials* **24**, 3805–3813 (2003).
39. Nechyporchuk, O., Belgacem, M. N. & Bras, J. Production of cellulose nanofibrils: A review of recent advances. *Ind Crops Prod* **93**, 2–25 (2016).
40. SEM micrograph of the cellulose nanocrystals isolated by a ‘polyol... | Download Scientific Diagram. https://www.researchgate.net/figure/SEM-micrograph-of-the-cellulose-nanocrystals-isolated-by-a-polyol-method_fig1_341190759.
41. Liao Kim Anh Pham Victor Breedveld, J., Liao Á A Pham Á V Breedveld, J. K. & Liao Á Breedveld, J. V. TEMPO-CNF suspensions in the viscoelastic regime: capturing the effect of morphology and surface charge with a rheological parameter. doi:10.1007/s10570-020-03572-1.
42. SEM micrograph of a bacterial cellulose sample showing a coherent 3-D... | Download Scientific Diagram. https://www.researchgate.net/figure/SEM-micrograph-of-a-bacterial-cellulose-sample-showing-a-coherent-3-D-network-formed-by_fig1_256463244.
43. Fibrillation Definition & Meaning - Merriam-Webster. <https://www.merriam-webster.com/dictionary/fibrillation>.
44. Heggset, E. B. *et al.* Cellulose nanofibrils as rheology modifier in mayonnaise-A pilot scale demonstration. (2020) doi:10.1016/j.foodhyd.2020.106084.
45. Barnat-Hunek, D., Szyman´ska, M., Szyman´ska-Chargot, S., Jarosz-Hadam, M. & Łagód, G. Effect of cellulose nanofibrils and nanocrystals on physical properties of concrete. (2019) doi:10.1016/j.conbuildmat.2019.06.145.
46. Tayeb, A. H., Amini, E., Ghasemi, S. & Tajvidi, M. molecules Cellulose Nanomaterials-Binding Properties and Applications: A Review. (2018) doi:10.3390/molecules23102684.
47. Wang, J. *et al.* Moisture and Oxygen Barrier Properties of Cellulose Nanomaterial-Based Films. *ACS Sustain Chem Eng* **6**, 49–70 (2018).

48. Hafez, I. & Tajvidi, M. Comprehensive Insight into Foams Made of Thermomechanical Pulp Fibers and Cellulose Nanofibrils via Microwave Radiation. (2021)
doi:10.1021/acssuschemeng.1c01816.
49. Hossain, R., Tajvidi, M., Bousfield, D. & Gardner, D. J. Multi-layer oil-resistant food serving containers made using cellulose nanofiber coated wood flour composites. *Carbohydr Polym* **267**, 118221 (2021).
50. Holomakoff, D. G. DigitalCommons@UMaine Nanocellulose Fibers as a Potential Material for Orthopedic Implantation Application. (2017).
51. compass. <https://compass.astm.org/document/?contentCode=ASTM%7CD0695-23%7Cen-US>.
52. compass. <https://compass.astm.org/document/?contentCode=ASTM%7CD0790-17%7Cen-US>.
53. compass. <https://compass.astm.org/document/?contentCode=ASTM%7CD0638-22%7Cen-US>.
54. Digitalcommons@umaine, D. & Chesley, M. P. The Influence of Processing and Additives on Cellulose Nanofiber The Influence of Processing and Additives on Cellulose Nanofiber Properties for Orthopedic Application Properties for Orthopedic Application. (2022).
55. Predicting the Future of Orthopaedic Trauma Implantology. doi:10.1007/978-981-19-7540-0_7.
56. Ren, L. *et al.* Dual modification of starch nanocrystals via crosslinking and esterification for enhancing their hydrophobicity. *Food Research International* **87**, 180–188 (2016).
57. Catanzano, O. *et al.* Macroporous alginate foams crosslinked with strontium for bone tissue engineering. *Carbohydr Polym* **202**, 72–83 (2018).
58. Min, Y., Yi, J., Dai, R., Liu, W. & Chen, H. A novel efficient wet process for preparing cross-linked starch: Impact of urea on cross-linking performance. *Carbohydr Polym* **320**, 121247 (2023).
59. Sharma, S. & Deng, Y. Dual mechanism of dry strength improvement of cellulose nanofibril films by polyamide-epichlorohydrin resin cross-linking. *Ind Eng Chem Res* **55**, 11467–11474 (2016).
60. Lopez-Esteban, S. *et al.* Bioactive glass coatings for orthopedic metallic implants. *J Eur Ceram Soc* **23**, 2921–2930 (2003).
61. Mosaner, P., Bonelli, M. & Miotello, A. Pulsed laser deposition of diamond-like carbon films: reducing internal stress by thermal annealing. *Appl Surf Sci* **208–209**, 561–565 (2003).
62. Mane, S., Ponrathnam, S. & Chavan, N. Effect of Chemical Cross-linking on Properties of Polymer Microbeads: A Review. **3**, 473–485 (2015).

63. Wei, Y. C., Hudson, S. M., Mayer, J. M. & Kaplan, D. L. The crosslinking of chitosan fibers. *J Polym Sci A Polym Chem* **30**, 2187–2193 (1992).
64. Celestine, A.-D. N., Agrawal, V. & Runnels, B. Experimental and numerical investigation into mechanical degradation of polymers. *Composites Part B* **201**, 108369 (2020).
65. Cheneler, D. & Bowen, J. Degradation of polymer films. doi:10.1039/c2sm26502h.
66. Feng, X. Chemical and Biochemical Basis of Cell-Bone Matrix Interaction in Health and Disease. doi:10.2174/187231309788166398.
67. What Is Bone? | NIAMS. <https://www.niams.nih.gov/health-topics/what-bone>.
68. Digitalcommons@umaine, D. & Chesley, M. P. Characterization of Nano-Cellulose Based Composites For Characterization of Nano-Cellulose Based Composites For Biomedical Applications Biomedical Applications.
69. Moreno, E. C., Gregory, T. M. & Brown, W. E. Preparation and Solubility of Hydroxyapatite. (1968).
70. Bosetti, M. & Cannas, M. The effect of bioactive glasses on bone marrow stromal cells differentiation. *Biomaterials* **26**, 3873–3879 (2005).
71. Tavakolizadeh, A. *et al.* Investigation of Osteoinductive Effects of Different Compositions of Bioactive Glass Nanoparticles for Bone Tissue Engineering. *ASAIO Journal* **63**, 512–517 (2017).
72. Buseti, F. Simulated annealing overview. (2001).
73. van Laarhoven, P. J. M. & Aarts, E. H. L. Simulated annealing. *Simulated Annealing: Theory and Applications* 7–15 (1987) doi:10.1007/978-94-015-7744-1_2.

BIOGRAPHY OF THE AUTHOR

Cameron Andrews was born in Lewiston, Maine, on June 15th 2001. Throughout his youth, he lived in New Gloucester, Maine, and graduated from Gray-New Gloucester High School in 2019. Following graduation, he continued his education at the University of Maine, pursuing a Bachelor's degree in biomedical engineering. In the fall of 2021, he started his research career as an undergraduate researcher in the Mason Lab. He continued working throughout his undergraduate career and graduated from the University of Maine with his Bachelor's degree in biomedical engineering in May 2023. He furthered his education in an accelerated Master's program in biomedical engineering that June. Cameron is a candidate for a Master of Science in biomedical engineering at the University of Maine in August 2024.